Technische Universität Berlin

Fakultät VII Wirtschaft & Management

Fachgebiet Wirtschafts- und Infrastrukturpolitik (WIP)

Demand Response in bottom-up planning models

Author:

Gro Lill Økland (0452815) - okland@campus.tu-berlin.de

Supervisors:

Prof. Dr. Christian von Hirschhausen

Leonard Göke

Berlin, Monday 28th February, 2022

Statutory declaration

Hereby, I declare that I have developed and written this research completely by myself and that I have not used sources or means without declaration in the text. Any external thought, content, media, or literal quotation is explicitly marked and attributed to its respective owner or author.
As of the date of submission, this piece of document and its content have not been submitted anywhere else but to my supervisors.

Berlin, Monday 28th February, 2022

Gro Lill Økland

Acknowledgement

I would like to take the opportunity to thank and acknowledge the help and encouragement that people have given me during the writing of this thesis. Many thanks to my supervisor Leonard Göke for his constructive comments and discussions. And a special thank you to my family and friends for their unwavering belief and support in me.

Abstract

The climate change crisis requires immediate action on a global and national scale to mitigate the Greenhouse Gas (GHG) emissions. In the next decades, the energy system will experience a considerable rise in Renewable Energy Sources (RES), leading to more fluctuating electricity generation from weather dependent Intermittent Renewable Energy Sources (IRES). This requires more flexibility in the energy system on both the supply and demand side. Demand Side Management (DSM), and specifically the category Demand Response (DR) has received increased attention for its ability in increasing the energy system flexibility. The thesis investigates two methods of DR in a bottom-up energy planning graph-based framework. An indirect method utilising the inherent temporal resolution mapping in the graph-based framework and a direct method implementing a DR formulation. The two methods are analyzed in a case study representing the German energy system with 100% share of RES in Germany in the bottom-up energy planning model. The evidence from the study suggest that a direct modelling approach is better for modelling load shifting compared to the indirect method. Considerable insights have been gained with respect to individual DR measures and how it affect the demand with the direct method. The findings shows that DR measures from $Washing\ Appliances$ and $Heat\ Storage$ mapped to the residential and commercial sector demand has the biggest contribution of load shifting in the energy system. The results from the indirect approach suggest that a two and four hour time-step temporal resolution can give a general indication on total system cost reduction from increasing the flexibility in the model. The case studies show that DR can contribute in increasing the system flexibility in the future energy system with high shares of renewable energy.

Contents

List of Figures

List of Tables

List of Acronyms

DR	Demand Response
DSM	Demand Side Management
EF	Energy Efficiency
GHG	Greenhouse Gas
IRES	Intermittent Renewable Energy Sources
OM	Operation and Maintenance
RES	Renewable Energy Sources
VRE	Variable Renewable Energy

1. Introduction

The climate change crisis requires immediate action on a global and national scale to mitigate the Greenhouse Gas (GHG) emissions to keep the temperature below 2°C aligned with the commitment from parties in the Paris Agreement (Climate Change, 2015). The European Union has committed to net-zero greenhouse gas emissions by 2050. To reach this Germany has set a target of 100% share of renewable energy sources by 2050. The power sector contributes approximately 25% of the total GHG emissions in Europe and is therefore an important sector for mitigation of climate change (Misconel et al., 2021). In the next decades the energy system will experience a considerable rise in Renewable Energy Sources (RES) to mitigate GHG emissions and increase in demand to meet the climate change targets. The increase in RES increases the fluctuations in the energy system as the Intermittent Renewable Energy Sources (IRES) is weather dependent and lead to fluctuating electricity generation. To address this issue a more flexibility from the energy system on both supply and demand side is required. The transition towards 2050 is generating considerable interest in terms of how to meet the increasing energy demand with increasingly higher shares of intermittent renewable energy sources. The renewable energy transition is recognised as being an important challenge for global society to mitigate climate change. One of the solutions that is interesting to look at is Demand Side Management (DSM). The main principle of DSM is changing the load shape of the energy demand, with various methods. In the recent years, there has been an increase in studies of different DSM applications and formulations. Demand Response (DR) is one of the DSM classifications showing promising result in increasing the load flexibility. To my knowledge, it has not yet been established a common way to formulate DR in an capacity model. The aim of the thesis is to evaluate different DR formulations in a bottom-up planning graph-based formulation. The thesis describes the implementation of DR in the graph-based framework, following a case study in modelling of DR in a bottom up energy planning model. Optimisation of direct modelling of DR in an energy system can be computationally demanding and time consuming. In addition, energy models representing RES can be difficult and time consuming to model the fluctuations from RES at a detailed level. The question is then how to model the system making it more efficient in computation time but still achieving a reliable operation. Therefore, an evaluation of the trade-off between an indirect method utilising the inherent flexible temporal resolution in the graph-based framework and the direct DR formulation is carried out in a case study representing the German energy system with 100% share of RES. The following sections in the paper is organised as follows: section 2 gives a brief overview of DSM and DR and its benefits is presented, following a review of DR model implementations in the literature. In section 3, the quantitative method of DR modelling is outlined following a presentation of the case study in section 4. Section 5 presents and discusses the result from the case study. Lastly, a conclusion is reached and suggested further research directions is mentioned in section 6.

2. Implementation of Demand Response in energy models

2.1. Role of Demand Side Management and Demand Response

The potential role of DSM remains unclear and has been largely neglected in relation to the transition towards net zero emissions by 2050. In the literature there exist many definitions of DSM, in general terms DSM can be defined as changes to the load shape and/or energy consumption pattern. DSM is a term that captures different ways of changing the energy demand consumption and as such has resulted in many different ways of achieving it. DSM is mainly categorised as either Energy Efficiency (EF) or DR. In addition, DSM can also be categorised into Time of Use and Spinning Reserve however, these have not received much attention in comparison to EF (Palensky and Dietrich, 2011). Major benefits of DSM include the increase in utilization of generation capacity and decrease of the required storage capacity. DSM can help reduce the transmission infrastructure and congestion in the grid (Strbac, 2008). DSM might be of benefit with regards to the power system stability in the grid. By decreasing the frequency fluctuations from Variable Renewable Energy (VRE) generation and at the same time increasing the share of renewable energy DSM can increase the power system stability (Gils, 2014). The two main strategies of DR measures are shifting load to an earlier or later time and load shedding. Considerable work on the theoretical and economical potential of DR has been done by Gils 2014; 2015; 2016. Gils (2014) assess the theoretical potential of DR, including both measures in Europe. It is based on the geographical distribution of consumers in residential, tertiary, and industrial sector in addition to a technological characteristics and load profile analysis. Based on 30 different electricity consumers, Gils finds that the aggregated average theoretical potential is 93 GW for load reduction and 247 GW for load increase in Europe. Gils also stresses the seasonal, geographical and sector variations have on the DR potential. The article highlights the importance of differentiating between theoretical, technical, economic, and practical DR potential and provides an approximate assessment of the theoretical potential in Europe. More specific case studies for a given market or region is needed, investigating the different variables, input data and DR formulation and market barriers hindering its entry and affecting the DR potential. With the predicted increase in shares of RES, DR can assist in balancing fluctuation in the grid, reducing load peaks and flatten the residual load. It would also be beneficial from the energy system point of view to adjust demand accordingly to avoid excessive overcapacity, simultaneously allowing for a higher penetration of RES and potentially decreasing the generation and storage capacity in the power system (Müller and Möst, 2018; Strbac, 2008; Gils, 2016). By adjusting according to the demand by DR measures, it is in essence increasing the flexibility of power system. Consequently, DR could play an important role in an energy system with large shares of intermittent RES, contributing to a more effective market and higher electricity system reliability and security (Müller and Möst, 2018). The remaining part of this section examines formulation of DR in different types of energy models.

2.2. Demand Response in market and dispatch models

2.2.1. BalmoREG, Demand flexibility in a market model

Roos and Bolkesjø (2018) analyze the impact of demand flexibility with regards to the electricity spot market and the reserve market for Germany in 2030 with a high share of VRE. Roos and Bolkesjø developed BalmoREG, a linear bottom-up planning model, the paper formulate energy system under the assumption of competitive markets with the objective of minimizing total costs. Roos and Bolkesjø (2018) assumed that the demand reduction potential is 6% of total demand in Germany. The modelling of demand flexibility was divided into long-term (LT) and short-term (ST) shifting in the electricity spot market. Equation 1 - 7 present the modelling of demand flexibility constraints in the study. Table 1 describes the sets, parameters, and variables used in the DR formulation. The free variables $d_{s,t}^{change\_ST}$ and $d_{s,t}^{change\_LT}$ define the demand flexibility by week s and time segment t. If the sign of the free variables is negative then the variables represent demand reduction, and if it is positive it is demand recovery. The constraints in Eq. 1 and 2 describe the lower bound given by the parameter's technical potential for short and long-term demand reduction ($d_{s,t}^{red\_LT}$ and $d_{s,t}^{red\_ST}$ [%]) multiplied by the electricity demand ($d_{s,t}^{base}$ [MWh]). The demand flexibility is constrained to shifting the load within a day (Eq. 3 and 4), reflecting the day ahead spot market. In addition, the short-term demand flexibility is constrained by a four hour recovery time resolution after demand reduction has occurred (Eq. 5). Lastly, a lower bound is defined for demand flexibility for upregulation in the reserve market in Equation 6 and 7.

$$d_{s,t}^{change\_LT} \geq -d_{s,t}^{base} \cdot d_{s,t}^{red\_LT} \qquad \forall s \in S, t \in T \tag{1}$$

$$d_{s,t}^{change\_ST} \geq -d_{s,t}^{base} \cdot d_{s,t}^{red\_ST} \qquad \forall s \in S, t \in T \tag{2}$$

$$\sum_{t \in DT} d_{s,t}^{change\_LT} = 0 \qquad \forall \text{ d} \in \text{D} \tag{3}$$

$$\sum_{t \in DT} d_{s,t}^{change\_ST} = 0 \qquad \forall d \in D \tag{4}$$

$$\sum_{t \in DT}^{t+H} d_{s,t}^{change\_ST} = 0 \qquad \forall \text{d} \in \text{D, where t + H = 4 hours} \tag{5}$$

$$R_{s,d}^{D} \leq d_{s,t}^{base} \cdot (d_{s,t}^{red\_ST} + d_{s,t}^{red\_LT}) \qquad \forall s \in S, t \in T \tag{6}$$

$$R^{D}_{s,d} \leq d^{base}_{s,t} \cdot (d^{red\_ST}_{s,t} + d^{red\_LT}_{s,t}) + d^{change\_LT}_{s,t} + d^{change\_ST}_{s,t} \qquad \forall d \in D, s \in S, t \in T \quad (7)$$

In addition to the demand flexibility constraints above for the spot and reserve market, demand flexibility is included in the electricity and the reserve balance equation. The results shows that demand flexibility is more beneficial on the reserve market than the spot market with a system of high VRE shares and decreased baseload capacity. Lastly, Roos and Bolkesjø stress the importance of a combined approach analysing the operational and economical sides when evaluating future power systems.

Table 1: Sets, parameters, and variables. Source: Roos and Bolkesjø, 2018

Item	Description	Unit
Sets and indices		
S	Weeks, s = {1,2,...,52}	Hours
T	Time segments, t = {1,2,...,168}	
D	Days in the week, d = {1,2,...,7}	
DT	Subsets of time segments t ∈ T defining hours of the day for each d ∈ D	
Parameters		
$d^{base}_{s,t}$	Electricity demand	MWh
$d^{red\_ST}_{s,t}$	Technical demand reduction potential with a short-term shifting horizon	% demand
$d^{red\_LT}_{s,t}$	Technical demand reduction potential with a long-term shifting horizon	% demand
Variables		
$d^{change\_ST}_{s,t}$	Demand change at time step t due to short-term demand shifting on the spot market	MWh
$d^{change\_LT}_{s,t}$	Demand change at time step t due to long-term demand shifting on the spot market	MWh
$R^{D}_{s,d}$	Upregulation reserve from flexible demand at time step t	MW

2.2.2. Bottom-up electricity market model with time availability and flexibility from Demand Response formulation

In Müller and Möst (2018), the authors investigate the time availability and flexibility of DR in Germany. Based on data from 2013, they quantified the technical potential from the theoretical potential of DR for 2035 and 2050. Then, utilising a bottom-up electricity market model Electricity Transshipment Model (ELTRAMOD), with a DR formulation together with the estimated DR potential, a case study of Germany with different share of VRE at respectively 60%, 80% were investigated. The model's objective were to minimize the cost of generation dispatched. The DR formulation in Müller and Möst (2018) are comprehensive and are presented in Eq. 8 to 20. Table 2 describes the sets, parameters, and variables used. The first two constraints (Eq. 8 and 9) restricts the DR application reducing ($DR^{DOWN}_{t,app}$) and increasing ($DR^{Up}_{t,app}$) the demand in time step t by the current demand

with the app in the DR application set and in the case of $DR^{Up}_{t,app}$, the maximum demand as well. A binary variable $DR^{ON}_{t,app}$ is utilized in Eq. 8, where the value one represent that the demand is reduced in time step t for a given DR application app. Additionally, Eq. 10 assures that the condition is enforced. The constraint Eq. 11 represent the energy balance with a supplier ($S_{p,t,c}$) and demand ($D_{c,t}$) for p in power plant and c in countries, to ensure that there are no changes in the total electricity demand by load shifting from a DR application. Load shifting is represented as a storage unit, since they operate in a similar fashion. This is expressed in Eq. 12; when the load is reduced the "storage unit" is charged, and similarly discharged when the demand is increased. The storage unit has to be zero for the load increase and decrease to be in balance when t is equal to $t^{balance}_{app}$ (Eq. 13). Additional restriction is implemented for DR applications to hinder loss of comfort by restricting the amount of interventions per day. Eq. 14 quantify the maximum quantity of decreased demand by multiplying the maximum number ($\mathbf{f^d}$) and the duration of each intervention ($\mathbf{t^{shed}}$) with the average electricity demand per day. The demand reduction variable ($DR^{DOWN}_{t,app}$) is in addition constrained by the demand and demand reduction in the previous time step to avoid consecutive hours of demand reduction after an intervention, as shown in Eq. 15. The sum of the binary variable $DR^{ON}_{t,app}$ in a given time frame t^{freq}_{app}, has to be less or equal to the time of intervention to further restrict the intervention time (Eq. 17). To describe starting up the load reduction ($DR^{DOWN}_{t,app}$), a binary variable $DR^{SU}_{t,app}$ is implemented. The value of the binary variable is one when $DR^{ON}_{t,app}$ goes from zero to one, otherwise the value is zero. The two last constraints Eq. 19 and 20 further limit the number of interventions, so that DR application can only start up once during the time frame t^{freq}_{app}. Lastly, it is worth noting that the DR formulation does not include cost, which would add further restrictions on the model.

$$DR^{DOWN}_{t,app} \leq dem^{DR}_{t,app} \cdot DR^{ON}_{t,app} \qquad \forall t \in T, app \in DR_{app} \tag{8}$$

$$DR^{UP}_{t,app} \leq dem^{max}_{t,app} - dem^{DR}_{t,app} \qquad \forall t \in T, app \in DR_{app} \tag{9}$$

$$DR^{DOWN}_{t,app} \geq 0,1 \cdot DR^{ON}_{t,app} \qquad \forall t \in T, app \in DR_{app} \tag{10}$$

$$S_{p,t,c} + DR^{DOWN}_{t,app} = DR^{UP}_{t,app} + D_{c,t} \qquad \forall t \in T, app \in DR_{app}, c \in C, p \in P \tag{11}$$

$$DR\_Sl_{t,app} = DR\_Sl_{t-1,app} + (DR^{DOWN}_{t,app})_{t,u} - DR^{UP}_{t,app} \qquad \forall t \in T, app \in DR_{app} \tag{12}$$

$$DR\_Sl_{t,app} = 0 \qquad \forall t \in t_{app}^{balance}, t_{app}^{balance} = \chi_{app} \cdot (t_{app}^{shed} + t_{app}^{shift}) + 1 \chi_{app} \in (0, 1..., f_{app} - 1) \tag{13}$$

$$\sum_{t\_start}^{t_{start}+23} DR_{t,app}^{DOWN} \leq \frac{\sum_{t\_start}^{t_{start}+23} dem_{t,app}^{DR}}{24} \cdot \mathbf{t^{shed}} \cdot \mathbf{f^{d}} \qquad \forall t_{start} = d \cdot 24 + 1, d \in (0, 1, ..., 364) \tag{14}$$

$$DR_{t,app}^{DOWN} \leq dem_{t-1,app}^{DR} - DR_{t-1,app}^{DOWN} \qquad \forall t \in T, app \in DR_{app} \tag{15}$$

$$t_{app}^{freq} = \frac{f_{app}}{8760} \qquad \forall app \in DR_{app} \tag{16}$$

$$\sum_{t\_start2_{app}}^{t\_start2_{app}+t_{app}^{freq}} DR_{t,app}^{ON} \leq t_{app}^{shed} \qquad \forall app \in DR_{app} \tag{17}$$

$$t\_start2_{app} = \chi_{app} \cdot t_{app}^{freq} + 1 \qquad \forall \chi_{app} \in (0, 1, ...f_{app} - 1) \tag{18}$$

$$DR_{t,app}^{SU} - DR_{t,app}^{SD} = DR_{t,app}^{ON} - DR_{t-1,app}^{ON} \qquad \forall t \in T, app \in DR_{app} \tag{19}$$

$$\sum_{t\_start2_{app}}^{t\_start2_{app}+tapp^{freq}} DR_{t,app}^{SU} \leq 1 \qquad \forall app \in DR_{app} \tag{20}$$

The result from the case study by Müller and Möst confirms the application of DR of balancing short-term fluctuations for smoothing the load curve and reducing the RES curtailment with a relative decrease of 26%. The results demonstrate that in periods of low RES feed-in or during peak loads the DR applications cannot always apply the maximum load reduction due to external variables. In addition, Müller and Möst stresses that the potential of DR potential will change as a result of market penetration thus changing the availability of DR. They conclude that further studies should focus on specific DR measures to minimize cost of the energy system in an efficient way.

Table 2: Sets, parameters, and variables. Source: Müller and Möst (2018)

Item	Description
Sets and indices	
app	DR application $app \in DR_{app}$
p	Power plant $p \in P$
t	Time step $t \in T$
c	Country $c \in C$
Parameters	
D	Electricity demand (of an country)
dem^{DR}	Electricity demand of an DR application
dem^{max}	Maximum demand of an DR application (equals its installed capacity)
f	Maximum numbers of interventions per year
f^{d}	Maximum numbers of interventions per day
$t^{balance}$	Time frame within the increased and decreased demand of an DR application needs to be balanced
t^{freq}	Time frame between interventions
t^{shed}	Maximum time for reducing electricity demand of an DR application
t^{shift}	Maximum shifting time of an DR application
Variables	
S	Supply (generation of all power plants)
DR^{DOWN}	Reduced electricity demand of an DR application
DR^{ON}	Binary Variable which is one, when the load of an DR is decreased
DR^{SU}	Binary Variable for starting up the load decrease
DR^{UP}	Increased electricity demand of an DR application
DR^{SL}	Virtual storage of an DR application for modelling load shifting

2.2.3. Bottom-up electricity market model with Demand Response in a centralized and decentralized European energy system

In Misconel et al. (2021), the authors question how DR can contribute in a decentralized and centralized European energy system with 100% renewable energy. The decentralized scenario has a higher share of PV rooftop capacity and the centralized scenario has a higher share of wind offshore capacity. They utilize the same optimization model as Müller and Möst (2018), ELTRAMOD, however the DR representation in the model differs. In contrast to other studies where shifting time and intervention time are investigated, Misconel et al. account for these technological constraint implicitly in the hourly DR potentials. The constraints described in Eq. 21 to 24 present the DR formulation added to the optimization model. Table 3 describes the sets, parameters, and variables used in the DR formulation. The variable $DR_{t,c}^{OPT}$ describes the optimal dispatch of DR for a given hour. It is constrained by the exogenously defined maximum increase and decrease of DR potential ($dr_{t,c}^{MAX}$, $dr_{t,c}^{MIN}$) in respectively Eq. 21 and 22, thus limiting the activation of DR. The total load increase is constrained to equal the load reduction, so the total demand remains unchanged (Eq. 23). Lastly, the optimized residual load ($RESDEM_{t,c}^{OPT}$) is defined as the subtraction of the unsmoothed residual load with the optimal DR dispatch, as shown in Eq. 24. Contrary to Müller and Möst (2018), Misconel et al. (2021) include activation cost of DR measures for a given country. The changes from the DR formulation in the

objective function and the energy balance is mentioned but not explicitly described.

$$DR_{t,c}^{OPT} \leq dr_{t,c}^{MAX} \cdot dr^{SHARE} \qquad \forall t \in T, c \in C \tag{21}$$

$$DR_{t,c}^{OPT} \geq dr_{t,c}^{MIN} \cdot dr^{SHARE} \qquad \forall t \in T, c \in C \tag{22}$$

$$\sum_{t=1}^{T} DR_{t,c}^{OPT} = 0 \qquad \forall t \in T, c \in C \tag{23}$$

$$RESDEM_{t,c}^{OPT} = resdem_{t,c} - DR_{t,c}^{OPT} \qquad \forall t \in T, c \in C \tag{24}$$

The outcome from the decentralized and centralized scenario, shows that DR implementation leads to a reduction of total system costs and CO_2 emission. The results show that a larger share of the DR potential is utilized in the decentralized scenario compared to the centralized scenario. The larger share results in a higher effect on smoothing the residual load per DR unit dispatched and as a result the RES curtailment is reduced. Their findings would seem to suggest that the feed-in pattern of PV corresponds better to the load shifting temporal pattern compared to wind.

Table 3: Sets, parameters, and variables. Source: Misconel et al., 2021

Item	Description
Sets and indices	
t ∈ T	Hour of a year
c ∈ C	Country of considered geographical scale (EU-27, United Kingdom, Norway, Switzerland, Balkan countries)
Parameters	
$dr_{t,c}^{MAX}$	Maximum positive hourly demand response potential (for residual load reduction)
$dr_{t,c}^{MIN}$	Minimum negative hourly demand response potential (for residual load increase)
dr^{SHARE}	Share of activated demand response potential
$resdem_{t,c}$	Residual load (unsmoothed)
Variables	
$DR_{t,c}^{OPT}$	Optimal hourly dispatch of demand response
$RESDEM_{t,c}^{OPT}$	Optimized residual load (smoothed)

2.2.4. Demand Response in a European power dispatch model

Göransson et al. (2014) investigates the role of DSM in reducing congestion in a case study of the European transmission grid for 2020 with a 17% share of renewable energy. In the paper, DSM is defined as DR load shifting, excluding load shedding. The European POwer Dispatch (EPOD), is a linear cost minimizing, short-term dispatch model, with the DC load flow formulation of the transmission system was utilized along with the load shifting formulation described in Eq. 25 to 27

below. Table 4 describes the sets, parameters, and variables used for formulating load shifting. The formulation is straightforward and minimal, where the two first constraints limit the time interval given by the delay time L, the demand put on hold ($dh_{i,t}$) must be balanced for i in regions and t in a time period. The formulation does not allow for an upward load shift before an amount of demand is put on hold. Demand put on hold is in Eq. 25 constrained by the sum of delayed demand ($dd_{i,t}$), and served demand ($ds_{i,t}$) in Eq. 26. Lastly Eq. 27 is the balance equation for demand put on hold. Other limits are mentioned in the article however not explicitly written. DR costs are not included in the analysis since the goal was to analyze how DR influences congestion in the European transmission system.

$$dh_{i,t} \leq \sum_{l=0}^{L-1} dd_{i,t-l} \qquad \forall i \in I, t \in T \tag{25}$$

$$dh_{i,t} \leq \sum_{l=1}^{L} ds_{i,t+l} \qquad \forall i \in I, t \in T \tag{26}$$

$$dh_{i,t} = dh_{i,t-1} + dd_{i,t} - ds_{i,t} \qquad \forall i \in I, t \in T \tag{27}$$

Table 4: Sets, parameters, and variables. Source: Göransson et al., 2014

Item	Description	Unit
Sets and indices		
i ∈ I	Regions	
t ∈ T	Time periods	Hours
Parameter		
L	Delay time	Hours
Variables		
$dh_{i,t}$	Hourly demand delayed	MWh
$dd_{i,t}$	Cumulative hourly demand put on hold	MWh
$ds_{i,t}$	Hourly demand served	MWh

The scenario results show that load shifting reduces the yearly transmission congestion. Göransson et al. reveal three types of congestion peak-load-hour congestion, low-load-hour congestion and all-hour congestion, where load shifting affects mainly the peak-load-hour congestion. However, the results show that reduction of congestion due to DR are highly dependent on the structure of the transmission system. Thus, when planning future expansion of the transmission grid it is important to consider load shifting on the specific connection as the impact of DR differs significantly in the network (Göransson et al., 2014).

2.3. Demand Response in bottom-up planning models

2.3.1. Energy system model Renewable Energy Mix for Sustainable Electricity Supply (REMix) with a Demand Response formulation

Gils (2016) introduce another representation for DR in a deterministic linear optimization model (REMix). The paper assesses the DR economical potential in a case study of Germany, based on the theoretical potential for Europe found in Gils (2014). The case study includes seven groups of DR technologies. The groups implemented in the case study contains in a total of 30 DR technologies with individual time shift parameter. The DR technologies are sector integrated to the industrial, commercial and residential loads. The DR modelling is adapted to fit REMix model, all equations for DR are outlined and is presented in Eq. 28 to 37. Table 5 describes the sets, parameters, and variables used to formulate load shifting. Similar to recent studies, the approach to model DR was to formulate it as a storage technology with specific constraints to emulate their definition of DR. Investment in DR capacity is constrained by the maximum available capacity potential (Eq. 28). To model load shifting, load shedding and balancing of load, four variables are introduced: $\mathbf{P}^{red}(t)$, $\mathbf{P}^{balRed}(t)$, $\mathbf{P}^{inc}(t)$, $\mathbf{P}^{balInc}(t)$ for time-step t. The balancing variables ensures that the shifted load is met after the time shift (t_{shift}), and that there are no changes to the total demand as shown in Eq. 29 and 30. Except in the case of load shedding (Eq. 31). Upper limits of load increase and decrease is described in respectively Eq. 32 and 33 and is calculated by the total installed DR capacity multiplied with a normalized hourly time series ($s_x^{free}(t)$, $s_x^{flex}(t)$) to capture the variation in DR potential.

$$P_x^{exCap} + \mathbf{P}_x^{adCap} \overset{!}{\leq} P_x^{maxCap} \qquad \forall x \in X \tag{28}$$

$$\mathbf{P}_h^{balRed}(t) \overset{!}{=} \frac{\mathbf{P}_h^{red}(t - t_h^{shift})}{\eta_h^{DR}} \qquad \forall h \in H \tag{29}$$

$$\mathbf{P}_h^{balInc}(t) \overset{!}{=} \mathbf{P}_h^{Inc}(t - t_h^{shift})\eta_h^{DR} \qquad \forall h \in H \tag{30}$$

$$\mathbf{P}_h^{balInc}(t) \overset{!}{=} 0 \qquad \forall h \in H \tag{31}$$

$$\sum_{H \to X} \mathbf{P}_h^{red}(t) + \mathbf{P}_h^{balInc}(t) \overset{!}{\leq} (P_x^{exCap} + \mathbf{P}_x^{adCap}) s_x^{flex}(t) \qquad \forall h \in H, x \in X \tag{32}$$

$$\sum_{H \to X} \mathbf{P}_h^{inc}(t) + \mathbf{P}_h^{balRed}(t) \overset{!}{\leq} (P_x^{exCap} + \mathbf{P}_x^{adCap}) s_x^{free}(t) \qquad \forall h \in H, x \in X \tag{33}$$

The storage level $\mathbf{W}^{levRed}(t)$ and $\mathbf{W}^{levInc}(t)$ represent respectively the reduced and increased load that will be balanced at a given time step t and the load shifted (Eq. 34, 35). The storage levels

upper bound for load shifted and unbalanced load is described in Eq. 36, 37. The limit is based on the maximum load change duration ($t_x^{interfere}$), the average load increase ($\overline{s}_x^{free}$) and load decrease ($\overline{s}_x^{flex}$) potential relative to installed capacity multiplied with the available DR load.

$$\sum_{H \to X} (\mathbf{P}_h^{red}(t) + \mathbf{P}_h^{balRed}(t) \cdot \eta_h^{DR}) \overset{!}{=} \mathbf{W}_x^{levRed}(t) - \mathbf{W}_x^{levRed}(t-1) \qquad \forall h \in H, x \in X \qquad (34)$$

$$\sum_{H \to X} (\mathbf{P}_h^{inc}(t) \cdot \eta_h^{DR} + \mathbf{P}_h^{balInc}(t)) \overset{!}{=} \mathbf{W}_x^{levInc}(t) - \mathbf{W}_x^{levInc}(t-1) \qquad \forall h \in H, x \in X \qquad (35)$$

$$\mathbf{W}_x^{levRed}(t) \overset{!}{\leq} (P_x^{exCap} + \mathbf{P}_x^{adCap}) \cdot \overline{s}_x^{flex} + t_x^{interfere} \qquad \forall x \in X \qquad (36)$$

$$\mathbf{W}_x^{levInc}(t) \overset{!}{\leq} (P_x^{exCap} + \mathbf{P}_x^{adCap}) \cdot \overline{s}_x^{free} + t_x^{interfere} \qquad \forall x \in X \qquad (37)$$

Constraints regarding the number of times and amount of energy shifted or shedded, are imposed and expressed in two ways: a yearly limit of DR interventions and a recovery time between two interventions in a day (Eq. 38, 39). The equations are expressed for load reduction, equivalent constraints for load increase are found by switching $\mathbf{P}^{red}$ with $\mathbf{P}^{inc}$ and s_{flex}^X with s_{free}^X. Finally, Eq. 40 to 42 describes the DR investment cost and operation cost from the supply and use of flexible loads in the model.

$$\sum_t \sum_{H \to X} \mathbf{P}_h^{red}(t) \overset{!}{\leq} (P_x^{exCap} + \mathbf{P}_x^{adCap}) \cdot \overline{s}_x^{flex}(t) \cdot t_x^{interfere} \cdot n_x^{yearLim} \qquad \forall h \in H, x \in X \qquad (38)$$

$$\sum_{H \to X} \mathbf{P}_h^{red}(t) \overset{!}{\leq} (P_x^{exCap} + \mathbf{P}_x^{adCap}) \cdot \overline{s}_x^{flex}(t) \cdot t_x^{interfere} - \sum_{t'=1}^{t'=t_x^{dayLim}} \sum_{H \to X} \mathbf{P}_h^{red}(t-t') \qquad \forall h \in H, x \in X \qquad (39)$$

$$\mathbf{C}_{invest} = \sum_X \mathbf{P}_x^{adCap} \cdot c_x^{specInv} \cdot f_x^{annuity} \qquad \forall x \in X \qquad (40)$$

$$f_x^{annuity} = \frac{i \cdot (1+i)^{t_x^{amort}}}{(1+i)^{t_x^{amort}} - 1} \qquad \forall x \in X \qquad (41)$$

$$\mathbf{C}_{op} = \sum_{X} \sum_{H \to X} \sum_{t} (\mathbf{P}_h^{red}(t) + \mathbf{P}_h^{inc}(t)) \cdot c_x^{OMVar} + \sum_{X} \mathbf{P}_x^{adCap} \cdot c_x^{specInv} \cdot c_x^{omFix} \qquad \forall h \in H, x \in X \tag{42}$$

Table 5: Sets, parameters, and variables. Source: Gils, 2016

Item	Description	Unit
Sets and indices		
x	DR technology $x \in X$	
t	Time-step $t \in T$	h
h	Shifting classes $h \in H$	
Parameters		
t_h^{shift}	DR shifting time (maximum duration until balancing)	h
η_h^{DR}	DR efficiency	$\frac{1}{100}$
$t_x^{interfere}$	DR interference time (maximum duration of load change)	h
$t_x^{dayLimit}$	Waiting time between two DR interventions	h
$n_x^{yearLimit}$	Annual limit of DR interventions	$\frac{1}{a}$
P_x^{exCap}	Installed capacity of all appliances in DR technology X	GW^{el}
P_x^{maxCap}	Maximum installable capacity of appliances in DR technology X	GW^{el}
$s_x^{flex}(t)$	Maximum load reduction relative to installed capacity	GW^{el}
$s_x^{free}(t)$	Maximum load increase relative to installed capacity	GW^{el}
$\overline{s}_x^{flex}$	Average load reduction potential relative to installed capacity	GW^{el}
$\overline{s}_x^{free}$	Average load increase potential relative to installed capacity	GW^{el}
$c_x^{specInv}$	Specific investment cost	k€/MW
c_x^{OMFix}	Operation and maintenance fix costs	%/year
c_x^{OMVar}	Operation and maintenance variable costs	$k/eMWh$
t_x^{amort}	Amortization time	years
i	Interest rate	%
$f_x^{annuity}$	Annuity factor	–
Variables		
$\mathbf{P}_h^{red}(t)$	Demand Response load reduction in shift class H	GW^{el}
$\mathbf{P}_h^{inc}(t)$	Demand Response load increase in shift class H	GW^{el}
$\mathbf{P}^{balRed}(t)$	Balancing of earlier load reduction in shift class H	GW^{el}
$\mathbf{P}^{balInc}(t)$	Balancing of earlier load increase in shift class H	GW^{el}
$\mathbf{W}_x^{levRed}(t)$	Amount of reduced and not yet balanced energy of technology X	GWh_{el}
$\mathbf{W}_x^{levInc}(t)$	Amount of increased and not yet balanced energy of technology X	GWh_{el}
P_x^{adCap}	Installed electric capacity of additionally DR consumers	GW^{el}
C^{invest}	Investment costs	k€/a
C^{op}	Operation and maintenance costs	k€/a

The case study finds that the DR load shifts corresponds with the residual peak load, which confirms previous findings observed in literature. The residential sector have a low utilization of the DR potential except for storage water heaters, in comparison to the industrial and commercial sector. This is attributed to the DR parameters regarding consumer participation, investment cost and operation hours. A key factor of the general DR capacity implementation in the energy system is the investment cost rather than the temporal availability potentials. Interestingly, Gils indicates

that DR implementation does not relate to a higher VRE integration on the generation capacity but rather to the application of residual load reduction. Sensitivities analysis on cost, DR frequency, DR potential and load shifting time show that yearly shifted and shedded energy ranges from 0.3 to 4.1 TWh which is less than 1% of the total yearly demand. Gils concludes that it is the provision of power DR measures should aim at, not provision of energy.

2.3.2. EMPIRE, power system capacity expansion model with Demand Response

Marañón-Ledesma and Tomasgard (2019) implemented a DR extension and analyzed DR in the European Power Market in a dynamic capacity expansion model (EMPIRE). EMPIRE is a multi-horizon stochastic model, with the object of minimizing total costs for optimal investment of capacity and transmission expansion in the electricity sector. Marañón-Ledesma and Tomasgard introduce a DR extension of EMPIRE formulating three DR measures: shiftable volume loads, curtailable loads and interruptible loads, based on a common formulation of flexible loads with additional constraints for the respective measures. The flexible load can change the hourly load profile with upward or downward regulation. The shiftable volume loads is load regulation of to the hourly load profile like flexible load, however the total energy cannot be changed and the load regulated has to be balanced. The curtailable load decreases the hourly load profile without balancing it at a later point. Finally an interruptible load is a curtailable load that is able to decrease the load to zero, otherwise it is left unmodified (Marañón-Ledesma and Tomasgard, 2019). The DR formulation by Marañón-Ledesma and Tomasgard is described in Eq. 21 to 24. To formulate the flexible loads, new variables, parameters, sets and constraints are introduced in the extension. Table 6 describes the sets, parameters, and variables used in the extension. Variables $y^{REG}_{fi\omega h}$, $y^{LOSS}_{fi\omega h}$ and $y^{DRCAP}_{fi\omega h}$ represent the load deviation, load loss and the potential flexible load for a flexible load f.

The DR available capacity also called the potential load, is the flexible load that can be utilized for DR measures and is defined by the installed DR capacity (v^{DR}_{fi}) and two scaling factors (α_{fih}, $\frac{\zeta^{load}_{ni\omega h}}{\hat{\zeta}_{ni\omega}}$) (Eq. 43). The realised DR load is given by the potential downward regulation and the DR load deviation (Eq. 44). The resulting load cannot be a negative value (Eq. 31). When $y^{REG}_{fi\omega h'}$ is equal to zero the load is unregulated, if $y^{REG}_{fi\omega h'}$ is larger than zero it is shifted upwards and if $y^{REG}_{fi\omega h'}$ is less than zero it is downward regulated. When shifting or curtailing the load profile, there are energy losses during the act that needs to be covered, thus increasing the energy demand. The energy loss, or rather the additional energy demand for flexible loads are given in Eq. 46. Furthermore, the upward regulation is constrained by an upper bound $U^{DR}_{fi\omega h}$ (Eq. 48), which is mathematically described in detail in the article. By restricting the up-regulation, the upper bound limit the load shifting in an effort to increase valley filling during peak hours.

$$y^{DRCAP}_{fi\omega h} = \alpha_{fih} \cdot \frac{\zeta^{load}_{ni\omega h}}{\hat{\zeta}_{ni\omega}} \cdot v^{DR}_{fi} \qquad \forall f \in F_n, i \in I, \omega \in \Omega_i, h \in H \tag{43}$$

$$y_{fi\omega h}^{DR} = y_{fi\omega h}^{DRCAP} + y_{fi\omega h'}^{REG} \qquad \forall f \in F_n, i \in I, \omega \in \Omega_i, h \in H \tag{44}$$

$$y_{fi\omega h}^{DR} \geq 0 \qquad \forall f \in F_n, i \in I, \omega \in \Omega_i, h \in H \tag{45}$$

$$y_{fi\omega h}^{loss} = \beta |y_{fi\omega h}^{DR}| \left(\frac{1 - \eta_f^{DR}}{\eta_f^{DR}} \right) \qquad \forall f \in F_n, i \in I, \omega \in \Omega_i, h \in H, n \in N \tag{46}$$

$$\beta_f := \begin{cases} 0.5 & f \in S \\ 1 & f \in C \end{cases} \tag{47}$$

$$y_{fi\omega h}^{DR} \leq U_{fi\omega h}^{DR} \qquad \forall f \in F_n, i \in I, \omega \in \Omega_i, h \in H \tag{48}$$

The constraints in Eq. 43 - 48 form the general description of a flexible load and applies to all DR measures. In addition to these constraint, Eq. 49 and 50 gives the formal description of a shiftable load. Equation 49 and 50 states that the upward or downward regulation has to be compensated at another time, so the total energy demand remain unchanged. The time-frame for when a load shifting can occur, is defined by $\{W_{fj}\}_{j \in J}$ in Eq. 49. Unlike shiftable loads, the curtailable loads decrease the total energy demand since curtailable load can only decrease the load (Eq. 51 - 53). The interruptible loads reduces the demand to zero, as shown in Eq. 54 and 55. Lastly, the sum of load deviation and losses from flexible loads ($\sum_{f \in F_n} y_{fi\omega h}^{REG} + y_{fi\omega h}^{loss}$) are added to the energy balance equation (Eq. 56).

$$\sum_{h \in W_{fj}} y_{fi\omega h}^{DR} = \sum_{h \in W_{fj}} y_{fi\omega h}^{DRCAP} \qquad \forall j \in J, f \in F, i \in I, \omega \in \Omega_i, \tag{49}$$

$$y_{fi\omega h}^{DR} = y_{fi\omega h}^{DRCAP} \qquad \forall f \in F, i \in I, \omega \in \Omega_i, h \in H \backslash (T_{f1}, T_{fN}) \tag{50}$$

$$y_{fi\omega h}^{DR} \leq y_{fi\omega h}^{DRCAP} \qquad \forall f \in F, i \in I, \omega \in \Omega_i, h \in (T_{f1}, T_{fN}) \tag{51}$$

$$y_{fi\omega h}^{DR} = y_{fi\omega h}^{DRCAP} \qquad \forall f \in F, i \in I, \omega \in \Omega_i, h \in H \backslash (T_{f1}, T_{fN}) \tag{52}$$

$$y_{fi\omega h}^{DR} \geq 0 \qquad \forall \omega \in \Omega, i \in I, f \in C \tag{53}$$

$$y_{fi\omega h}^{DR} = \delta \cdot y_{fi\omega h}^{DRCAP} \qquad \forall h \in (T_{f1}, T_{fN}) \omega \in \Omega, i \in I, f \in C \tag{54}$$

$$\delta \in \{0,1\} \qquad \omega \in \Omega, i \in I, f \in C \tag{55}$$

$$\begin{aligned}\sum_{g\in G_n} y^{gen}_{gi\omega h} + \sum_{b\in B_n} \eta^{dischrge}_{b} y^{dischrge}_{bi\omega h} - y^{chrge}_{bi\omega h} + \sum_{a\in A^{in}_n} \eta^{tran}_{a} y^{flow}_{ai\omega h} - \sum_{a\in A^{out}_n} y^{flow}_{ai\omega h} \\ = \zeta^{load}_{ni\omega h} + \sum_{f\in F_n} y^{REG}_{fi\omega h} + y^{LOSS}_{fi\omega h} - y^{ll}_{ni\omega h} \qquad n \in N, h \in H, \omega \in \Omega, i \in I\end{aligned} \tag{56}$$

The flexible load capacity constrains are outlined in Eq. 57 - 60. The maximum of DR capacity investment (X^{DR}_{fi}) restricts the capacity investment (57). The correlation between aggregated DR capacity and the capacity investment is described in 58, and depends on the operational life of the flexible load investment. The aggregated DR capacity of a flexible load (v^{DR}_{fi}) is bound by the maximum DR capacity as stated in Eq. 59. The changes brought by the DR formulation cause an extension of the objective function to incorporate the flexible loads investment and operation cost. It is important to remark that any changes of the original load due to a flexible load is penalised by a cost, regardless if it is upward or downward regulation (Marañón-Ledesma and Tomasgard, 2019).

$$x^{DR}_{fi} \leq X^{DR}_{fi} \qquad \forall f \in F, i \in I \tag{57}$$

$$v^{DR}_{fi} = v^{DR}_{f0} \cdot \chi(DRL - i) + \sum_{j=0, j<i}^{DRL} x^{DR}_{fi-j'} \qquad \forall f \in F, i \in I \tag{58}$$

$$v^{DR}_{fi} \leq Y^{DR}_{fi} \qquad i \in I, f \in S \cup C \tag{59}$$

$$\chi(x) = \begin{cases} 0 & x \leq 0 \\ 1 & x > 0 \end{cases} \tag{60}$$

Most of the DR input data in the cases study is based on Gils (2014), Gils (2015), Gils (2016). It analyzes seven types of electricity consumers: Heating and AC, HVAC, Cooling and water, Process shift, Washing appliances, Heat storage, and Process shedding that is applicable as DR technologies. According to Marañón-Ledesma and Tomasgard (2019), Heat storage final demand users is the most significant group for load shifting, Heat storage also have very flexible time-frames. The results show that the countries with the highest share of IRES also have the highest amount of DR investment as it provides an efficient way to manoeuvre intermittent energy. In addition, a correlation between the countries with the highest share of solar capacity in Europe is the ones with most installed DR capacities is found.

Table 6: Sets, parameters, and variables. Source: Marañón-Ledesma and Tomasgard, 2019

Item	Description
Sets and indices	
$f \in F = \mathrm{S} \cup \mathrm{C}$	Index and set of flexible loads
$f \in F_n$	Set of flexible loads that belong to node n
$f \in S$	Set of shiftable loads
$f \in C$	Set of curtailable loads
$i \in I$	Set of long-term periods where investments take place
$\omega \in \Omega_i$	Set of operational scenarios in long-term period
$h \in H$	Set of hours in each operational scenario
$j \in J$	Set of hours where a load can be shifted in time window $\{W_{fj}\}_{j \in J}$
Parameters	
c_{fi}^{DR}	DR investment cost
q_{fp}^{REG}	DR operational cost
α_{fih}	DR load profile
X_{fi}^{DR}	Maximum DR capacity investment
$U_{fi\omega h}^{DR}$	Maximum upward regulation of group f
Y_{fi}^{DR}	Maximum DR capacity of group f
t_f^{shift}	Maximum load time shift of group f
η_f^{DR}	Efficiency of flexible load f
Q_{fi}^{REG}	DR baseline operational costs
m_{REG}	DR operational cost scaling factor
μ_{fp}^{REG}	Special Ordered Set of type 2 intervals
DRL	Operational life a DR investment
Variables	
x_{fi}^{DR}	DR capacity investment of group f in period i
x_{gi}^{gen}	Capacity investment of generator type g in period i
v_{fi}^{DR}	Aggregated DR capacity of group f
v_{gi}^{gen}	Aggregated capacity of generator type g
$y_{fi\omega ph}^{DR}$	Actual DR load of group f
$y_{fi\omega ph}^{DRCAP}$	Potential downward regulation of group f
$y_{fi\omega ph}^{REG}$	DR load deviation
$\lambda_{fi\omega ph}^{REG}$	Special Order Set 2 DR regulation variables

2.3.3. DIETER Zerrahn

Zerrahn and Schill (2015) present a novel DSM formulation based on the work of Göransson et al. (2014). Like Göransson et al., DSM is meant as DR load shifting in the paper. The formulation was then implemented in the Dispatch and Investment Evaluation Tool with Endogenous Renewables model (DIETER) described in Zerrahn and Schill (2017). A companion paper (Schill and Zerrahn, 2018), analyzed the role of storage and DR with high shares for VRE in a greenfield system of Germany. Equation 61 to 65 present the constraints formulating the DR, and the sets, parameters, and variables is described in Table 7. The formulation introduces two variables for upward (DSM_t^{up}) and downward ($DSM_{t,tt}^{do}$) shifting of load for a given time t. The constraint Eq. 61 guarantees that the upward load shift in a given time t is compensated by the sum of downward shifted demand within a time interval surrounding time t. The downward variable has two time indices (t, tt) to

reflect downward shift in time tt from the upward shift in t. Thus, the downward shift can occur both before and after an upward load shift. The upward and downward variable is constrained by the installed capacity parameter for hourly upward and downward load shifts (C^{up}, C^{do}) in Eq. 62 and 63. Furthermore, Eq. 64 ensure that the maximum capacity is not used for both upward and downward shift simultaneously. Finally, Zerrahn and Schill introduces a constraint (Eq. 65) covering a recovery time to hinder unrestrained use of load shifting.

$$DSM_t^{up}\eta = \sum_{tt=t-L}^{t+L} DSM_{t,tt}^{do} \quad \forall t \in T \tag{61}$$

$$DSM_t^{up} \leq C^{up} \quad \forall t \in T \tag{62}$$

$$\sum_{t=tt-L}^{tt+L} DSM_{t,tt}^{do} \leq C^{do} \quad \forall tt \in T \tag{63}$$

$$DSM_{tt}^{up} + \sum_{t=tt-L}^{tt+L} DSM_{t,tt}^{do} \leq \max(C^{up}, C^{do}) \quad \forall tt \in T \tag{64}$$

$$\sum_{tt=t}^{t+R-1} DSM_{tt}^{up} \leq C^{up} \cdot L \quad \forall t \in T \tag{65}$$

Table 7: Sets, parameters, and variables. Source: Zerrahn and Schill, 2015

Item	Description	Unit
Sets and indices		
$t, tt \in T$	Time periods	Hours
Parameters		
C^{up}	Installed capacity for hourly downward shifts	MWh
C^{do}	Installed capacity for hourly upward shifts	MWh
η	Efficiency	
L	Delay time	Hours
R	Recovery time	Hours
Variables		
$DSM_{t,tt}^{do}$	Hourly downward load shifts for hour t in hour tt	MWh
DSM_t^{up}	Hourly upward load shifts	MWh

The findings in the article by Schill and Zerrahn (2018), shows that the role of storage and flexibility in an energy system with a high share of VRE is crucial. When comparing the result from the two cases with a share of 80% and 100% VRE, the requirement for storage and flexibility increases from 12 GW to 34 GW, resulting in a factor of 2.83 increase in storage capacity. A sensitivity analysis on the cost and availability of storage and RES, find that the storage demand depend heavily on the cost and availability on flexible storage options for an energy system with high shares of RES. Their

findings confirm the importance of load shifting and load curtailment, as it is found to be dominant options to meet the storage requirement. This underlines how important the role of DR is in a future 100% renewable energy system.

3. Qualitative Method of Demand Response modelling

In order to investigate DR formulation based on the previous analysis, two modelling methods of DR were investigated in a bottom-up planning graph-based formulation. The first method is based upon the temporal resolution in the graph-based formulation. While the second method is an DR extension in the graph-based framework based on the DR formulation by Zerrahn and Schill. It was decided that the best procedure for the study was to investigate the two DR modelling methods of DR in graph-based framework to evaluate the impact the DR extension have. More details on the methods will be given in the following subsections. The graph-based formulation for bottom-up planning model was implemented in the AnyMOD.jl framework, and a detailed mathematical equations of the framework is described in Göke (2021). It is an open-source bottom-up energy planning model, implemented with Julia Language and available on GitHub. The graph-based formulation allows for a short-term and long-term modelling horizon, sector integration of energy carriers and multiple capacity expansion periods.

3.1. Indirect representation of Demand Response in graph-based formulation

The temporal resolution in the graph-based formulation is modelled as a rooted hierarchical three, and a reduced form of two ways the time-steps can be modelled shown in Figure 1 and 2. The vertices depth in the threes represent how the time-step are ordered in the model. The figures differs in how the two last vertices are defined. The last vertices depth represent the hourly steps in two-hour (Fig. 1) and four-hour (Fig. 2) time-steps. The hierarchy three is also analogous to the way regions and energy carriers are modelled in the framework. An expansion would usually have a yearly resolution, whereas the dispatch depends on the energy carrier temporal resolution. The indirect method splits the time-steps defined in the day vertices into hourly groups in the hierarchical three, since it is the hourly time-steps in a day that is relevant for DR modelling.

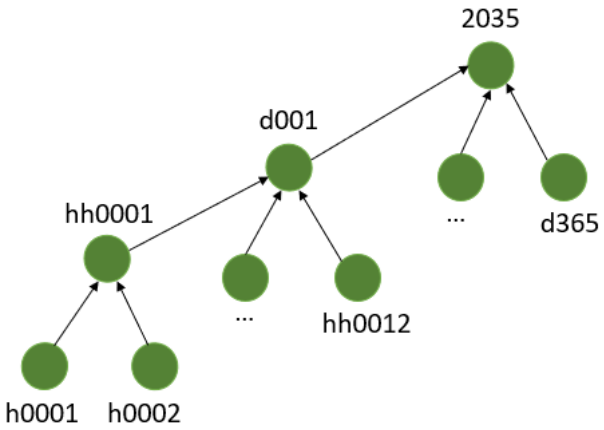

Figure 1: Rooted hierarchical tree with a two-hour time-steps

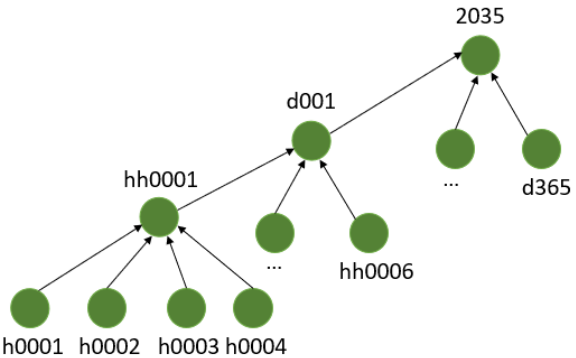

Figure 2: Rooted hierarchical tree with a four-hour time-steps

By exploiting the framework of how time-steps and energy carriers are organised, it allows for a practical way to model DR in the energy system without any changes to the graph-based formulation.

In order to do that, the demand time series are modelled as energy carriers within the model. In addition, "dummy technologies" was added to map the actual energy carriers to the "demand carrier". The "demand carriers" can then be defined as an hierarchical three and the subdivided demands then share a common ancestor. This allows for easy changes of the time-step vertices for dispatch and expansion for "demand carriers". Thus, a subdivided "demand carrier" can then change from a hourly resolution to for example four-hour time-steps temporal resolution. The larger hourly time-step granularity allows the model to optimise with more freedom within the temporal resolution. It is anticipated that the higher flexibility will reduce the system cost, and the cost reduction can then be described as the economic value of the flexibility. By adjusting graph-based formulation specific time-step granularity for "demand carriers", the temporal resolution can then be used as indirect method of representing DR in the graph-based formulation.

3.2. Direct representation of Demand Response in graph-based formulation

This section describes the method and changes to the DR formulation implemented into the graph-based formulation. The formulation is based on Zerrahn and Schill (2015) described in the previous section 2.3.3, who present a DR representation based on the Göransson et al. (2014) formulation. Some alteration of the formulation was carried out to implement it in the graph-based formulation. Various approaches of formulating DR have model it as a short term storage technology, based on the resemblance to storage technologies. The energy in to the storage technology is equivalent to load increase, and energy out is equivalent to the load reduction. The load shifting formulation by Zerrahn and Schill (2015) was therefore implemented as a storage technology in the graph-based formulation. This enables the use of existing parameters, variables, and constraints in the graph-based formulation for the DR formulation. Additional parameters and variables was necessary for formulate the new DR constraints. The constraints implemented in the graph-based formulation is described in Eq 66 to 70, and Table 8 describes the sets, parameters, and variables. Two new parameters are added, labelled $drTime$ and $drRecoveryTime$ and represent respectively the parameter L and R in the Zerrahn and Schill formulation. The $drTime$ parameter differentiate the DR technologies from the other storage technologies and ensure that the DR constraints are not enforced on the other storage technologies. If $drRecoveryTime$ is not given by the input data, its default value is none and the recovery constraint (Eq. 70) is not enforced. The DR the graph-based framework existing parameter $effStIn$ describes the efficiency for energy in and is utilised as the efficiency parameter η for upward load shift in Zerrahn and Schill Eq. 61 (See Eq. 66). The default value for $effStIn$ is 1 if no value is given in the input data. The efficiency parameter can be used to describe losses or rebound effects from upward load shifting. Since DR is implemented as a storage technology, it uses the existing $costExpStIn$ for investment cost [M€/GW], $costOprStIn$ for fixed Operation and Maintenance (OM) cost [Mil.€/GWh/a], and $costVarStIn$ for variable OM costs [€/MWh] parameters in the framework to affect objective function. Consequently no changes of the objective function is necessary. Next,

a description of how the two variables DSM_t^{up} and $DSM_{t,tt}^{do}$ was implemented in the graph-based formulation from Zerrahn and Schill DR formulation. The variable DSM_t^{up} reuses the existing variable $stExtIn$ for storage technologies in the bottom-up planning model. However the variable $DSM_{t,tt}^{do}$ require a new variable due to the additional time-step index and therefore cannot use the existing definition of the $stExtOut$ variable in the graph-based framework. As a consequence, $stExtOut$ is redefined as $\sum_{t=tt+L}^{tt+L} DSM_{t,tt}^{do}$, so that the storage constraint formulation reflect the DR load shifting behaviour. The main modification from the Zerrahn and Schill formulation is due to the parameter C^{up} and C^{do}, the parameters is changed to variables to align with the capacity expansion modelling in the graph-based formulation. The parameters C^{up} and C^{do} utilise the existing variables: $capaStIn$ and $capaStOut$. Constraint 69, is changed from an upper bound of the highest value of either parameter C^{up} or C^{do} to an upper bound of variable $capaStOut$. The upper and lower load shifting installed capacity ($capaStOut$ and $capaStIn$) is then constrained by the two parameter $capaStOutUp$ and $capaStInUp$ from an existing constraint in the graph-based formulation. By defining the ratio between storage-output and storage-input to 1 in the input data, the parameter $capaStOutUp$ and $capaStInUp$ is the same and there will be no issues with changing the constraint. Constraint 70 is implemented in the DR extension, however it is not purpose of the thesis to evaluate recovery of load shifting, and is therefore not used and analysed in the following case study.

$$stExtIn_{t,r,c} \cdot stEffIn = \sum_{tt=t+drTime}^{t+drTime} DSM_{t,tt,r,c}^{do} \quad \forall t \in T, r \in R, c \in C \tag{66}$$

$$stExtIn_{t,r,c} \leq capaStIn_{t,r,c} \quad \forall t \in T, r \in R, c \in C \tag{67}$$

$$\sum_{t=tt+drTime}^{tt+drTime} DSM_{t,tt,r,c}^{do} \leq capaStOut_{r,c} \quad \forall tt \in T, r \in R, c \in C \tag{68}$$

$$stExtIn_{tt,r,c} + \sum_{t=tt+drTime}^{tt+drTime} DSM_{t,tt,r,c}^{do} \leq capaStIn_{r,c} \quad \forall tt \in T, r \in R, c \in C \tag{69}$$

$$\sum_{tt=t}^{t+drRecoveryTime-1} stExtIn_{tt,r,c} \leq capaStIn_{r,c} \cdot drTime \quad \forall t \in T, r \in R, c \in C \tag{70}$$

Table 8: Sets, parameters, and variables for modelling DR in a graph-based formulation

Item	Description	Unit
Sets and indices		
t, tt $\in$ T	Time periods	Hours
r $\in$ R	Regions	-
c $\in$ C	Carriers	-
Parameters		
$stEffIn$	Efficiency	%
$drTime$	Load shift time	Hours
$drRecoveryTime$	Recovery time	Hours
Variables		
$capaStIn$	Capacity of storage-input	GW
$capaStOut$	Capacity of storage-output	GW
DSM^{do}	Hourly downward load shifts	GWh
$stExtIn$	Hourly upward load shifts	GWh

4. Quantitative case study

In order to investigate the two load shifting methods presented in the previous section, a case study on the German energy sector was carried out using the conditions described in the following section. In the case study, a reference case of the energy system without any load shifting is carried out to enable comparison between two load shifting methods. The case study is normative, as in they result in different pathways to achieve the same target, i.e. meeting the energy demand with the objective of minimising the cost.

4.1. Reference case

The reference case model the German energy system with 100% renewable energy for 2035. There are three energy carriers implemented: electricity, hydrogen and syntactic gas. Five storage technologies; batteries (lithium-ion), CAES, hydrogen storage, pumped hydroelectric storage and synthetic gas storage are included. In addition to the storage technologies, the subsequent conversion technologies are modelled: on-shore and off-shore wind, rooftop photovoltaic, open-space photovoltaic (ground-mounted), agricultural photovoltaic (solar panels mounted above partial shade crops), hydrogen plant, electrolyzer and methanation. The upper limit of installable capacity for photovoltaic is 198 GW, 707 GW for photovoltaic roof, 1700 GW for photovoltaic agriculture, 84 GW for wind offshore and lastly 297 GW for wind onshore. Zamora Blaumann et al. (2021) present a more detailed description of the reference model and the input data. Figure 3 shows the modelled technologies and the energy carriers implemented in the case study.

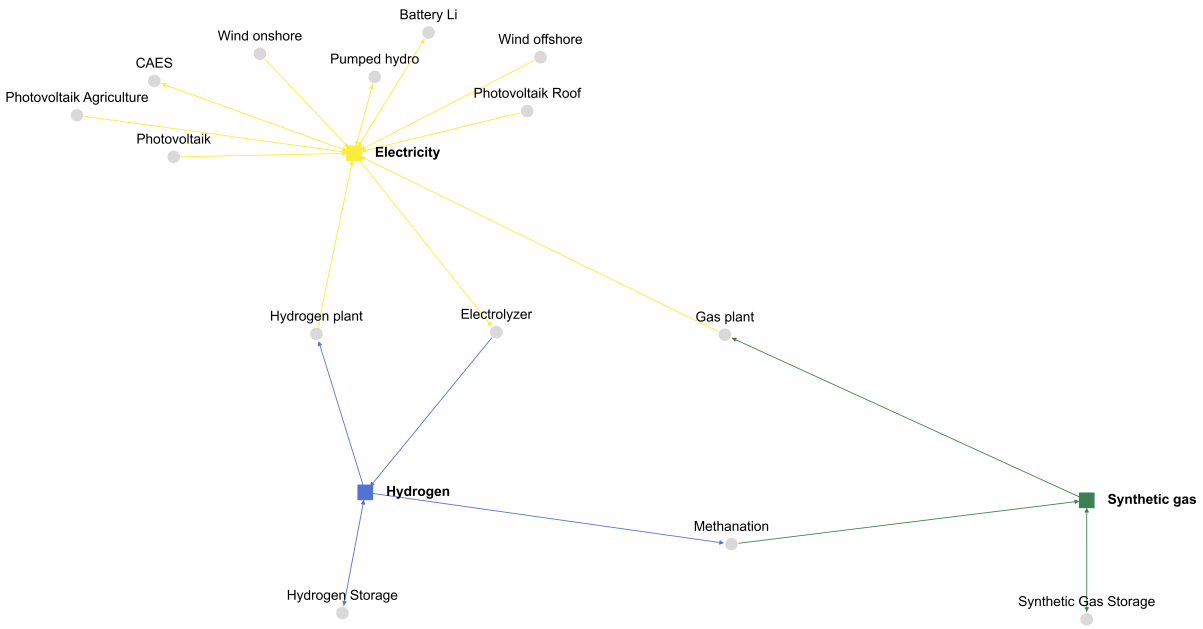

Figure 3: Energy flow graph, for the reference case

Three energy sectors are modelled, the conventional electricity sector (20.4%), heat sector (54.0%) and the transport sector(25.6%) from the total yearly energy demand (1465.21 TWh). Furthermore,

the conventional electricity demand is divided into: 45.8 % industry, 25.3% residential and 28.9% commercial sector. The heat sector is split into residential and commercial heat demand (20.9%), process heat low (9.7%), medium (47.8%) and high (21.6%) temperature demand. Lastly the transport sector is divided into freight transport, air 68.1%, rail 6.4 %, road 4.7% and passenger transport air 2.8%, rail 3.4%, road 14.7%. The flow diagram in Figure 4 illustrates the quantitative energy flow for the reference case and the sector demand. These demands are mapped to their respective "demand carrier" with a "dummy technology" allowing for conversion mapping the "demand carrier" to an energy carrier.

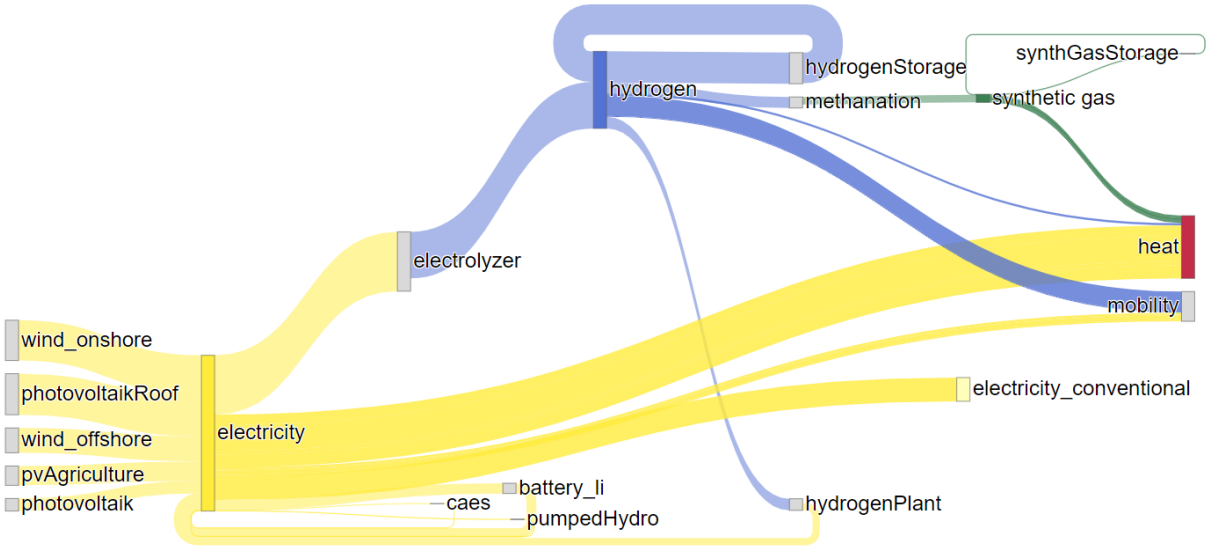

Figure 4: EW-PJS Qualitative energy flow diagram for the reference case

4.2. Temporal Resolution scenarios

The temporal resolution cases is based on the graph-based formulation indirect approach explained in section 3.1. The difference between the reference case and the TR cases is the temporal resolution of the "demand carriers". Specific demand carriers used to increase flexibility in the energy system from the heat sector is: process heat (medium) and residential and commercial heat demand, and the electricity sector: industrial, commercial and residential electricity demand. The transport sector is not used to increase the flexibility in the system. Five cases are run with the indirect method on temporal resolution in the graph-based formulation, with the temporal resolution of "demand carrier" set to: 2, 4, 6, 8, and 12-hour time-steps and named respectively TR_2, TR_4, TR_6, TR_8, TR_{12}. These cases does not have any additional costs, as it is only the "demand carrier" temporal resolution that differs from the reference case. This is important to acknowledge when comparing the results between the two methods of including DR measures. It is assumed that these cases will be quicker to compute compared to the scenarios below, since there is no extra constraints in comparison to the direct method.

4.3. Demand Response parameters and scenarios

The quantitative DR parameters for the DR reference case is based on Gils (2014), Gils (2015), and Gils (2016). Table 9 defines the grouping of DR technologies and its processes. The maximum installable DR capacity potentials for Germany is based on Gils (2016), and is shown in Table 9. In contrast to both Gils (2014) and Gils (2016) the processes are not individually implemented but rather the overall groups to minimise computation time and model size in the case study. In addition process shedding is not implemented as the DR formulation does not describe load shedding.

Table 9: Grouping of DR technology and installable capacity DR potential Source: Gils (2016)

Technology	Processes	Sector	Installable capacity MW
Heat storage	Residential storage water Residential storage heater Commercial storage water Commercial storage heating	Residential Commercial	8518
Heating and AC	Freezers/refrigerators Residential AC Heat circulation pump	Residential	5120
Process shift	Pulp Paper Recycling paper Cement Calcium carbide Air separation	Industry	2352
Washing appliances	Washing machines Tumble dryers Dish washers	Residential	15393
HVAC	Industrial ventilation Commercial ventilation Cooling retailing Commercial AC;	Commercial Industry	6427
Cooling and water	Industrial cooling Cooling hotels/restaurants Cold storages Water supply Water treatment	Commercial Industry	1107
Process shedding	Aluminium Copper Zinc Chlorine Steel	Industry	2084

Table 10: Demand Response parameter values. Source: (Gils, 2015) (Gils, 2016)

Technology	Investment cost M€/GW	Fixed OM Cost €/MW (3%)	Variable OM Cost €/MWh	Efficiency η	Time shift $drTime$
Heat storage	20	600	10	0.98	12
Heating and AC	250	7500	10	0.97	2
Washing appliances	30	900	50	1.0	6
Process shift	0	0	150	0.99	24
HVAC	10	300	5	0.97	2
Cooling and water	5	150	20	0.98	6

The parameter values used for the investment and operational cost for a given DR measure is from Gils (2016) and is described in Table 10. The DR groups are mapped to the final demand in the energy sectors listed in Table 9. The Figure 5 visualise how the DR processes is mapped to the a specific sectors demand. The three energy carriers is linked to the electricity, transport and heating sector, then the DR processes is directly connected to a specific demand time series in a sector. Along with the demand response module presented in section 3.2, this forms the base of all demand response cases. A baseline DR case DR_{Base}, was created with the parameters described in Table 10. Additionally, two cases was considered, with half and double of the time shift $drTime$ quantity of the DR_{Base} case named respectively DR_{Half} and DR_{Double}

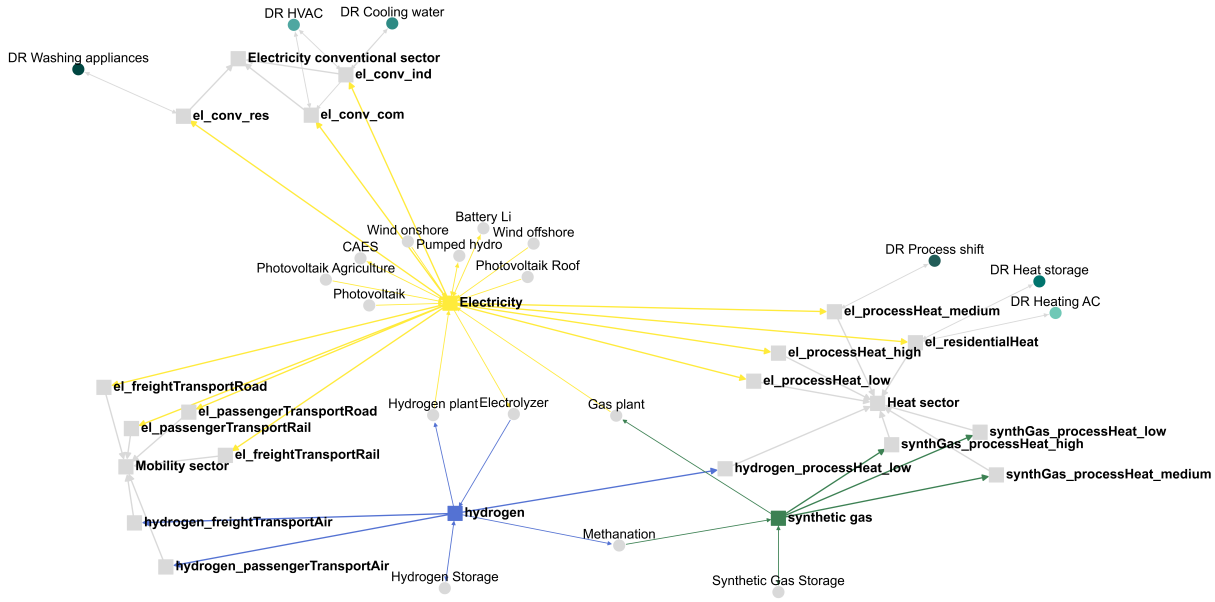

Figure 5: Energy flow graph, with Demand Response and sector mapping

5. Results and discussion

5.1. Load shifting analysis from the direct Demand Response formulation

In this section, an analysis of cases with the direct DR formulation approach in the graph-based formulation described in Section 3.2 and the DR cases presented in Section 4.3 is discussed. Starting with an investigation on the overall change in the demand, giving an overview of how load shifting affects the total demand, following with a closer inspection on load shifting from the individual DR technologies.

5.1.1. Total impact on the load profile from Demand Response

The total impact of all DR technologies on the total demand curve is shown for DR_{Base}, DR_{Half} and DR_{Double} in Figure 6, 7 and 8. The figures show a similar load shifting pattern throughout the year, and the installed capacity for upward and downward load shifting is 38.92 GW for all DR cases. General for all cases, is that there are distinct periods with higher quantity of upward and downward load shifting, there are no time-steps at maximum downward shifting capacity and almost no time-steps is at maximum of the installed capacity for upward shifting. Looking at the timesteps with maximum upward shifts it can be seen that there are fewer hours with maximum upward shift for DR_{Half} than DR_{Base}, and DR_{Double} have almost the double amount of maximum upward shifts compared to DR_{Base}. This is a direct consequence of change in the parameter $drTime$ for shifting time. The model have more flexibility to affect the demand curve with a bigger time-shift window compared to a smaller window for shifting load upward and downwards for a given hour by increasing the parameter $drTime$. The quantity and frequency of downward and upward load shifting is therefore distinctly reduced for DR_{Half} compared to DR_{Base} and DR_{Double}. On the figures, the smaller quantities of increased and decreased load is hard to see, however the changed demand curve shows that there is overall a consistent utilization of the DR measures. The average downward and upward shift is 5.48 GW and 5.57 GW for DR_{Base}, 3.67 GW and 3.74 GW for DR_{Half}, and 6.75 GW and 6.87 for DR_{Double}. As a result, the average utilization of load shifting capacity ranges from 9.43% to 17.65% of the installed DR capacity. The quantity for downward shifting is the sum of all hours where the index $t = t$, i.e. different tt indices, see definition of the variable $stExtOut$ in Section 3.2. The DR-to-Demand ratio is found by dividing total load shifted upwards or downwards by the total energy demand from the original demand curve. The DR-to-Demand can then be used to compare the share of demand changed between cases. The upward and downward DR-to-Demand ratio for DR_{Base} is 3.33% and 3.28%, for DR_{Half} it is 2.23% and 2.20%, and for DR_{Double} it is 4.10% and 4.03%. There is a relative small differences between the total demand from original to the total demand with DR measures. This is a result from the DR measures which has efficiency factor for upward shifting, therefore increasing the total demand, the efficiency factors ranges from 97-100%. The share of demand changed is small for all cases, with DR_{Double} having the highest DR-to-Demand ratio, e.g. a higher utilization of installed DR capacity. The share is of DR of the

total yearly demand is higher than the findings of Gils (2016), who found that the shifted load was less than 1% of the total yearly demand in Germany, however Gils only has a 17% share of RES.

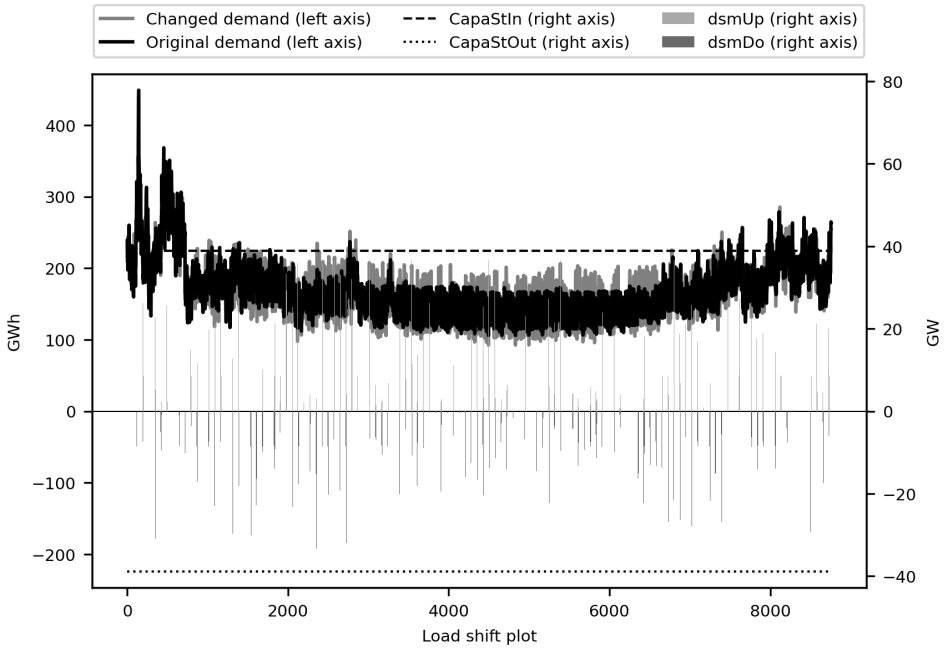

Figure 6: Load profile for DR_{Base} time-step 0-8760

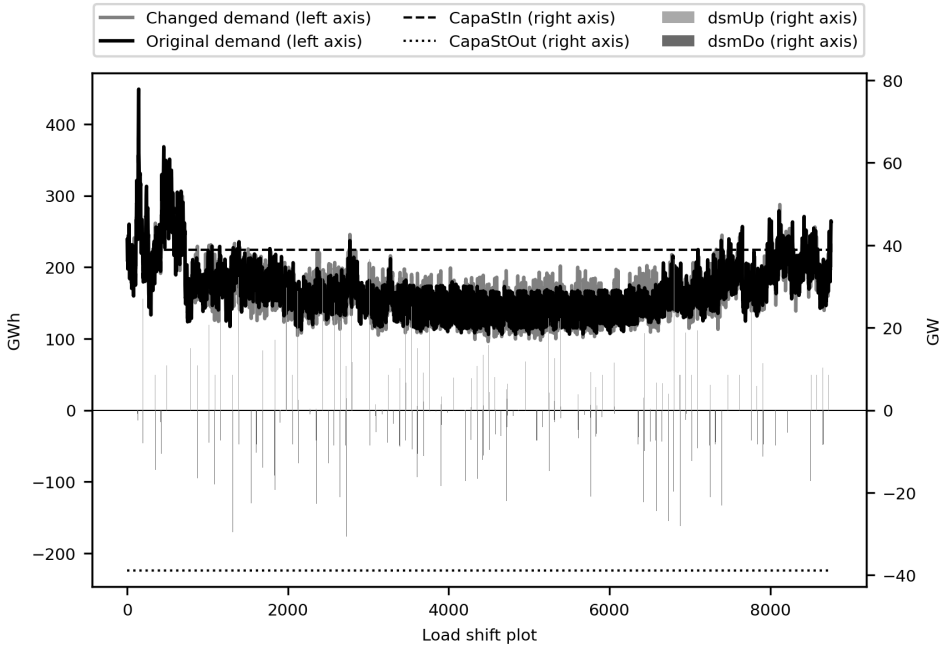

Figure 7: Load profile for DR_{Half} time-step 0-8760

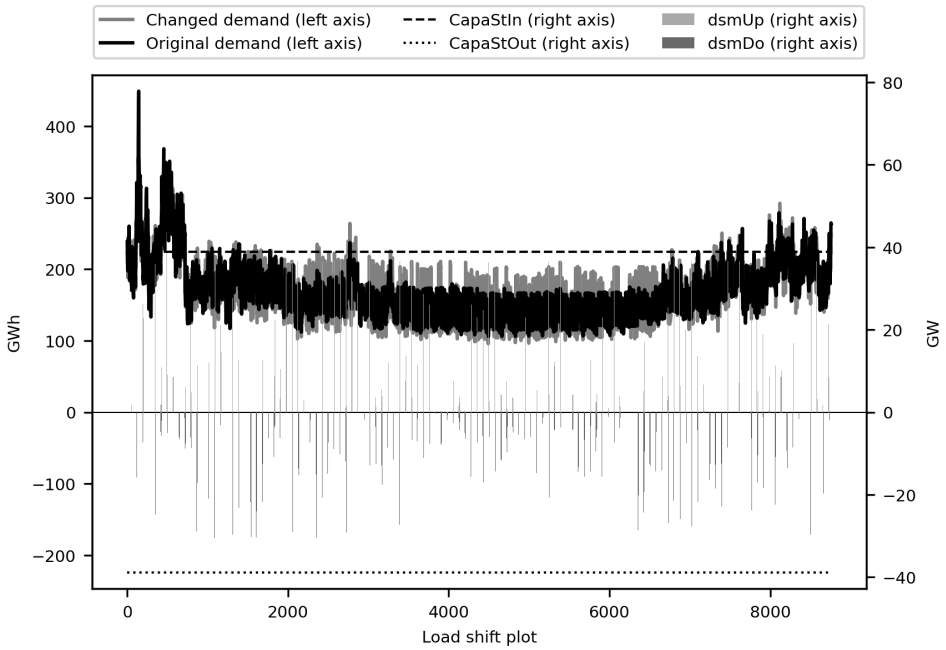

Figure 8: Load profile for DR_{Double} time-step 0-8760

A closer examination of DR_{Base} (Fig. 9), DR_{Half} (Fig. 10) and DR_{Double} (Fig. 11) during the time-period 96-288 in January, containing the peak load hour of in the total demand curve at 448.8 GW in hour 144 is carried out. It is observed that both DR_{Base} and DR_{Double} (Fig. 9 and 11) are able to reduce the peak load from 448.8 GW to 440.46 GW, resulting in a 1.85% decrease. Whereas DR_{Half} is not able to reduce the peak demand by upward shifting at an earlier or later point, this could indicate that DR_{Half} does not provide enough flexibility. DR_{Base} and DR_{Double} does not reduced the peak load at maximum downward shifting capacity in DR_{Base} and DR_{Double}, the DR-to-Peak ratio is 8.67% (installed DR capacity divided by peak load), it would therefore have been possible with a larger reduction of peak load. For DR_{Base}, the largest quantity shifted upwards is 34.41 GW at hour 109, and 29.76 GW at hour 191 for downward shifting. In the DR_{Half} case, 26.97 GW in hour 196 is largest quantity shifted upwards and the largest downward shift is 22.46 GW in hour 193. Lastly, DR_{Double} maximum upward shift and downward shift is 36.56 GW in hour 108 and 30.46 GW in hour 190. The upward and downward DR-to-Demand ratio in this time period is 0.61% and 0.72% for DR_{Base}, 0.33% and 0.32% DR_{Half}, and 1.1% and 1.40% for DR_{Double}. Looking at the share of total shifted demand, it is observed that DR_{Base} and DR_{Double} compensate for upward shifting before the time-frame 96-288, as the total downward shifting is higher than upward shifting. In contrast to DR_{Half} which is not affected by earlier or later load shifting.

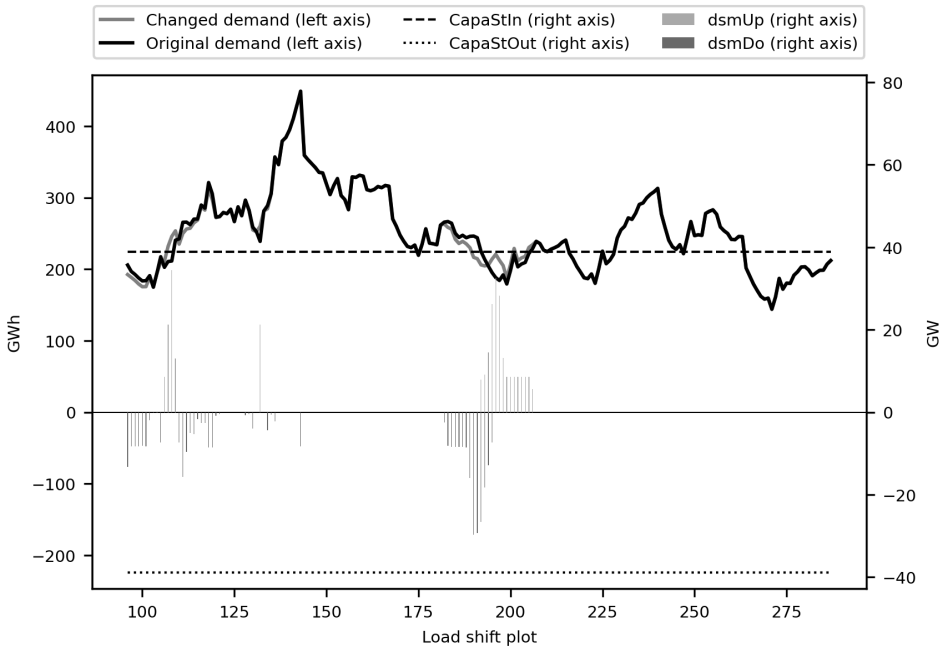

Figure 9: Load profile for DR_{Base} time-step 96-288

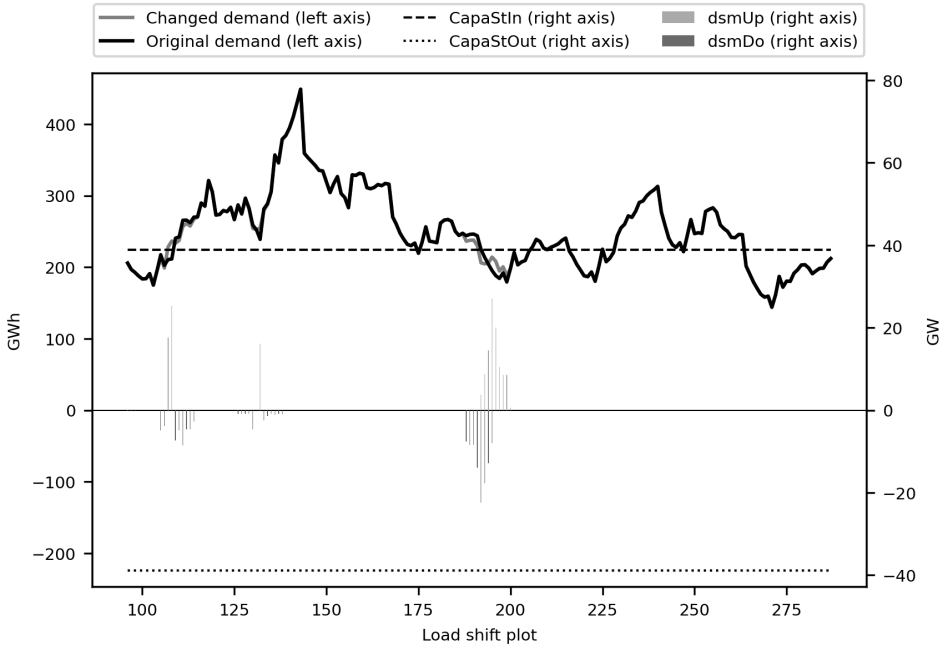

Figure 10: Load profile for DR_{Half} time-step 96-288

Continuing the analysis of the total demand, another time period (hours 1584-1880) is analysed, this period has a distinctly different demand pattern than in the previous evaluated period. The change in demand in time period 1584 to 1880 hour for DR_{Base}, DR_{Half} and DR_{Double} is shown in respectively Figure 12, 13 and 14. The upward and downward DR-to-Demand ratio for DR_{base} is 5.10% and 5.20%, 3.69% and 3.76% for DR_{Half}, and 6.03% and 6.10% for DR_{Double} in this time period. Compared to the DR-to-Demand ratios for time-period 96-288, this is a high share of load shifting. In addition, there is a slight increase for all three cases in the time period 1584-1880

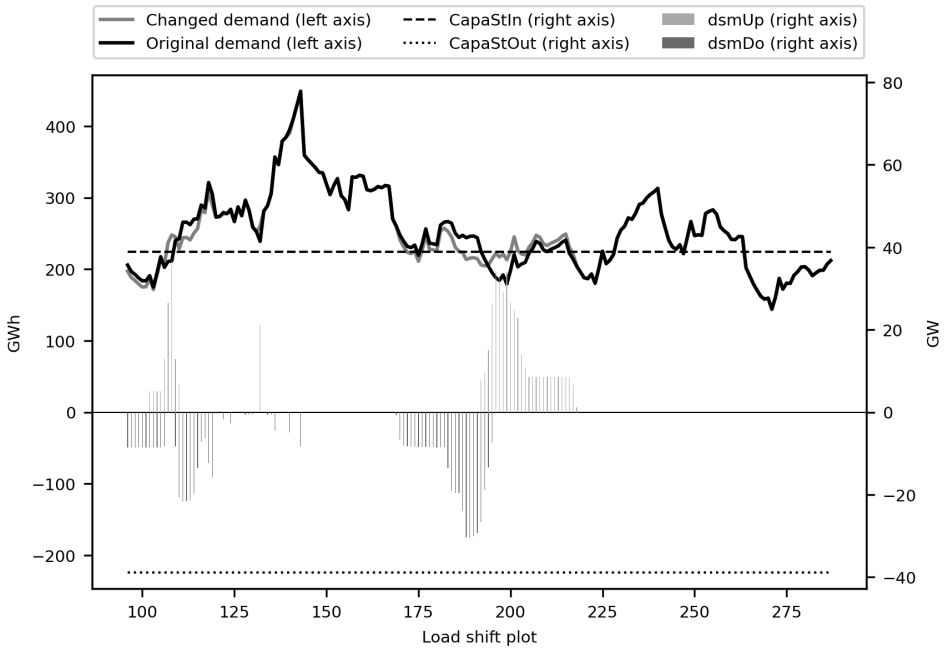

Figure 11: Load profile for DR_{Double} time-step 96-288

compared to the overall DR-to-Demand ratio. Looking at the changed demand curve for the cases, there are some peak reduction from the original demand curve, and at the same time, new and similar high peaks of demand occur at other points in time. The load shifting results in deeper valleys and new valleys in the changed demand curve. The DR formulation does not enforce a more even and stable demand curve such as valley filling strategies could have had. The load shifting rather follows the feed-in energy pattern, and with a case of 100% intermittent renewable energy, this leads to more fluctuations in the demand curve. The points in time changing the demand curve is more or less the same in all cases, with DR_{Half} having a bit fewer hours of load shifting and DR_{Double} more load shifts compared to DR_{Base}. When taking a closer look at time of load shifting, it can be observed that there are few hours with both upward and downward load shifting at the same time, compared to exclusively either upward or downward load shifting. There is a distinct time period with low or no load shifting as can be seen in Figures 12, 13 and 14. This could come from limited feed-in energy in surrounding hours or that excess feed-in energy is stored in other storage technologies alternatives for a later point where the flexibility from the DR measures is not enough to compensate for general storage technologies.

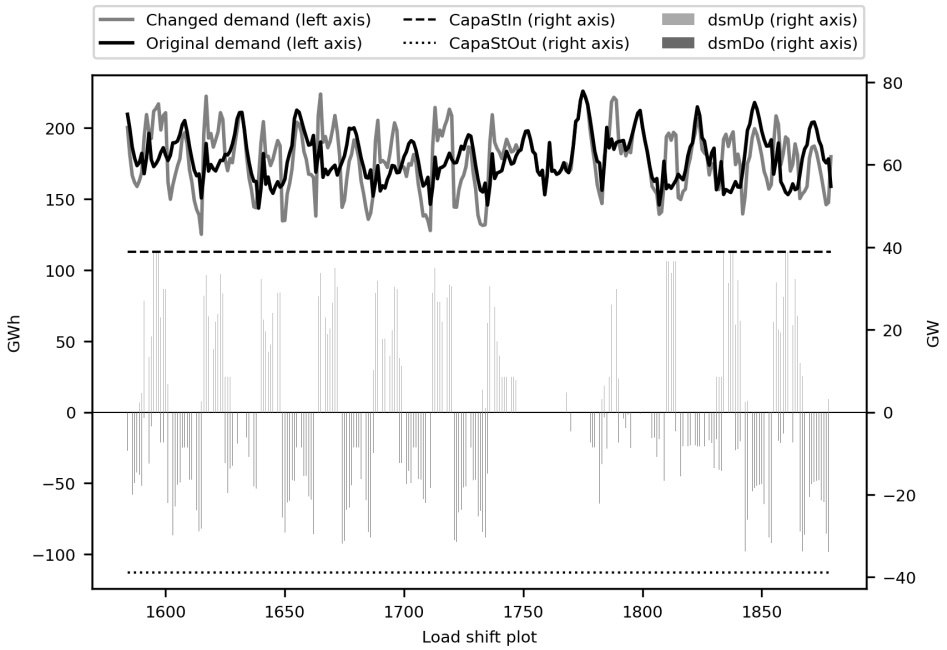

Figure 12: Load profile for DR_{Base} time-step 1584-1880

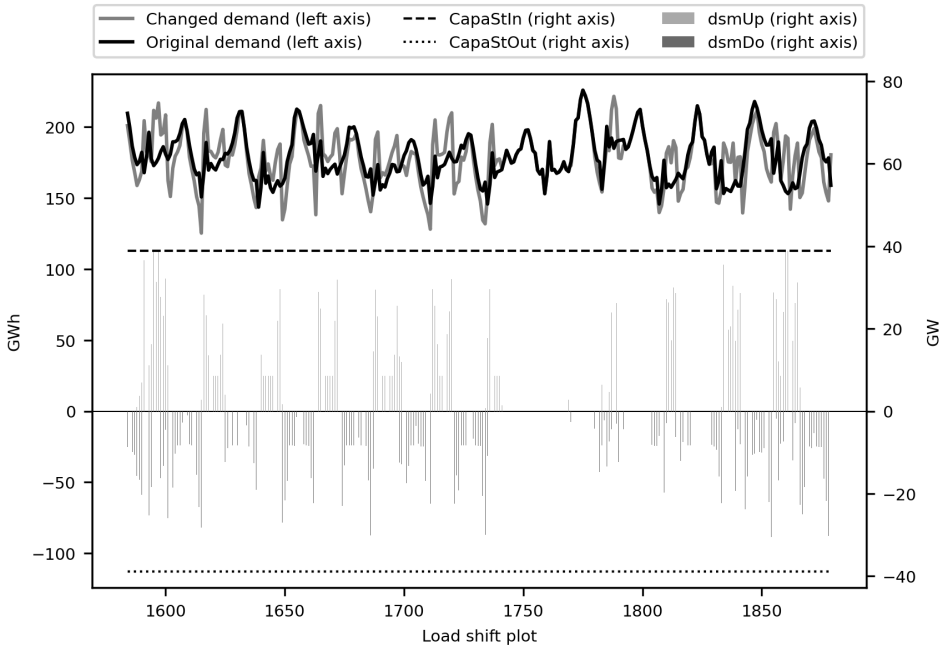

Figure 13: Load profile for DR_{Half} time-step 1584-1880

5.1.2. Impact on residential and commercial heat load profile from Heat Storage

Following the evaluation of the total impact on the demand, an in-depth examination of how load shifting from the DR measure $Heat\ Storage$ affect the residential and commercial heat demand is discussed. $Heat\ Storage$ installed upward and downward load shifting capacity is 8.518 GW, which is its maximum installable capacity potential, see Table 9. DR_{Base} (Fig. 15), DR_{Half} (Fig. 56) and DR_{Double} (Fig. 57) has frequent load shifting at maximum upward and downward capacity, with a slight difference when the load is shifted. Overall the shifted residential and commercial demand

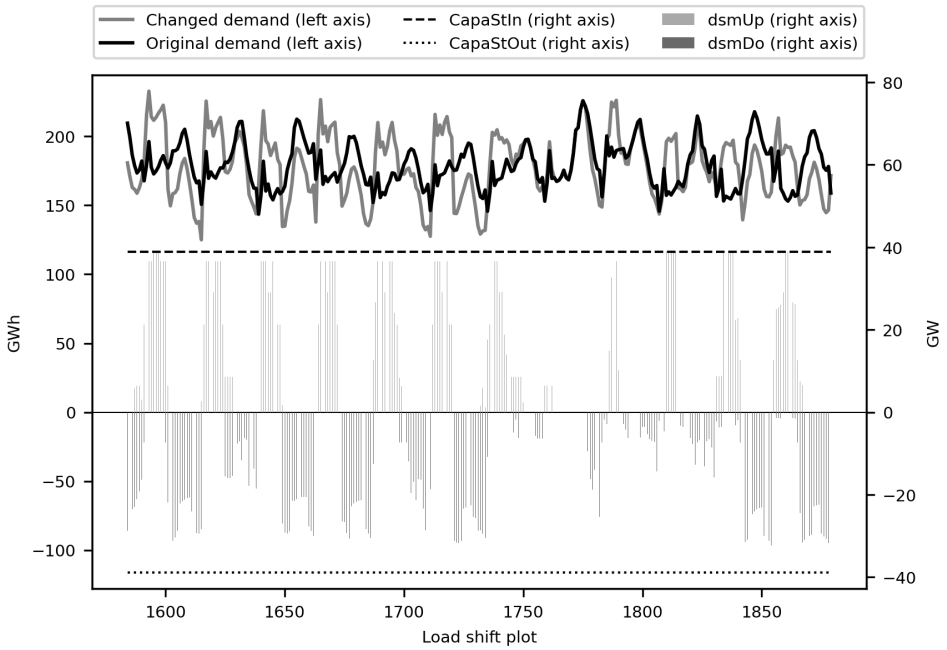

Figure 14: Load profile for DR_{Double} time-step 1584-1880

upwards and downward DR-to-Demand ratio is 10.40% and 10.20% for DR_{Base}, 8.48% and 8.31% for DR_{Half} and 12.10% and 11.90% for DR_{Double}. Load shifting from $Heat\ Storage$ occurs more often during the winter months when the demand is high. Even if the demand is lower during the summer, there is still load shifting. This implies that for a cost-minimisation objective, the model follows the pattern of feed-in energy from wind and photovoltaic. This energy would instead come from storage technologies in the reference case with no flexibility from DR measures.

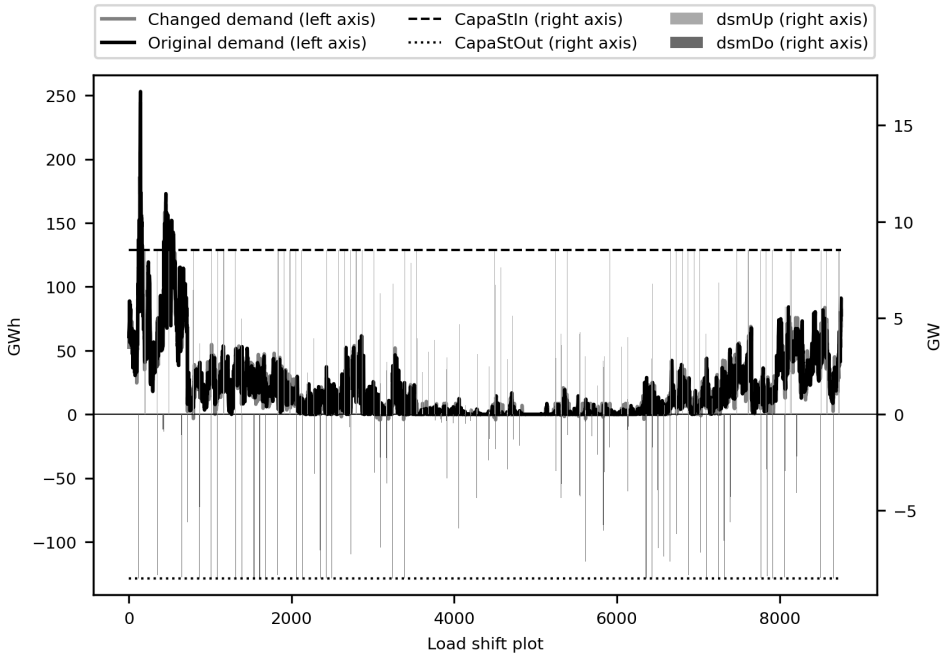

Figure 15: Load profile for DR_{Base} time-step 0-8760, $Heat\ Storage$

Similarly to the previous section on the total load profile, a closer look at how $Heat\ Storage$ affect the residential and commercial heat demand in time-period 96-288 and 1584-1880 is analysed. Figure 16, 17, 18 shows the load profile for residential and commercial heating demand during time-steps 96-288 and Figure 19, 58 and 59 shows the time-period 1584-1880 for DR_{Base}, DR_{Half}, and DR_{Double}. The peak demand of residential and commercial heat is 252.97 GW in hour 144, thus the residential and commercial demand is 56.40% of the total peak demand. From Figure 16, 17, and 18, it can be observed that in DR_{Base} and DR_{Double} the peak demand is reduced. The load reduction corresponds to the total peak load reduction of 8.34 GW discussed previously. As a result, $Heat\ Storage$ is the only DR measure which reduces the total peak demand. $Heat\ Storage$ has a time shift parameter $drTime$ of 12, 6, 24. Similar to the evaluation of the total demand in the time-frame 96-288, some quantities of downwards shifting is compensating for earlier upward load shifting in DR_{Base} and DR_{Double} from $Heat\ Storage$ as can be seen in Figure 16 and 18. It is clear that the change in load shift length $drTime$, has a great impact on load shifting of the residential and commercial demand. A closer look of the load profiles confirms that the direct approach allows for load shifting to occur before and/or after a time-step where the demand is altered. In Figure 17, there are three periods of load shifting with one period starting with upward load shift and the two other with a downward load shift. The first one shows an upward load shift thereby increasing demand, then compensating with downward load shifts afterwards. The second shift period, the downward shift occurs both before and after the upward shift. Lastly, the third period fully compensates with load reduction before the upward shift.

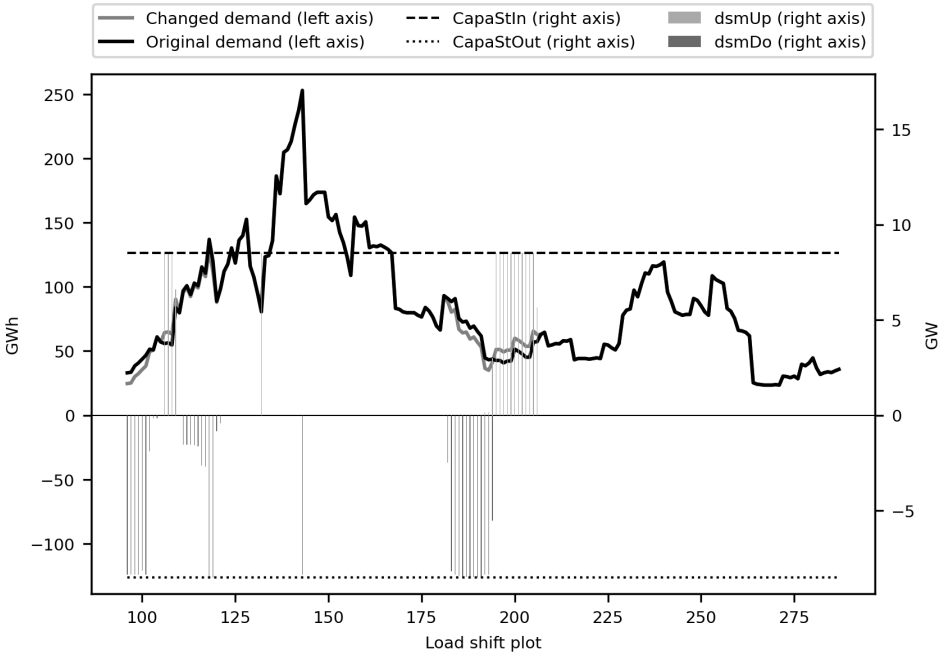

Figure 16: Load profile for DR_{Base} time-step 96-288, $Heat\ Storage$

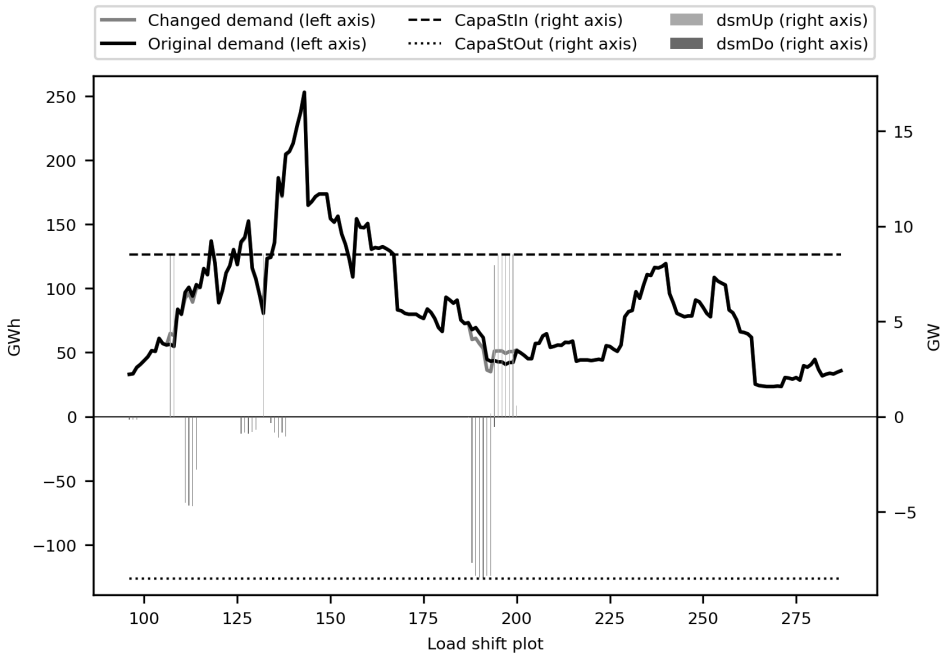

Figure 17: Load profile for DR_{Half} time-step 96-288, $Heat\ Storage$

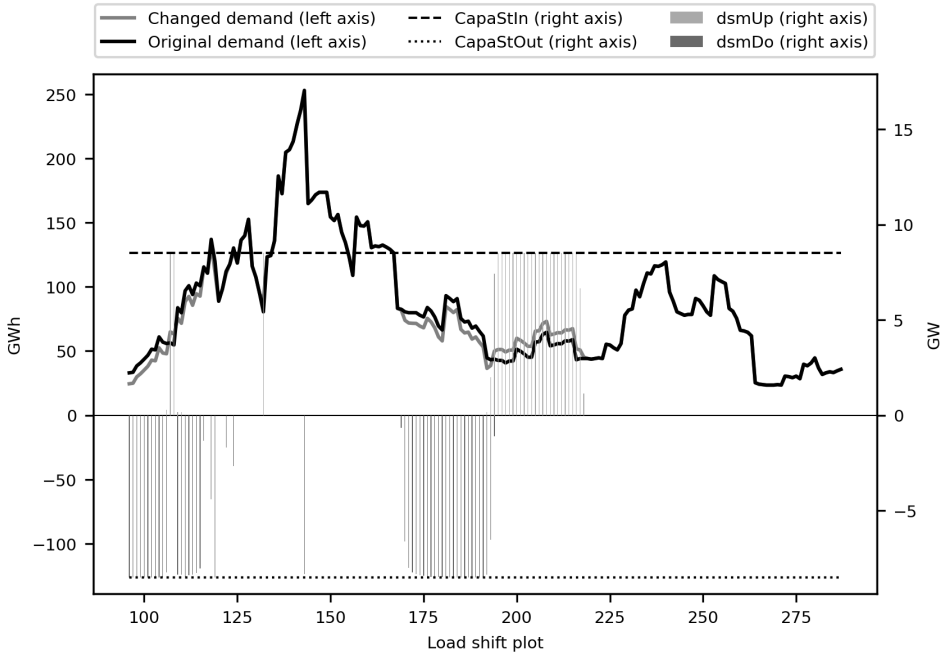

Figure 18: Load profile for DR_{Double} time-step 96-288, $Heat\ Storage$

Figure 19, 58, and 59 present the residential and commercial heat load profile between hour 1584 to 1880 for respectively DR_{Base}, DR_{Half}, and DR_{Double}. The demand profile in 1584-1880 for residential and commercial heat demand differs greatly from the demand profile in the 96-288 time period. Looking at the load shifts, it can be seen that the $Heat\ Storage$ upwards and downward capacity is fully utilized in several timesteps in all DR cases. Both the original and changed demand profile have large fluctuations in the demand profile. The residential and commercial demand have

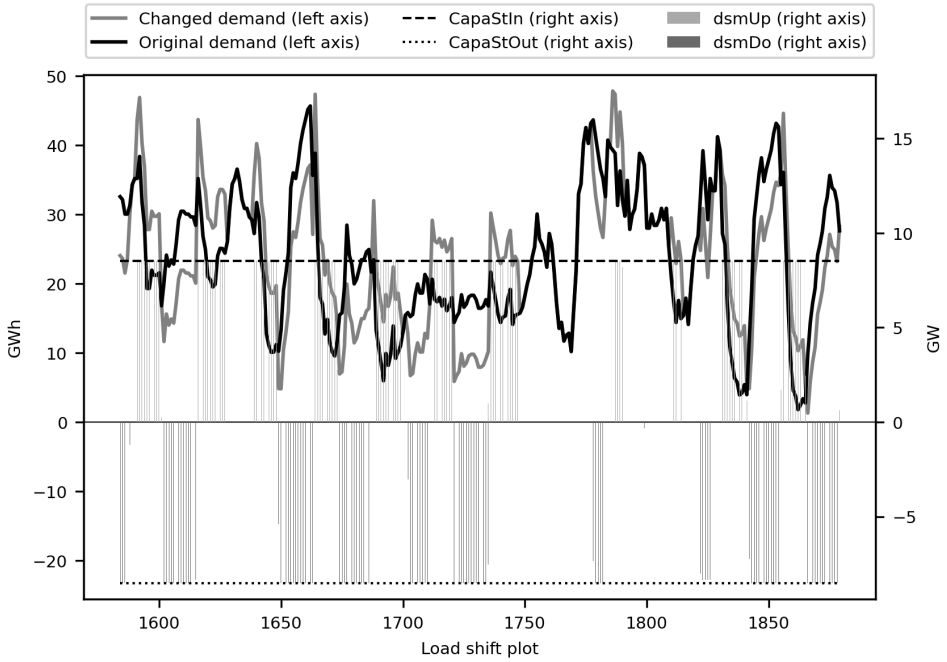

Figure 19: Load profile for DR_{Base} time-step 1584-1880, $Heat\ Storage$

more fluctuating demand curve compared to for example process industries that have a predictable and/or constant demand pattern. This affect how $Heat\ Storage$ is utilized in the case study. In addition, the residential and commercial heat demand depends on factors such as the temperature, changing the demand pattern during a year and over the years. With an 100% intermittent renewable energy, the results could vary over the years, therefore case studies with different feed-in pattern for different years should be studied further to evaluate the DR measures mapped to the residential and commercial heat demand.

5.1.3. Impact on residential and commercial heat load profile from Heating AC

Following the analysis of the impact on the residential and commercial demand from $Heat\ Storage$, an in-depth examination of how load shifting from $Heating\ AC$ affects the residential and commercial heat demand is carried out. Unexpectedly, the observations of $Heating\ AC$ is similar to $Heat\ Storage$, as both are mapped to the residential and commercial heat demand. However, $Heating\ AC$ has higher investment cost and fixed operation cost than $Heat\ Storage$. With limited feed-in energy from photovoltaic during the winter $Heating\ AC$ is utilized for load shifting like $Heat\ Storage$. However, it is not cost efficient to use $Heating\ AC$ when $Heat\ Storage$ is a cheaper option for shifting the same demand during the summer when the feed-in energy has higher shares of PV before after $Heat\ Storage$ load shifting is at maximum capacity. The maximum of potential load shifting capacity is installed for $Heating\ AC$ at 5.12 GW, which is lower than the installed capacity for $Heat\ Storage$. The DR-to-Demand ratio from the total upwards and downwards load shifted from $Heat\ Storage$ of residential and commercial heat demand is 3.31% and 3.21% for DR_{Base}, it is 1.94% and 1.88% for DR_{Half}, and it is 4.47% and 4.34% for DR_{Double}. Unexpectedly, the halving and doubling of

parameter $drTime$, does not correlate to a halving or doubling of the total shifted demand. This highlight the importance of evaluating the utilization of DR measures with sensitivity studies of DR parameters, for example cost sensitivities.

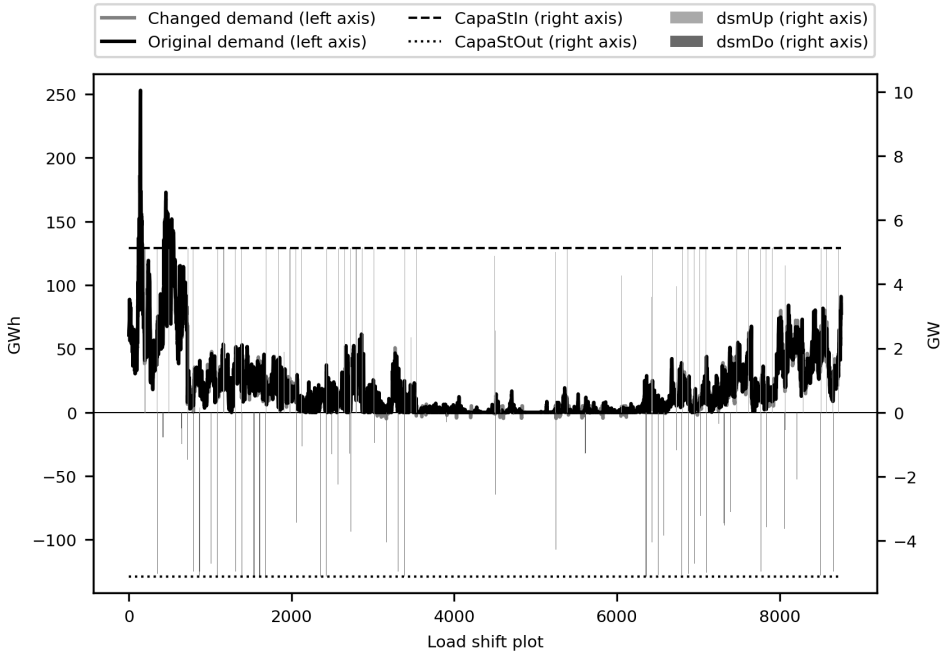

Figure 20: Load profile for DR_{Double} time-step 0-8760, $Heating\ AC$

Comparing $Heating\ AC$ with $Heat\ Storage$ for any of the cases in the time period 96-288, it can be seen that the time of load shifting is similar, aside from the smaller quantities shifted due to the higher costs, length of shifting and installed capacity. $Heating\ AC$ has a time shift parameter $drTime$ of 2, 1, 4 for DR_{Base}, DR_{Half}, and DR_{Double} compared to $Heat\ Storage\ drTime$ of 12, 6, and 24. It is clear that the change in length of $drTime$, and therefore a smaller time-window for shifting has a great impact on the load shifting of the residential and commercial heat demand. This results in $Heating\ AC$ not being able to reduce the peak load 252.97 GW in hour 144 for any of the DR cases as seen in Figure 21, 62, and 63 as $Heat\ Storage$ was able to with a larger downward load shifting time-period.

Like $Heat\ Storage$, the change in demand in time-period 1584-1880 for $Heating\ AC$ shows that the difference between the original demand and the changed demand is large as seen in Figure 22, 64, and 65. This is due to upward and downward capacity for $Heating\ AC$ is often utilized at maximum. However, with a smaller installed capacity and $drTime$ parameter, $Heating\ AC$ has less shifted load than $Heat\ Storage$. Comparing the two DR measures affecting the residential and commercial heat demand for DR_{Base} it is found that upward DR-to-Demand ratio is 12.56% for $Heat\ Storage$ and 5.83% for $Heating\ AC$ of the total demand in this time period.

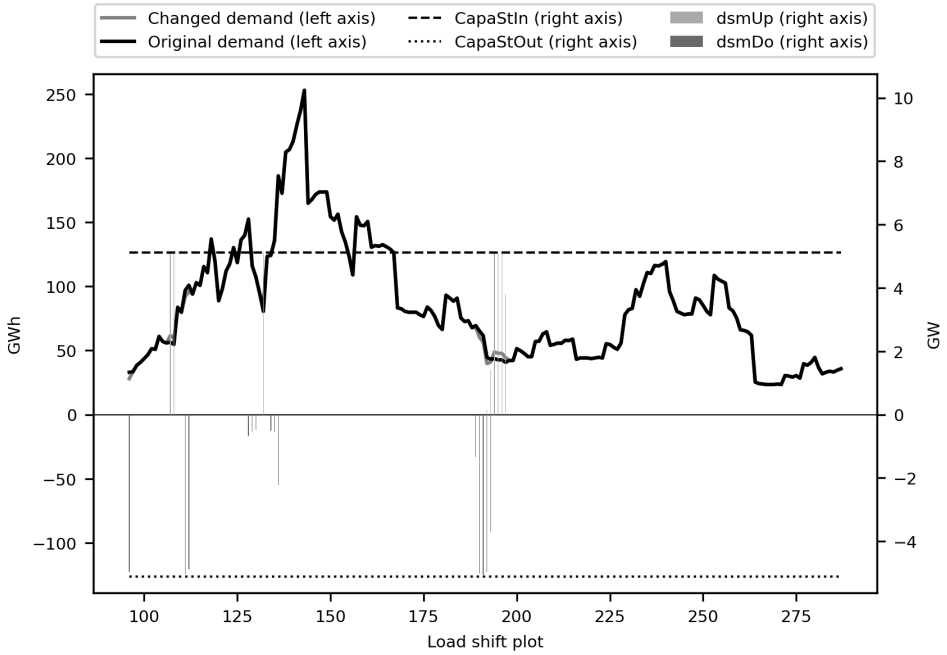

Figure 21: Load profile for DR_{Base} time-step 96-288, $Heating\ AC$

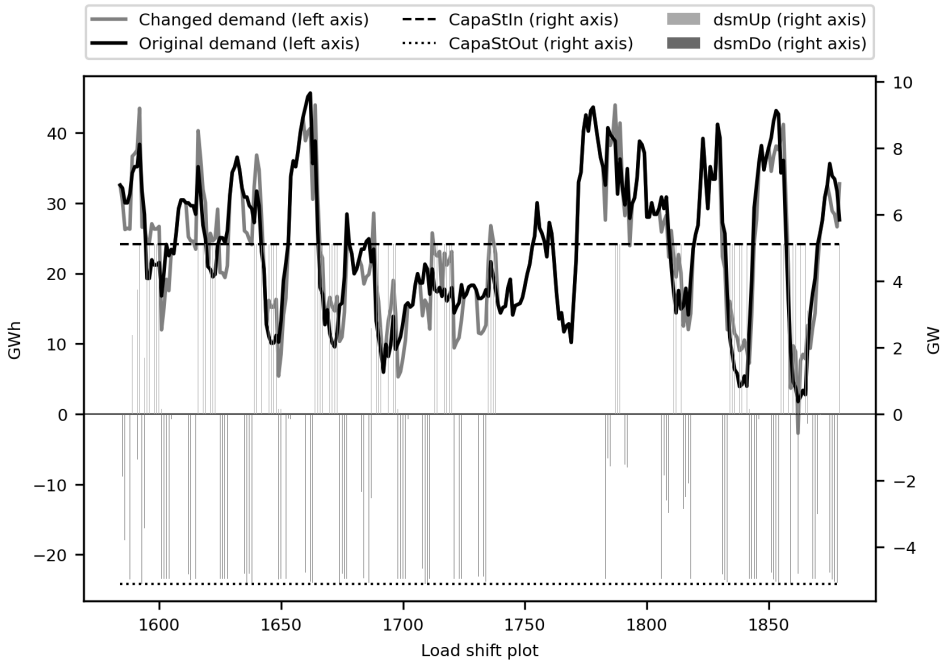

Figure 22: Load profile for DR_{Base} time-step 1584-1880, $Heating\ AC$

5.1.4. Impact on electricity for process heat load profile from Process Shift

The demand pattern of the electricity demand for process heat medium temperature overwrites the changed demand from load shifting as can be seen in Figure 23, 66, and 67 for case DR_{Base}, DR_{Half}, and DR_{Double}. However it is possible to observe the change in demand by looking at the downward load shifting bars (dsmDo bar) in the plot, from the figures it can be seen that there is only a few times of load shifting. There is almost no load shifting from $Process\ Shift$ resulting in a small DR-

to-Demand ratio. The upward and downward installed capacity for $Process\ Shift$ is 2352 MW. The DR-to-Demand ratio for upward shifting on process heat demand is 0.04% for DR_{Base}, 0.03% for DR_{Half}, and 0.04% DR_{Double}. The expansion cost parameter is 0 M€/GW and operation cost is 0 €/MW, the only cost is the variable cost at 150€/MWh, and while the efficiency parameter is 0.99 and there is large flexibility from $drTime$ of 24, 12, 48 in all cases, it is most likely the combination of low potential for installed capacity $Process\ Shift$ and high variable cost that hinder shifting of more load. On the other hand, it could be a result of the demand profile pattern. There is no change in demand in the time period 96-288 with the total peak demand for all three cases (Fig. 24, 68, and 69), as the available feed-in energy is utilized for load shifting other demand series rather than the process heat demand.

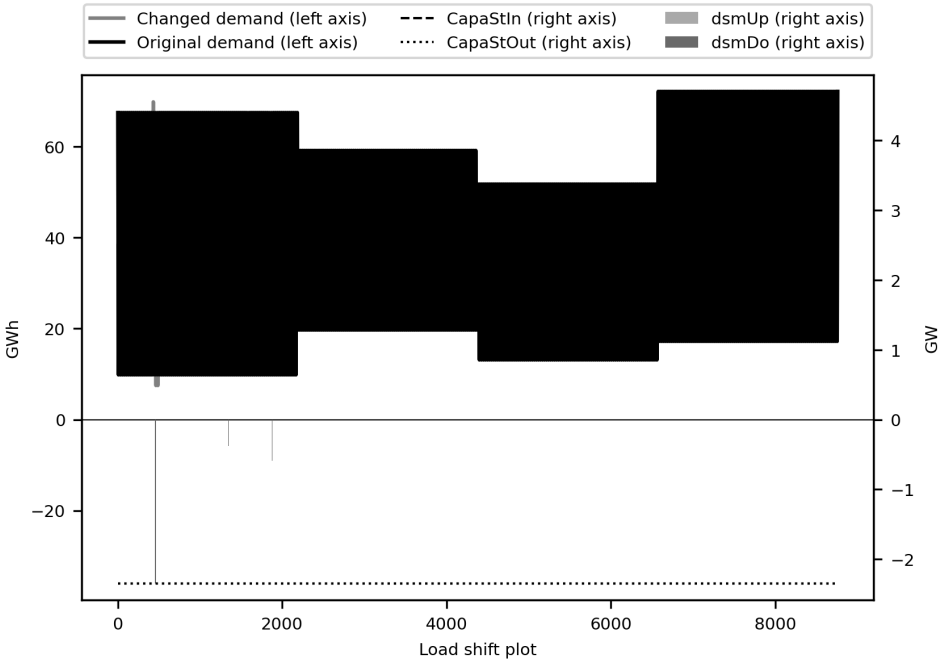

Figure 23: Load profile for DR_{Base} time-step 0-8760, $Process\ Shift$

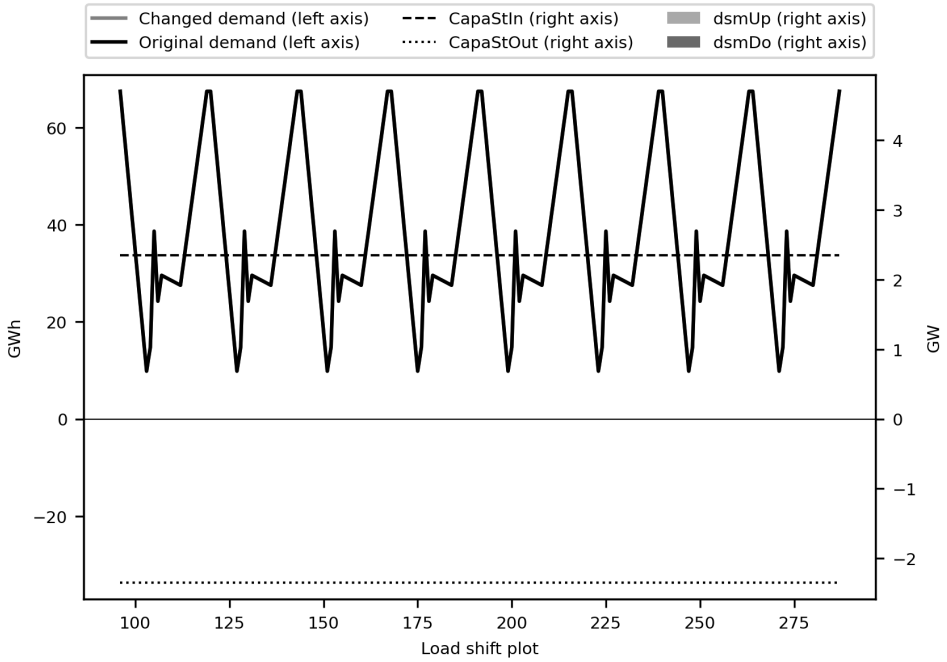

Figure 24: Load profile for DR_{Base} time-step 96-288, *Process Shift*

Figure 25, 70 and 71 have the same distinct pattern as time-period 96-288 however it is more frequent. The demand pattern is periodic, it can be observed that the increase and decrease of load occurs at specific points in the periodic pattern from the changed demand curve in the figures. There is small variations between the three cases with different quantities of shifted load, with DR_{Double} shifting one more "signal" than DR_{Base} and DR_{Half}.

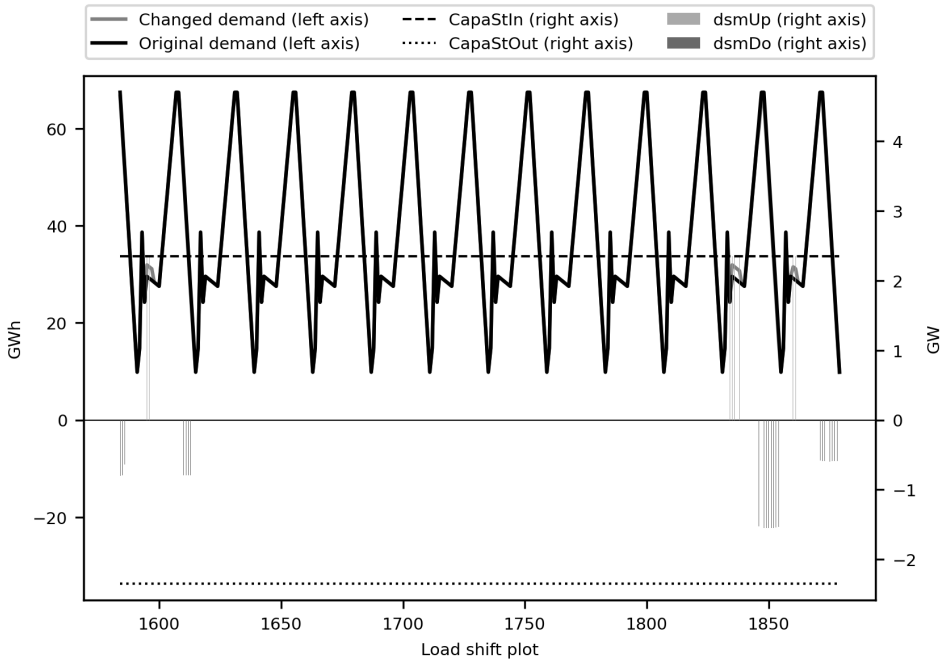

Figure 25: Load profile for DR_{Base} time-step 1584-1880, *Process Shift*

5.1.5. Impact on the residential electricity load profile from Washing appliances

The load shifting from the DR measure $Washing\ Appliances$, mapped to the residential conventional electricity demand is discussed. The demand pattern is drastically changed over the year, as can be seen in the load profile for DR_{Base}, DR_{Half} and DR_{Double} in Figure 26, 72, and 75. The peak demand is often more than doubled in the changed demand series, and compensating the increase, there are now frequent hours with no demand. The changed demand becomes more fluctuating. This observation is applicable to all three DR cases with the direct method as seen in Figure 26, 72, and 73. DR_{Half} change in demand curve is similar to DR_{Base}, but the shifts occur less frequently, while DR_{Double} have a more constant average downward shift of demand. There is no time-steps where downward capacity is at maximum, however the upward capacity is. This shows that the installed upward and downward capacity does not have to be equal to reach the same load shift pattern. $Washing\ Appliances$ total installed upward and downward load shifting capacity is 15.393 GW. The DR-to-Demand ratio for DR_{Base} is 21.3%, DR_{Half} is 12.3%, and for DR_{Double} is 23.9%. $Washing\ Appliances$ have a efficiency factor of 100%, thus the downward load shifting is equal to upward load shifting ratio.

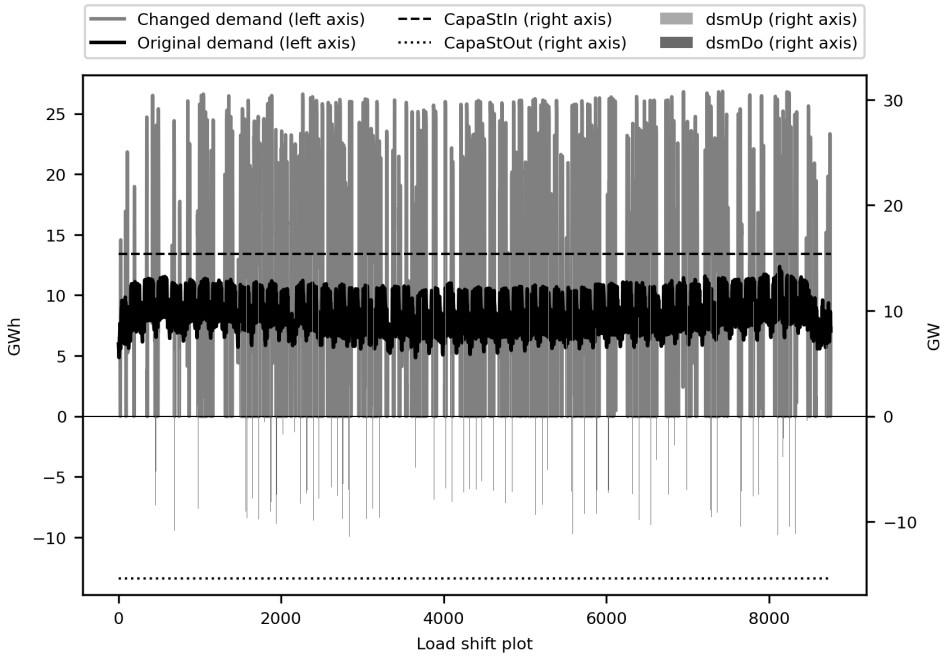

Figure 26: Load profile for DR_{Base} time-step 0-8760, $Washing\ Appliances$

The load shifting from $Washing\ Appliances$ for DR_{Base} in time-period 96-288 (Fig. 27), shows that the change in demand in hours 190-199 (22:00-07:00), is shifted from evening to morning. The downward shift starts at 22:00 and ending at 01:00 o'clock, the shift results in no demand hour 23:00-01:00. The upwards shift then starts in hour four o'clock and ending at seven o'clock. Upward shift leads to over doubling of the original load at five and six o'clock. A limitation of the study is that the market electricity price is not included, which is a factor when deciding what time load shift

shall occur. The electricity price is normally more expensive in the morning than the evening, so by including varying electricity prices, shifting load from the evening to the next morning might not have occurred with respect to minimising cost.

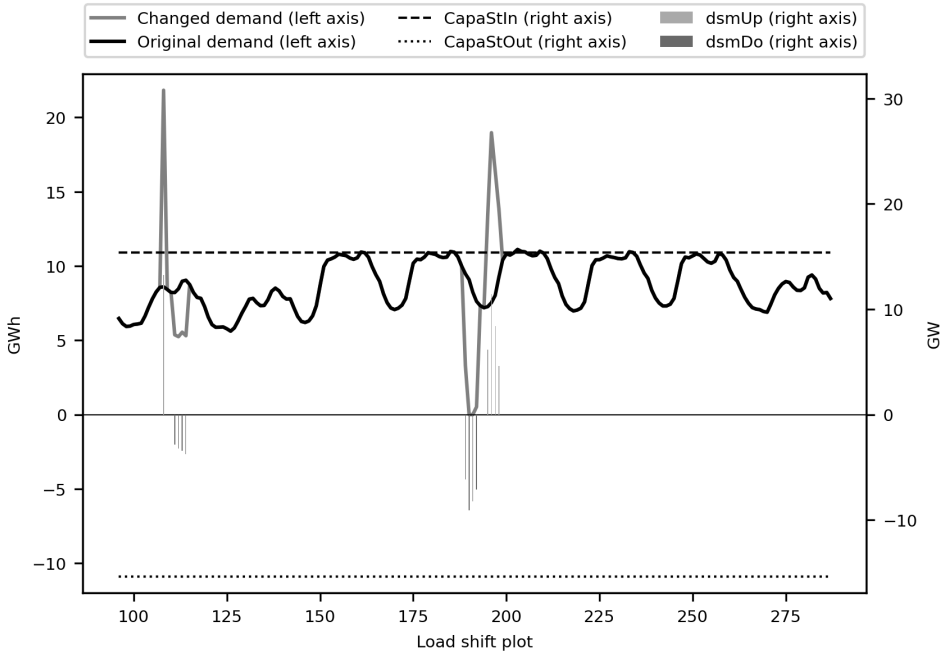

Figure 27: Load profile for DR_{Base} time-step 96-288, *Washing Appliances*

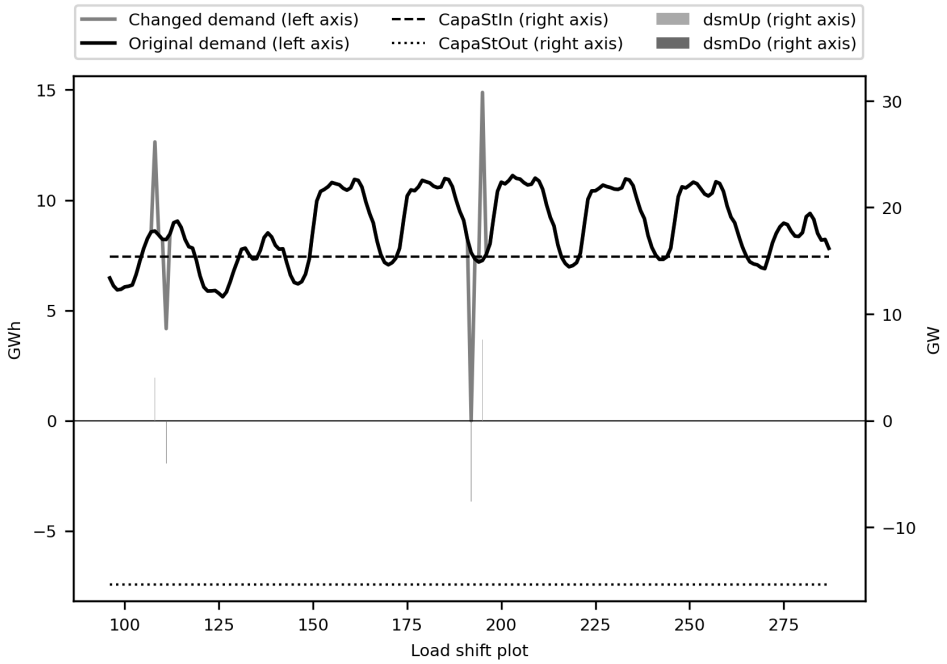

Figure 28: Load profile for DR_{Half} time-step 96-288, *Washing Appliances*

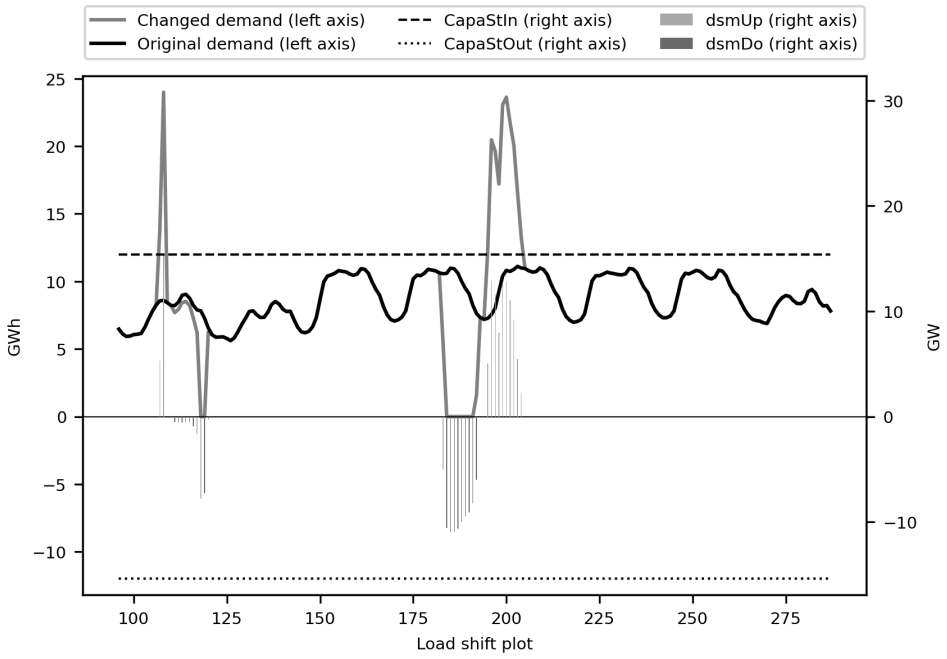

Figure 29: Load profile for DR_{Double} time-step 96-288, *Washing Appliances*

Compared to time-period 96-288, time-period 1584-1880 load shifts from *Washing Appliances* occur more frequently, however the load shifting pattern is approximately the same. Downward load shifts occur both during day and night and demand is zero during most of these shifts. There is small difference between the cases, due to $drTime$ resulting in high peaks from upward shifting lasting longer in DR_{Double}, whereas they are shorter for DR_{Half}. For the three DR cases there is a period with no load shifting, this is also observed in load shifting from other DR measures.

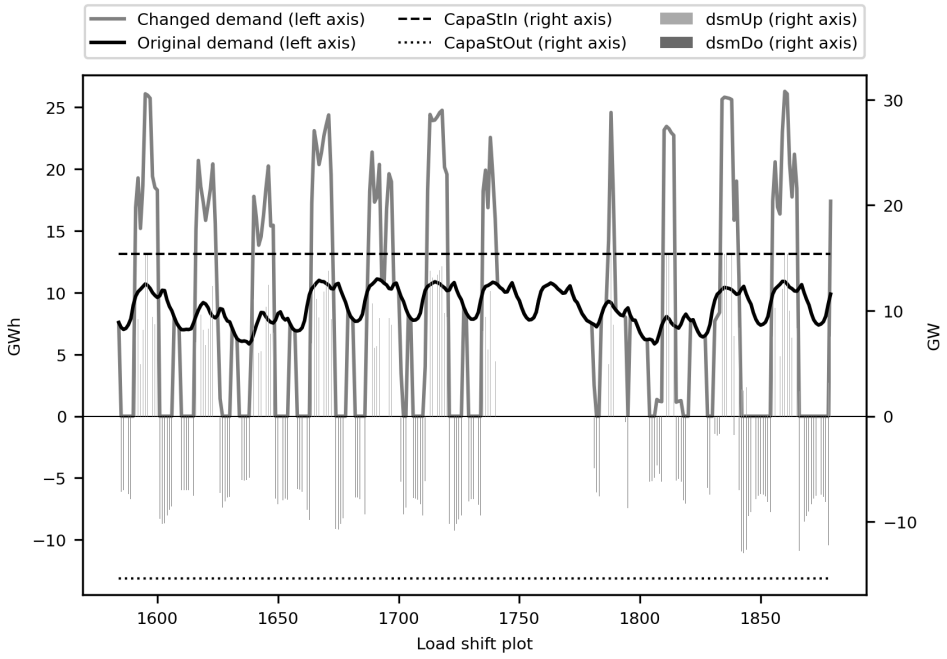

Figure 30: Load profile for DR_{Base} time-step 1584-1880, *Washing Appliances*

5.1.6. Impact on commercial and industrial electricity load profile from HVAC

This section discusses the impact $HVAC$ has on the commercial and industrial electricity demand. Figure 31, 76, and 77 shows the load profile from the commercial and industrial electricity demand for DR_{Base}, DR_{Half} and DR_{Double}. The change in demand pattern is similar, disregarding the difference in frequency of load shifting the $drTime$ parameter has. The maximum potential for $HVAC$ is installed at of 6.427 GW for upward and downward shifting capacity. The demand curve has an average electricity demand 25.53 GW and a peak demand of 36.51 GW, leading to a DR-to-Peak ratio of 17.6%. With the DR-to-Peak ratio being neither very high nor very low, and with a small time-frame for load shifting $drTime$ is 2, 1, 4 for respectively DR_{Base}, DR_{Half} and DR_{Double}, it is interesting to find that the total upward and downward change in demand is on the smaller scale. The upward and downward DR-to-Demand ratio for DR_{Base} is 3.94% and 3.82%, for DR_{Half} it is 2.44% and 2.37%, and for DR_{Double} it is 5.72% and 5.56%. The share of load shifting of total commercial and industrial electricity demand from $HVAC$ is higher than the DR-to-Demand ratio from all DR measures. The ratio increase ranges from 8.0% to 40.0%, with DR_{Half} having the least increase and DR_{Double} having the highest increase in ratio.

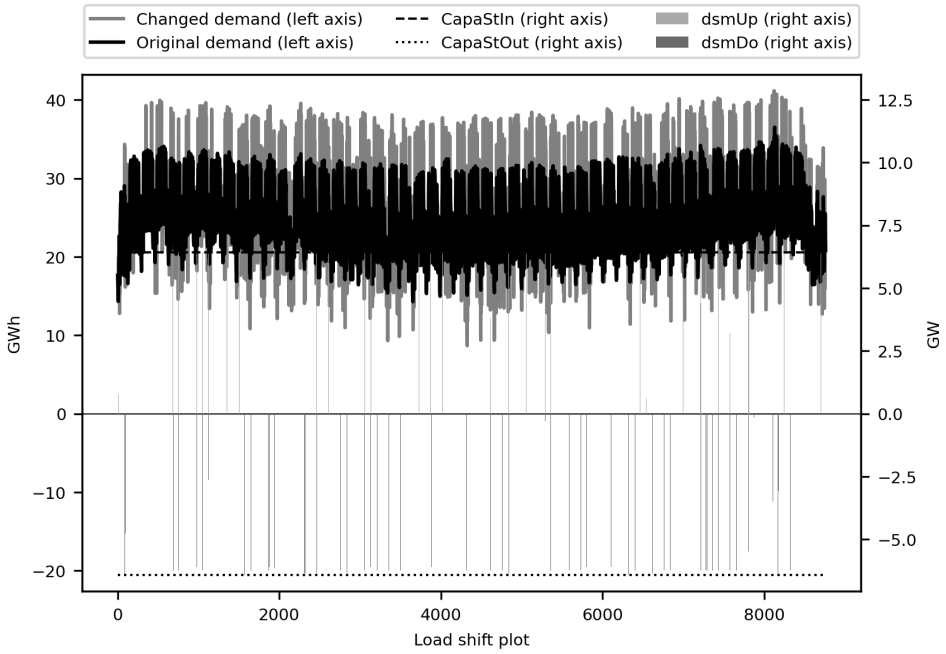

Figure 31: Load profile for DR_{Base} time-step 0-8760, $HVAC$

Closer observations of time-period 96-288 shows that load shifting from $HVAC$ occurs three times for all cases, as can be seen in Figure 32, 33, and 34. Analysing the figures, a clear trend can be seen from the time period that the changed demand from downward load shifting is not to smaller than the original minimum load even if it is possible. Looking at one specific upward shift (time-step 133) in the load profiles, the affect of changing the parameter $drTime$ on downward load shifting can be found from observing figures. For DR_{Base} (Fig. 32) a $drTime$ of 2, time-window for downward

shifting is 131-135 for time-step 133. With a four hour window for downward load shifting, and one hour at maximum upward capacity load shift, it is found that the downward shift is split in two hours, time-steps 131 and 135. The largest share for compensation of the upward shift occur in time-step 135, it is then better to shift more in time-step 135 than equal distribution of downward load shifting or a higher share in time-step 131. In contrast to DR_{Base} the upward shift in hour 133 is not at maximum capacity in DR_{Half} (Fig. 33). DR_{Half} has a two hours window from the $drTime$ is 1, forcing the downward shift to time-step 132 and 134. As can be observed in the figure, the downward shifting only occur in time-step 134. Looking at the load shifting for DR_{Double} shown in Figure 34, with a $drTime$ of 4, thus a 8 hour window for downward shifting, there is still no other upward shift in the surrounding hours. Time-step 133 has a upward shift at maximum, the same as DR_{Base} however other times for downward shifting. With the bigger time-window from time-step 129 to 137, it is found that the main downward shift occurs in the last hour, with smaller quantities in other hours except in time-step 132 and 134. From the three cases, it is evident that downward shifting in time-step 132 and 134 is avoided.

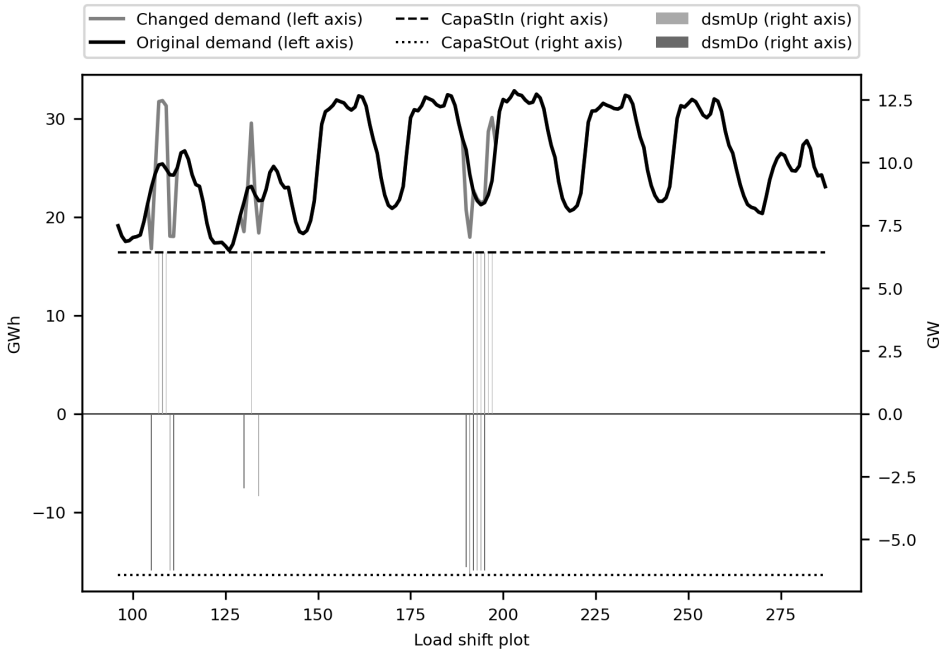

Figure 32: Load profile for DR_{Base} time-step 96-288, $HVAC$

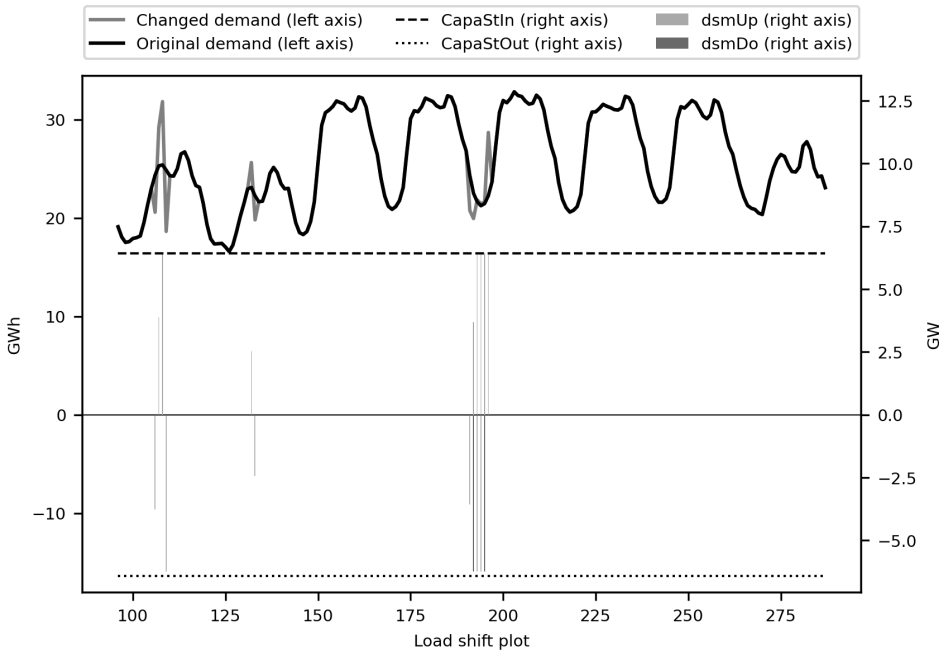

Figure 33: Load profile for DR_{Half} time-step 96-288, $HVAC$

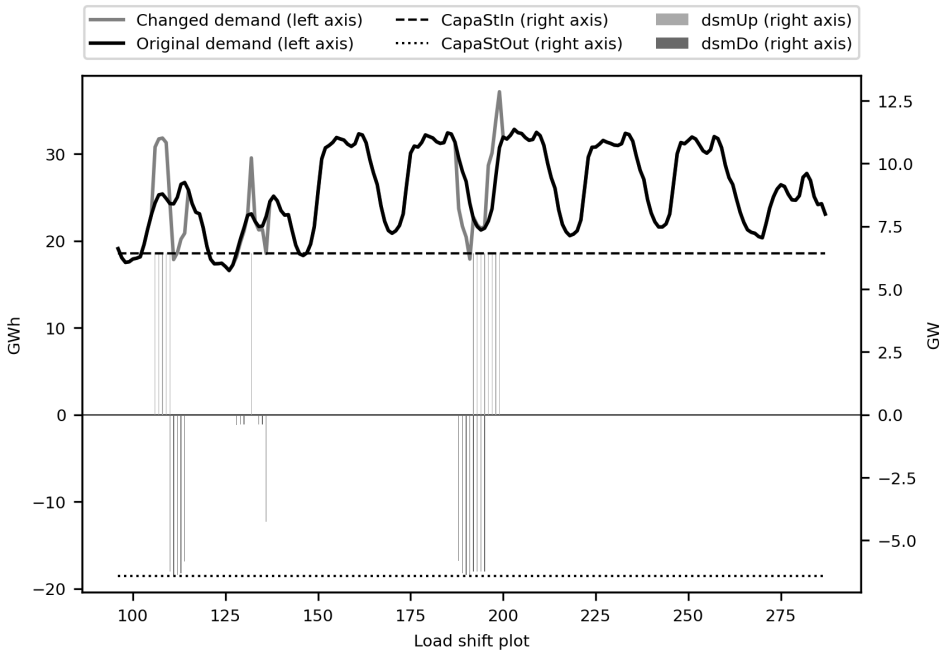

Figure 34: Load profile for DR_{Double} time-step 96-288, $HVAC$

In contrast to time period 96-288, a new minimum load is found in the changed demand profile (Fig. 35, 78 and 79). In addition, load shifting occur more frequently. The DR cases share similar time-steps for load shifting and both upwards and downwards shifting is close to or at maximum capacity, there is seldom shifting of smaller quantities of the installed capacity, resulting in steeper valleys and higher peaks.

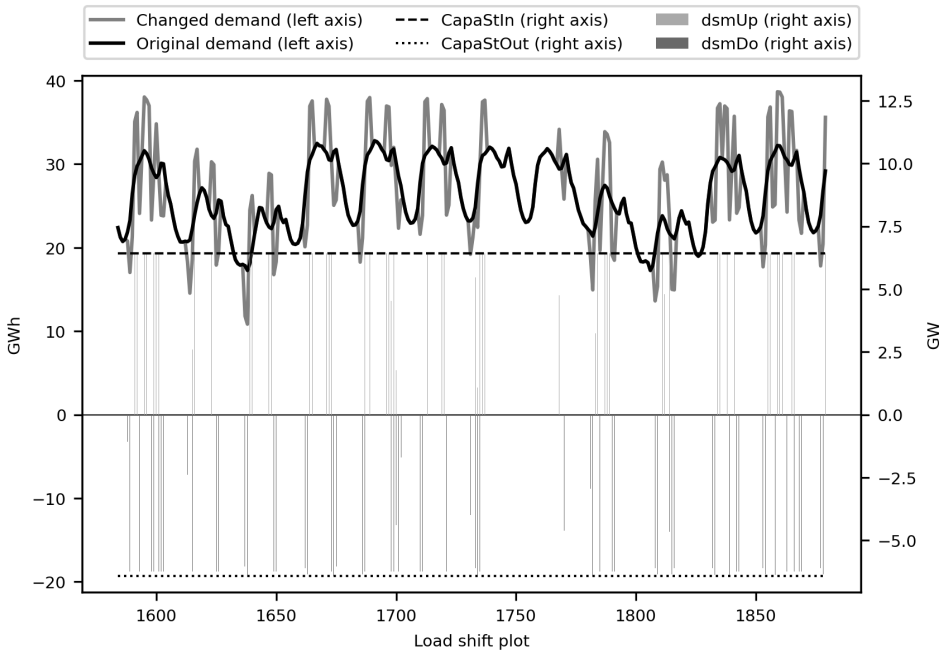

Figure 35: Load profile for DR_{Base} time-step 1584-1880, $HVAC$

5.1.7. Impact on commercial and industrial electricity load profile from Cooling and Water

When analysing the load profiles from $Cooling\ and\ water$, it is clear that the DR measure has almost no impact on the commercial and industrial electricity total yearly demand. The average demand is 25.54 GW and the peak demand remains unchanged for all DR cases at 36.51 GW in time-step 8130 as can be seen in the Figures 36, 80, and 81. The installed capacity for $Cooling\ and\ water$ is 1107 MW. Resulting in a DR-to-Peak ratio of 3.03%. The upward and downward DR-to-Demand ratio of the total commercial and industrial electricity demand for DR_{Base} is 0.49% and is 0.48%, for DR_{Half} it is 0.28% and 0.27%, and for DR_{Double} it is 0.78% and 0.76%. The combination of a small installed capacity with a relative small to large time-window for load shifting ($drTime$ is 6, 3, and 12 for respectively DR_{Base}, DR_{Half}, and DR_{Double}), it is interesting to find that the share of total upward and downward change in demand is small for all three cases. Since $Cooling\ and\ water$ and $HVAC$ are mapped to the same demand, it is interesting to compare how they differ. While $Cooling\ and\ water$ have installed the maximum upward and downward load shifting potential of 1107 MW, whereas $HVAC$ has an installed capacity of 6427 MW, leading to $HVAC$ having a factor of 5.8 times the installed $Cooling\ and\ water$ capacity. Unexpectedly, $HVAC$ has a higher DR-to-Demand ratio and a higher DR-to-Peak ratio than $Cooling\ and\ water$. Comparing the difference input parameter between $HVAC$ and $Cooling\ and\ water$, it is found that variable cost is 4 times higher for $Cooling\ and\ water$, however its investment and fixed OM cost is half of $HVAC$ cost, additionally the time-shift parameter $drTime$ is larger. With the low investment and fixed OM cost and the lower DR-to-Demand ratio, $Cooling\ and\ water$ has a lower total cost. This is a direct consequence of lower potential capacity than $HVAC$ and a higher variable cost. Even if cooling has lower total cost, it is not used all the

time, and $HVAC$ is used instead with its shorter load shifting window and lower variable cost.

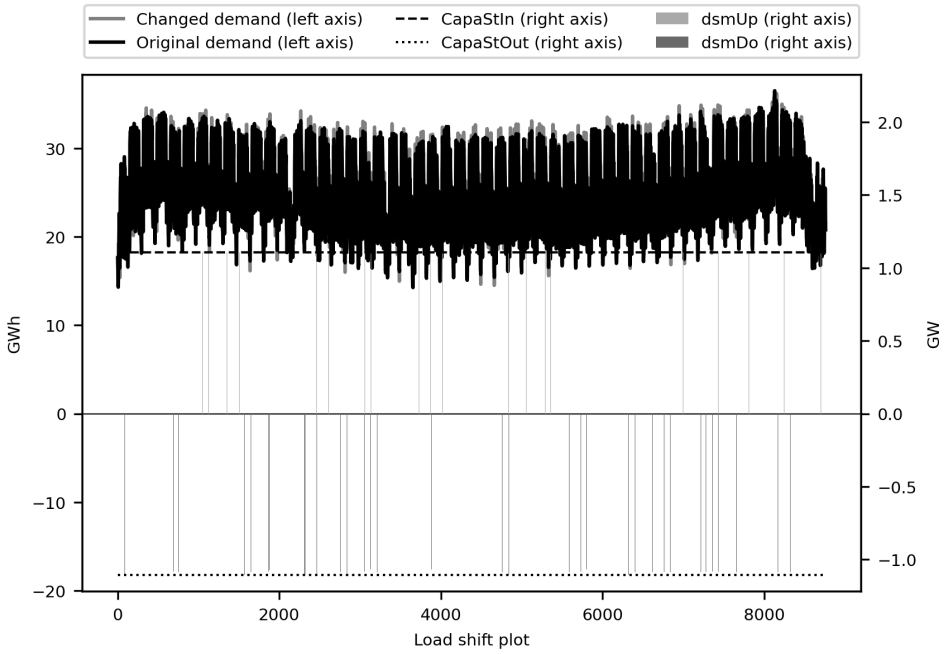

Figure 36: Load profile for DR_{Base} time-step 0-8760, $Cooling\ and\ water$

There is minimal load shifted in time-period 96 to 288 from $Cooling\ and\ water$ on the commercial and industrial electricity demand for the three cases, as shown in Figure 37, 38, and 39. This is consistent with the changes from $HVAC$ in the same period on the commercial and industrial electricity demand. In Figure 37 and 39 the load shifting is centred around three time-periods. The load shifts from $Cooling\ and\ water$ occurs during or around the same time-steps as $HVAC$ load shifts. For DR_{Half} (Fig. 38), the smaller time window causes the removal of one of the times of load shifting seen in 37 and 39. Therefore it is reasonably to assume that there is excess feed in energy in the surrounding area of the downward shifts, however the installed capacity put a limitation on how much load is optimal to be shifted, in contrast to $HVAC$, which have a smaller $drTime$ and higher installed capacity.

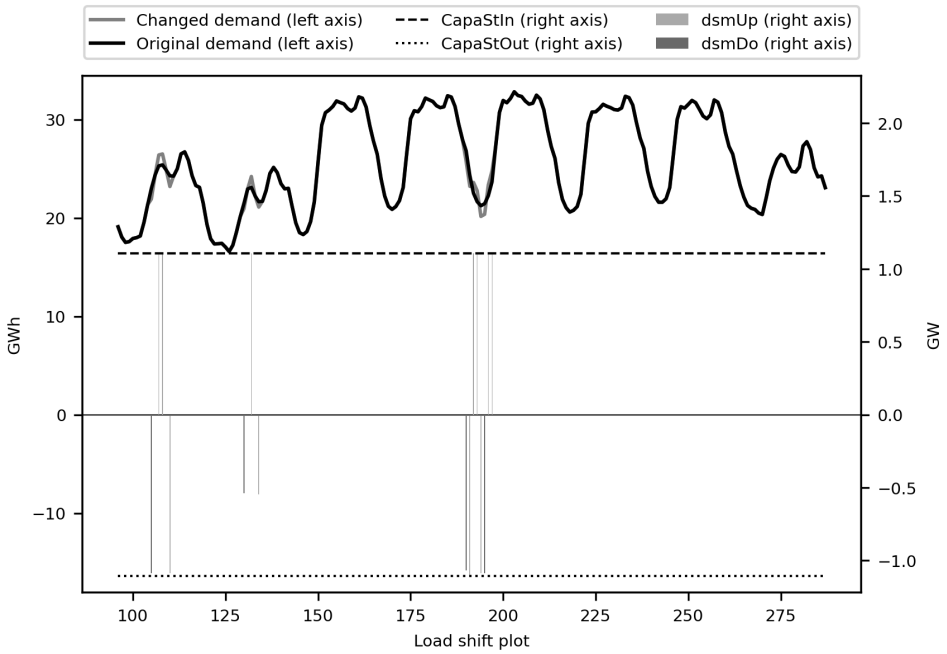

Figure 37: Load profile for DR_{Base} time-step 96-288, $Cooling\ and\ water$

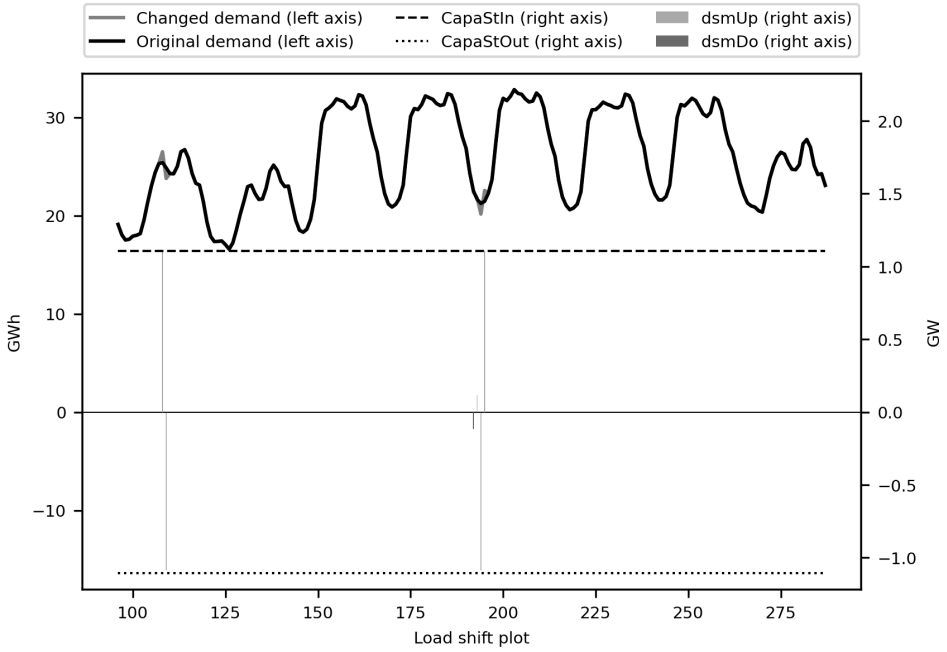

Figure 38: Load profile for DR_{Half} time-step 96-288, $Cooling\ and\ water$

Studying the change from $Cooling\ and\ water$ in the load profile in time-period 1584-1880 (Fig. 40, 82, and 83), it is observed that the frequency of shifting is ramped-up, compared to hours 96-288. This is similar to the observed changes in $HVAC$ in these time periods. The shifting pattern from $Cooling\ and\ water$ is relatively the same between the DR cases, with small increase and reduction of different peak loads. Most of the upward and downward load shifts is at maximum capacity (Fig. 40). DR_{Double} has of predicable the most change, as the bigger $drTime$ can therefore shift downwards at periods with lower load demand (i.e. during the night). Overall it is the shifting capacity that limits

load shifting of the demand profile.

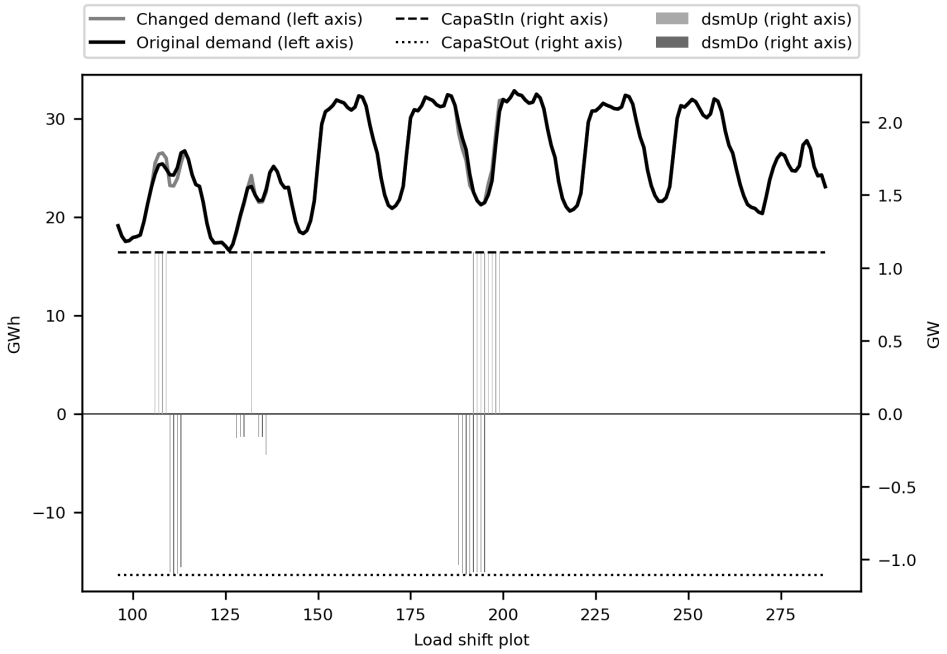

Figure 39: Load profile for DR_{Double} time-step 96-288, *Cooling and water*

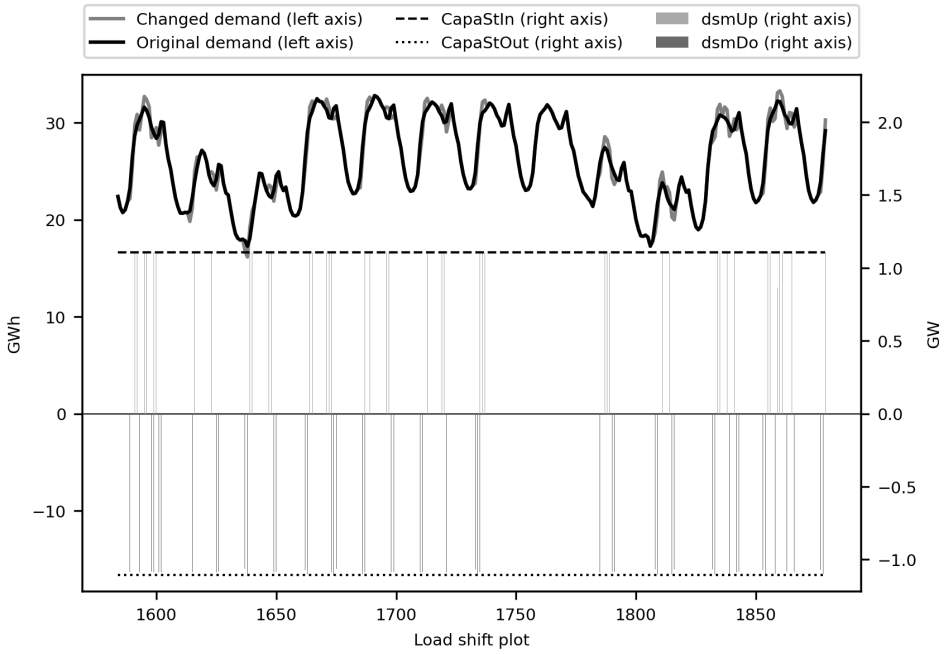

Figure 40: Load profile for DR_{Base} time-step 1584-1880, *Cooling and water*

5.2. Load shifting analysis from the indirect Demand Response formulation

This section discusses the results from the TR cases described in section 4.2 by the indirect DR formulation described in section 3.1. The change in load profile for the TR cases with the indirect method is shown in Figure 41, 42, 43, 44, and 45. When comparing the overall change in the load profile from the indirect method with the DR cases (Fig. 6, 7, and 8), it is only the two-hour shift

(TR_2) that seems to have a somewhat close resemblance to the changed demand profile in the DR cases. The other TR cases have significantly higher peak loads, for example TR_{12} have a new peak load over 500 GW. Thus a detailed examination of the flexibility "capacity" and load shifted from the indirect method is carried out compared to the results from the direct method. When analysing the largest upward and downward shift, it is found that they have significantly higher capacity quantity than the installable DR potential (seen Table 9). The maximum upward and downward shift for TR_2 is 89.66 GW and 89.66 GW. This is a factor of 2.3 in comparison to DR cases with a maximum potential of 38.92 GW. For TR_4 the largest upward and downward shift is 168.78 GW and 139.42 GW, resulting in a factor of respectively 4.34 and 3.58. Case TR_6 maximum increase and decrease of demand is 183.96 GW and 119.04 GW, a factor of 4.73, 3.06. For TR_8 largest upward and downward shift is 282.65 GW and 129.18 GW, ending up at a factor of respectively 7.26 and 3.32. Lastly, TR_{12} maximum increase is 359.17 GW and max decrease 138.75 GW, a factor of 9.23 and 3.57 of the DR potential. While TR_2 has equal upward and downward load shifted due to the temporal resolution, there are no constraint telling that the upward and downward shifting of load have to be equal. The downward factor seems to be "saturated" around a factor of three, suggesting that the energy system distributes the downward load shifting over several time-steps. In contrast, the upward factor becomes increasingly higher by increasing the temporal resolution in the TR cases. The system moves the upward shifts of the demand to periods with excess feed-in energy, to reduce the system cost. The results show that the average values for downward and upward shifting is 9.09 GW and 9.56 GW for TR_2, 12.04 GW and 12.57 GW for TR_4, 15.17 GW and 15.78 for TR_6, 15.38 GW and 15.98 GW for TR_8, 34.36 GW and 34.88 GW TR_{12}. All the average values are higher than the average quantities shifted either upwards or downwards in the DR cases. From the smallest shift 2-hour, the average values is almost the double of the average quantity in DR_{Base}, which has an average downward and upward load shifted of 5.48 GW and 5.57 GW. In addition, the average quantities for shifting TR_{12} is almost the same as the DR cases maximum installed capacity. The downward and upward DR-to-Demand ratio is 5.44 % and 5.72% for TR_2, 7.20% and 7.51% for TR_4, 9.07 and 9.43% for TR_6, 9.19% and 9.55% for TR_8, and finally 20.54% and 20.86 % for TR_{12}. The increase in DR-to-Demand was expected, however not the degree of difference between the DR-to-Demand ratio with the indirect method and the direct method. The indirect method can give an indication on the amount of capacity needed for flexibility in the energy-system. However, there is no constraints or parameters restricting the method, allowing the system to freely optimise with the flexibility given by the temporal resolution of the demand profile. From the load profiles it can be concluded that the indirect method of flexibility does not give a realistic load shifting. Moreover, the maximum load shifting quantities is unrealistic with regards to the German DR potential found in Gils (2014) and Gils (2016). Compared to shifted values in the DR cases, the flexibility from the indirect method is resulting in an over-estimation of the load shifting in the energy system when system is allowed to

freely change the demand.

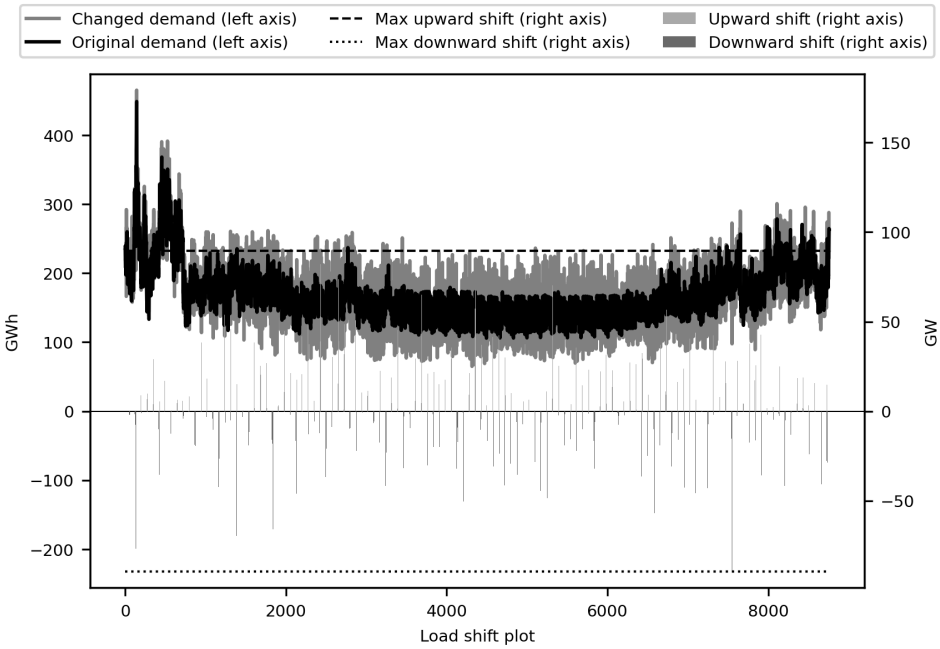

Figure 41: Load profile for TR_2 time-step 0-8760

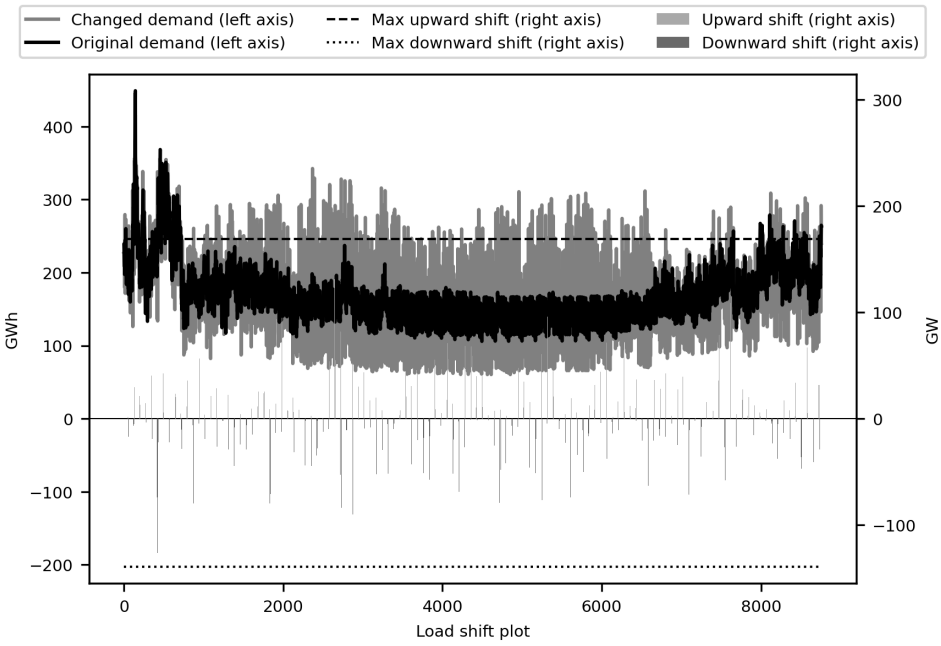

Figure 42: Load profile for TR_4 time-step 0-8760

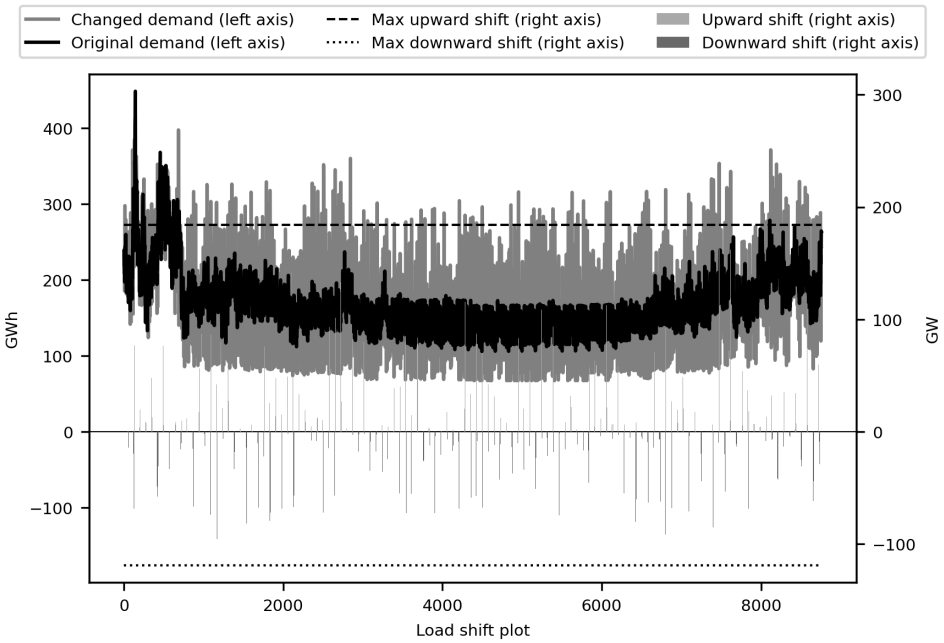

Figure 43: Load profile for TR_6 time-step 0-8760

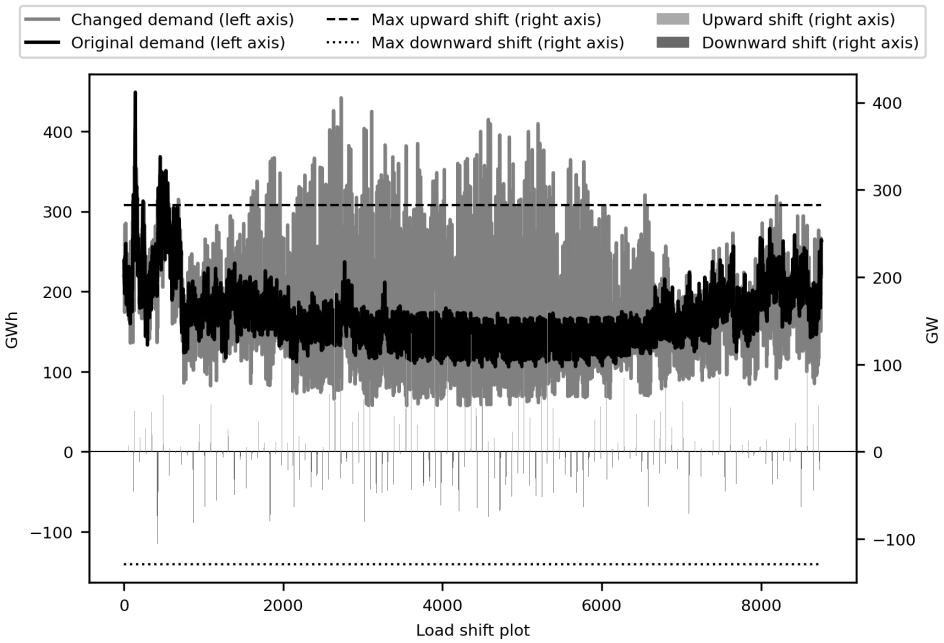

Figure 44: Load profile for TR_8 time-step 0-8760

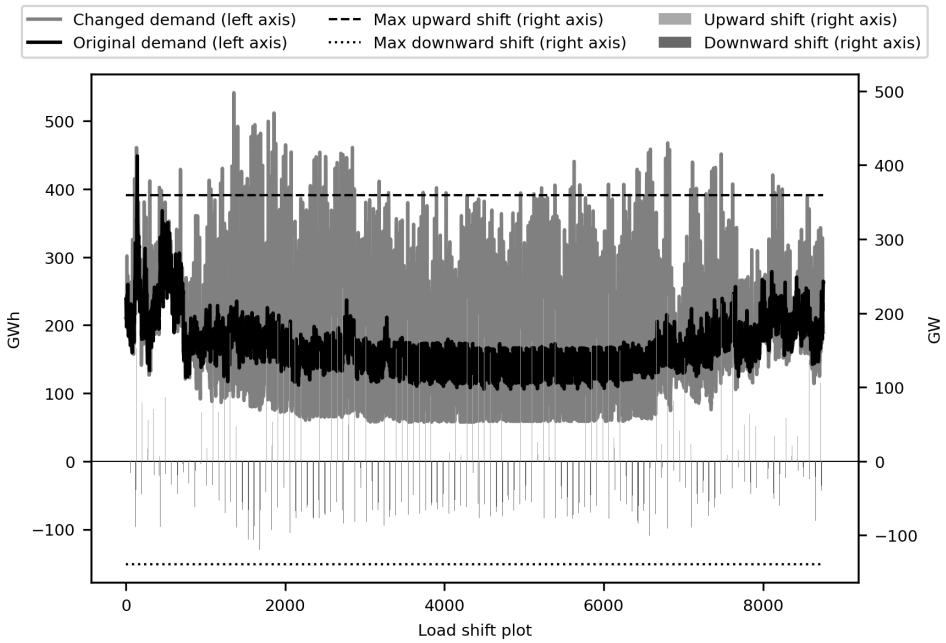

Figure 45: Load profile for TR_{12} time-step 0-8760

Based on the findings of change in the total load profile, it was decided to only proceed with a further examination in two time-periods for TR_2, which was done for the DR cases. Figure 46 and 47 shows the load profile for the time period 96-288 and 1584-1880. The equivalent plots for the remaining cases can be found in the Appendix A.2. Since the system can change the demand in 2 hour time-steps, i.e. increasing the load in one hour and reduced it in the other. The system then has three options, either shift first upwards, or start with downward shift or not change the demand at all. This can be observed in Figure 46, the original peak load is reduced, however to compensate for the reduction the previous time-step is increased and result in a higher peak load than the original. Since the 2 hour time-steps is defined in the input data, it cannot have downward shift for the peak load in the following hour based on the temporal resolution. The temporal resolution of the input data fixes the window for which time-steps the load can be shifted with, compared to direct method which consider demand increase in every hour, with downward shifting window to that specific time-step. The time-period 96-288 has more frequent load shifting compared to the total change in DR cases in the same period. With frequent shifting, the difference in demand from one time-step to the next is increased. When looking at time-period 1584-1880 in Figure 47, the observed change in time-step 1865 and 1866 shows a 48.53% increase in demand in time-step 1865 demand and a 48.25% decrease in demand in time-step 1866 in comparison to original demand. The upward and downward DR-to-Demand ratio for this period is 6.62% and 6.45%, approximately 1% higher than the overall DR-to-Demand ratio from TR_2, in addition it is also higher than the DR-to-Demand ratio for the DR cases in the same period.

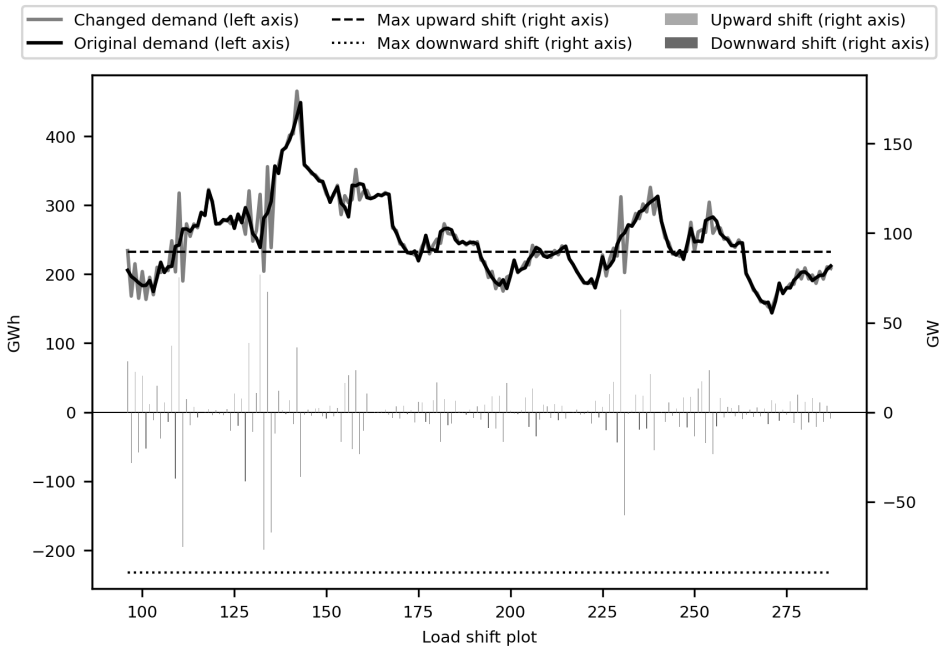

Figure 46: Load profile for TR_2 time-step 96-288

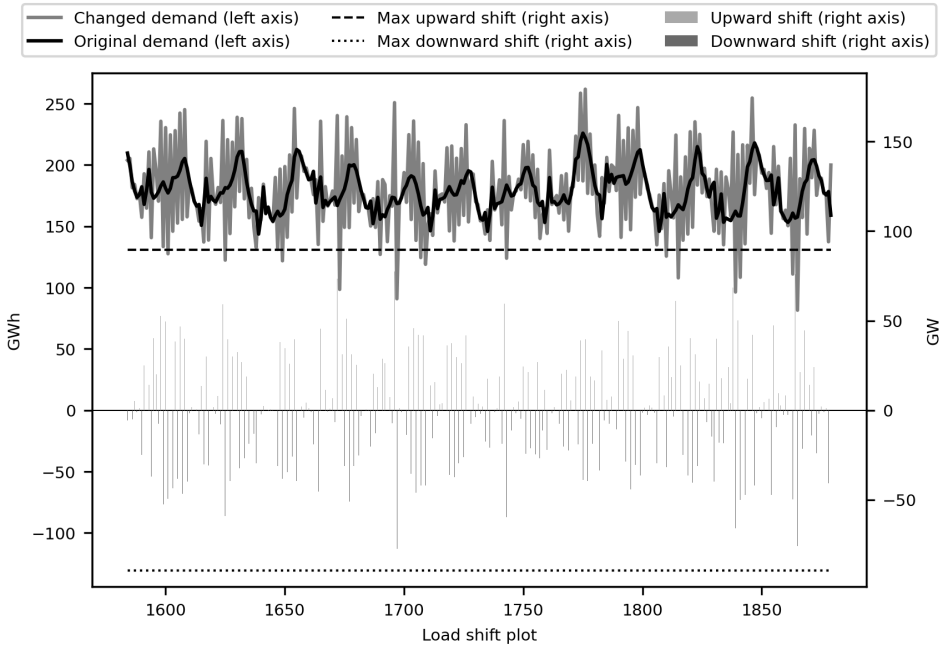

Figure 47: Load profile for TR_2 time-step 1584-1880

5.3. Impact on storage and capacity expansion

Given the substantial findings on how the direct and indirect method affect the load profile, the impact on storage and capacity expansion is deliberated. The load flexibility influence of the storage capacity is shown in Figure 48 for the indirect method. The findings show that it is battery storage and hydrogen storage that is mainly reduced. Battery has a higher expansion cost and is the first technology that experience capacity reduction, to minimise the system costs. Hydrogen storage does not have high expansion cost, however the hydrogen plant and electrolyzer which utilise the stored

hydrogen have high expansion cost. It is interesting to note that TR_4 experience an increase of hydrogen storage capacity, and a decrease in battery storage. TR_8 have also unexpected result where the hydrogen storage is higher than hydrogen storage share in TR_6 and that battery storage is larger than the reference value. This result was not anticipated, however the reason for this is likely the dividing of daily time-steps in the temporal resolution and the demand profile.

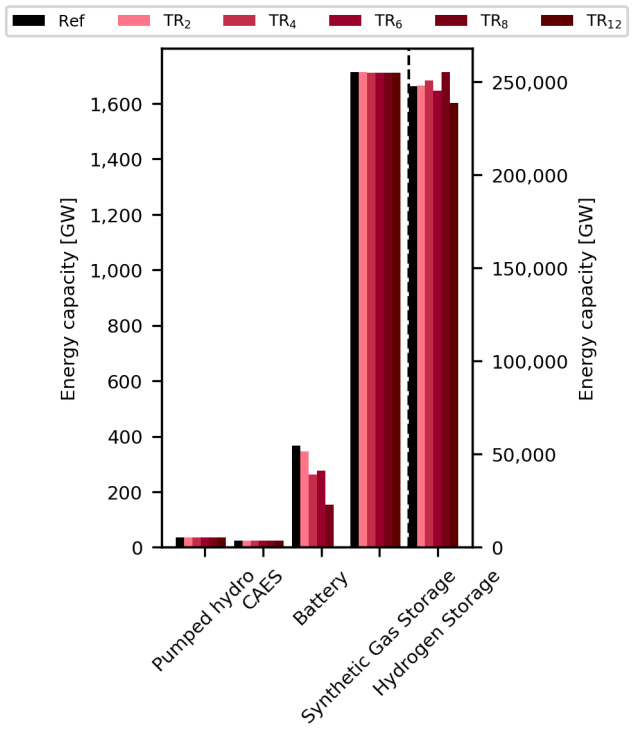

Figure 48: Energy capacity of storage technologies for TR cases

For all DR cases, the maximum potential for upward and downward load shifting capacity is implemented of 38.92 GW as stated earlier (Section 5.1). The equal capacity for upward and downward shifting is a result of a input parameter, fixing the ratio between energy in and out of a storage technology to 1. This was set as to not complicate the constraints by finding the maximum of the two capacity variables (See Eq. 69 and 64). This is a limitation of the model implementation since the potential of upward and downward load shifting is not necessarily the same (Gils, 2014). It is interesting to evaluate how the $drTime$ parameter has affected the storage technologies in the individual cases since the installed capacity is the same in all three cases. As can be seen in Figure 49, DR_{Base} have a reduction in battery and hydrogen storage as seen in the TR cases. In the DR_{Half} case, the flexibility from the DR technologies is not enough to cover the demand when there is low input of variable renewable energy, thus more storage is needed to increase the flexibility in the energy system. The load flexibility introduced by both DR and TR cases reduces the storage capacity. And in both cases, it is the battery storage and hydrogen storage that is reduced.

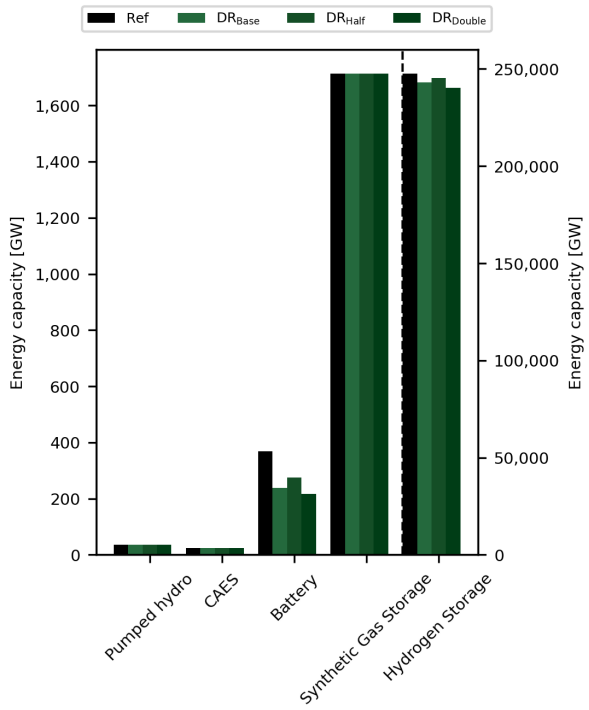

Figure 49: Energy capacity of storage technologies for DR cases

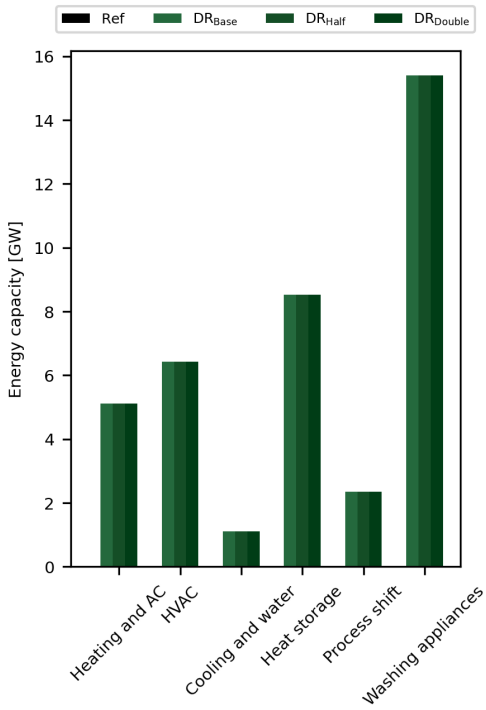

Figure 50: Energy capacity of DR technologies for DR cases

The total renewable energy capacity installed in the reference case is 1495.98 GW. DR_{Base} has a 1.41% decrease in energy capacity, DR_{Half} has a 0.75% decrease, and DR_{Double} has a 1.87% decrease. In the reference scenario, photovoltaics roof and onshore wind power have the largest capacities installed. The photovoltaic, wind offshore and wind onshore installable capacity is fully utilized, this is true for all cases as can be seen in Figure 51 and 52. In comparison, photovoltaic roof and agriculture is not installed at maximum capacity. Comparing photovoltaic roof to photovoltaic agriculture, it has a higher expansion cost but a lower operation cost. All DR and TR cases except from TR_8 have a reduction of photovoltaic roof capacity. The TR_8 photovoltaic roof capacity is 1.3% larger than the Ref case, this result was not expected. Disregarding TR_8, there is almost no difference in photovoltaic roof between TR_2, TR_4 and TR_6 with regards to the reference case before a 7.6% decrease in TR_{12}. The findings from the DR cases are as expected, with a larger installed renewable energy capacity in DR_{Half} than DR_{Base} with a smaller flexibility from DR measures and that DR_{Double} have the smallest capacity.

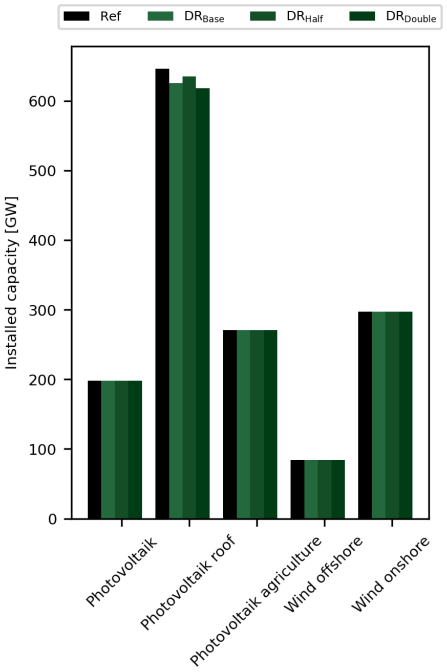

Figure 51: Installed capacities for DR cases

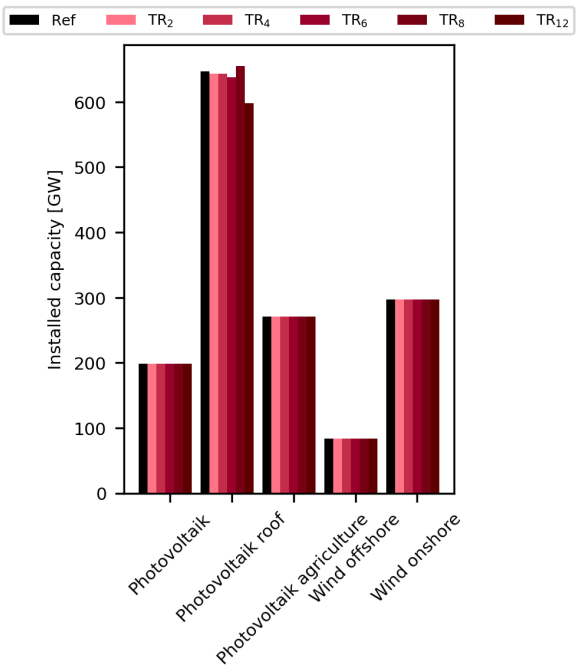

Figure 52: Installed capacities for TR cases

5.4. Impact on the system costs

In this section the resulting system costs is discussed. Figure 53 shows the total system cost for all of the cases run in this case study. As can be seen, the reference case has a total system cost of 121690.64 M€. From the extra flexibility, either from the indirect or the direct method, a reduction in total system cost is achieved for all cases. The temporal resolution case TR_{12} has the highest decrease in total cost at 9.7% compared to the reference case. As a result, the economic potential of the flexibility from the 12-hour time-step is 11805.71 M€. However, it is important to keep in mind that the indirect method does not have any cost of load shifting. Table 11 presents the absolute difference between the reference case, the DR cases and the TR cases. The cost matrix shows how the total cost correlates between two given cases. It is interesting to see how the difference in system cost vary in column TR_8 compared to the adjacent columns, as the total cost increases from TR_6 before a large decrease in TR_{12}. The cost increase from TR_6 to TR_8 and the large cost reduction TR_{12} does not seem realistic. The result could be a consequence of how the time-steps in a day were defined in the rooted three. The reason for this rather contradictory result is still not completely clear, and utilizing temporal resolution of eight and twelve hour time-steps should therefore be avoided. The single most striking observation to emerge from the data comparison is the small difference between TR_6 and DR_{Double}. This emphasises that the a 6-hour time-step and the DR technologies implemented with a half load shifting time have approximately the same amount of cost reduction with two very different DR-to-Demand ratio in the energy system.

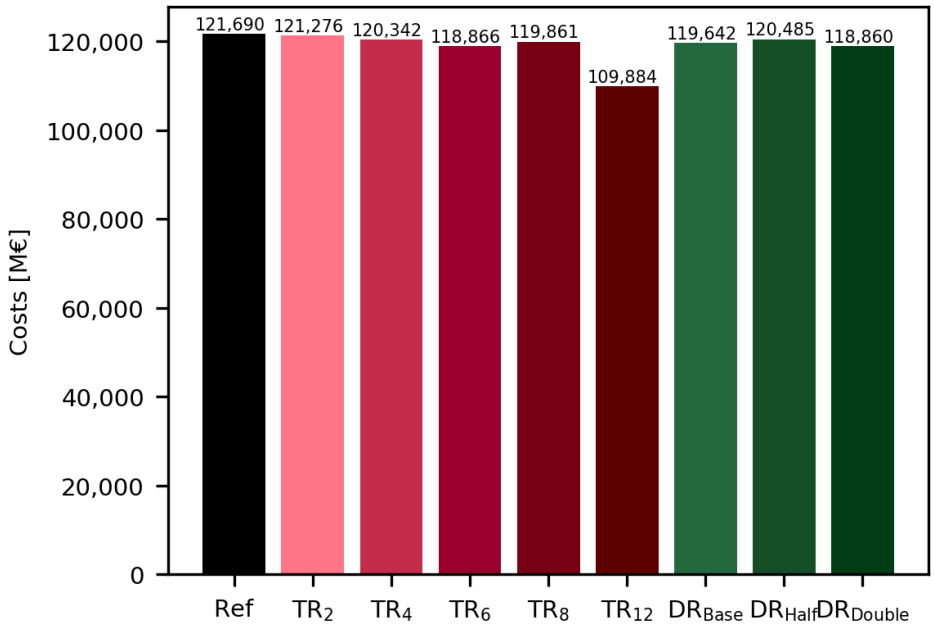

Figure 53: Total system cost

Table 11: Total system cost matrix

	Ref	TR_2	TR_4	TR_6	TR_8	TR_{12}
Ref	0.0	414.09	1348.48	2823.75	1829.12	11805.71
DR_{Base}	-2047.93	-1633.84	-699.45	775.83	-218.81	9757.78
DR_{Half}	-1204.75	-790.67	143.72	1619.0	624.37	10600.96
DR_{Double}	-2830.43	-2416.34	-1481.95	-6.67	-1001.31	8975.28

The cost matrix present the absolute difference between the scenarios. The matrix is calculated by subtracting a column value from the row values.

To distinguish where the changes in cost arise, the conversion technology, storage and the renewable energy cost are plotted in Figure 54 and 55 for respectively the TR and the DR cases. The figures shows the change in cost for the respective technologies. Photovoltaic roof is the only renewable energy with the cost reduction, the reduction varies due to the change in installed capacity and the operation cost. The results from the indirect method show that four of the five storage technology implemented in the cases has a change in cost. While battery, CAES and pumped hydro has varying reduction in cost with regards to the reference values, hydrogen storage has increased cost for TR_2, TR_4, and TR_8 and decrease in cost in TR_6 and TR_{12} with regards to the reference value. In comparison, the costs from the direct method (Fig. 55) show that CAES and pumped hydro has an increase in cost with regards to the reference value, while battery and hydrogen storage have a reduction in cost with regards to the respective reference cost. Gas plant is not installed in the indirect and direct cases, thus there is no cost associated with gas plant, additionally the methanation cost is the same for all cases. Looking at figure 54, there is a negligible increase in hydrogen plant cost, whereas the electrolyzer cost has a decrease in TR_6 and TR_{12} and an increase in the three remaining cases. from figure 55, a reduction in cost of the conversion technologies electrolyzer and hydrogen

plant is found for the direct method. The direct method quantifies the cost from the DR measures *Heat Storage*, *Washing Appliances*, *Process shift*, *Cooling and water*, *HVAC* and *Heating AC*. The Figure 55 shows that DR have low costs, overall, the total share of DR costs is rather small in comparison to the other storage technology costs. Implementing DR flexibility leads to a cost reduction in mainly photovoltaic roof, battery, electrolyser and hydrogen plant.

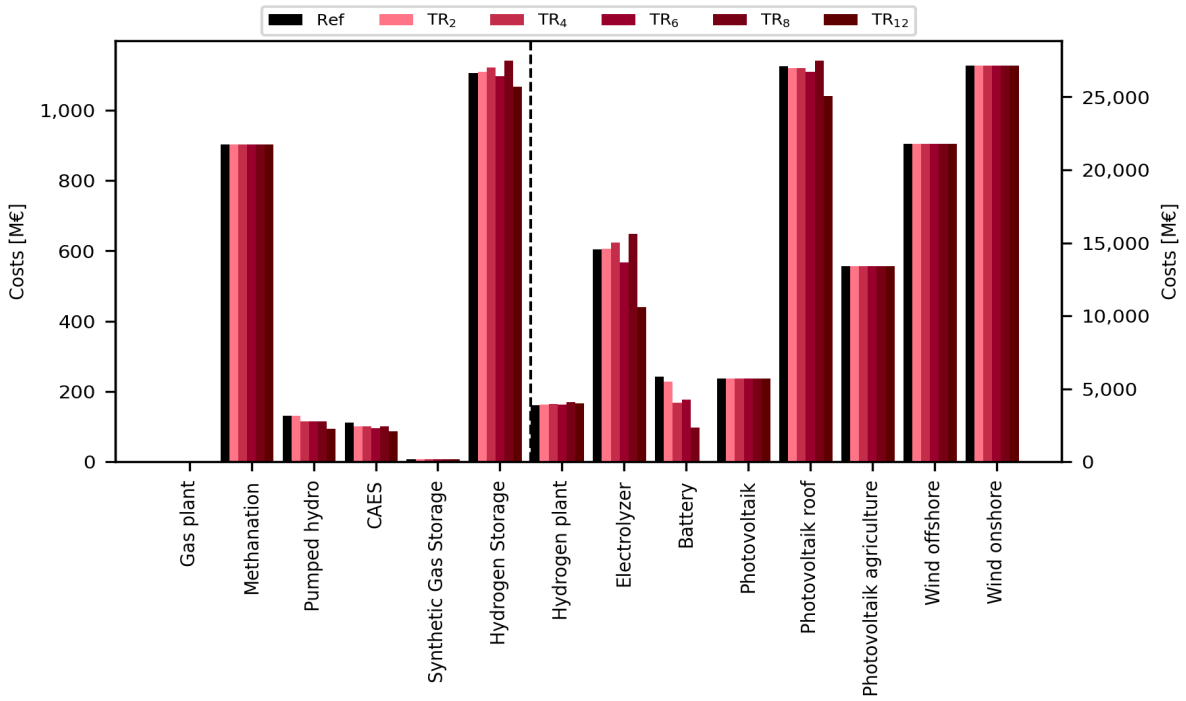

Figure 54: Cost of individual technologies for TR cases [M€]

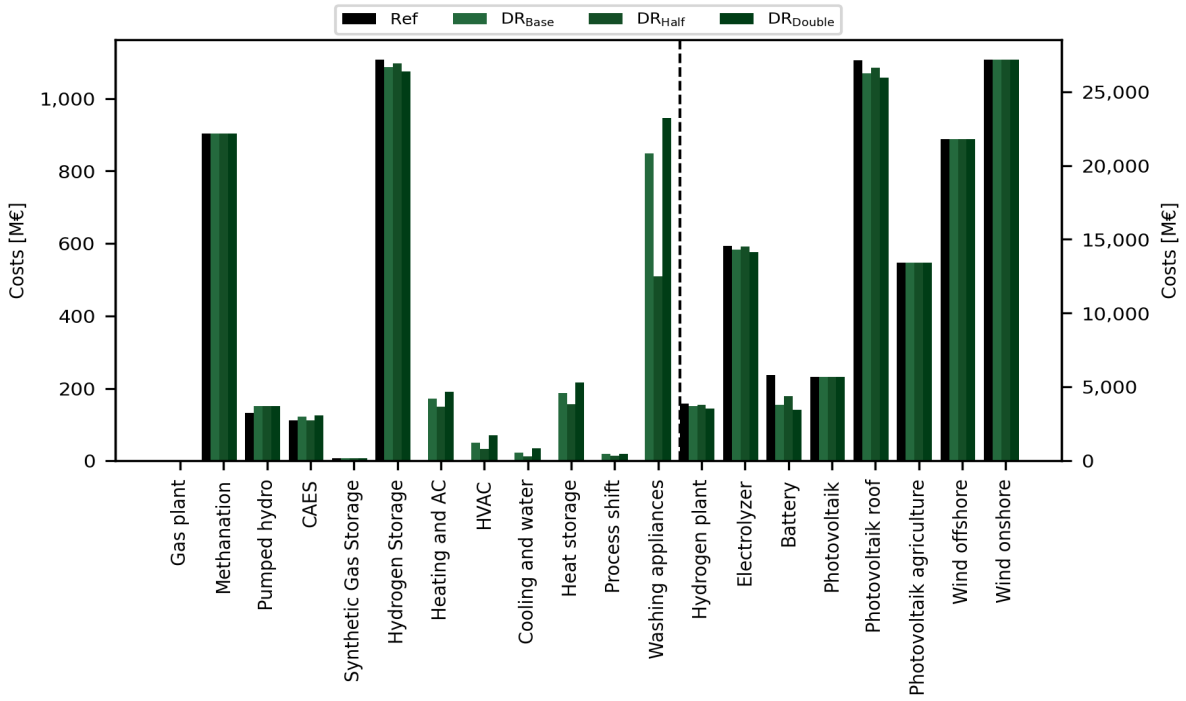

Figure 55: Cost of individual technologies for DR cases [M€]

6. Conclusion

This thesis has investigated two methods of DR representation in a graph-based framework. The evidence from this study suggest that a direct modelling approach is better for modelling load shifting. The indirect method splits the time-steps defined by vertices in the hierarchical three. For DR modelling it is the daily hourly time-steps that is relevant for load shifting, the vertices splits the daily timesteps into groups, and load shifting cannot occur between two groups. By splitting the hourly timesteps in a day in different groups, it can neglect the actual optimal time-steps relevant for load shifting. The graph-based framework cannot then optimally shift load between hours in two different groups if that would have been the best for load shifting based on the input data. As opposed to the direct approach where an upward load shift is balanced with downward load shift(s) optimally over a window of time-steps before and after the upward shift. The findings from the DR cases with the direct approach show satisfactory results demonstrating how the load shifting pattern changes with regards to available feed-in energy and the demand.

Considerable insights have been gained with respect to individual DR measures and how it affect the demand. The DR measures $Heat\ Storage$, $Washing\ Appliances$, $Process\ shift$, $Cooling\ and\ water$, $HVAC$ and $Heating\ AC$, are directly mapped to the final energy carrier demand from different sectors. The findings demonstrate that the $Washing\ Appliances$ and $Heat\ Storage$ mapped to the residential and commercial sector has the biggest contribution of load shifting. Whereas $Process\ shift$ and $Cooling\ and\ water$ has the smallest impact on the load profile. The result form the DR cases are consistent with previous findings, showing that the heat storage final demand users is the most significant demand profile for load shifting, and further work should therefore focus on the residential and commercial heat demand (Marañón-Ledesma and Tomasgard, 2019). However, it is important to recognise that the existing and future DR potential is dependent on the development in these sectors.

The results from the indirect approach suggest that a short time-step resolution can give a general indication on total system cost reduction from increasing the flexibility in the model. Further work needs to be carried out to establish whether or not a short time-step resolution with the indirect approach is applicable for modelling load shifting in the graph-based framework. To do so, modelling the sector coupling in detail is the key; implementing actual technology with capacity limit such as heat pumps instead of the "dummy technologies" in this study. Taken together, the findings suggest that a indirect approach can give an indication in the total system cost reduction but should not be utilized for load shifting studies without a detailed modelling of sector coupling.

The prospect of being able to increase the flexibility in an energy system with DR and reduce the system costs, increases the incentive for future research. Further sensitivity analysis on individual DR measure are needed to estimate the individual role of DR in the energy systems, to support policy decisions on DR. And additional constraints should be implemented in the direct method to hinder loss of comfort by restricting the amount of load shifting interventions per day. The case studies

show that DR can play a role in the future energy system with high shares of renewable energy to increase the system flexibility. The case results are promising and should be further studied for a longer time period and in a more complex energy-system, implementing CO_2 costs, and allowing trade and exchange between regions, to determine what role DR can have on the pathway to a 100% renewable energy system in 2050.

References

Climate Change, U. N. F. C. on (2015). *The Paris Agreement*. Available at: https://unfccc.int/sites/default/files/english_paris_agreement.pdf. Paris: UN General Assembly.

Gils, H. C. (2014). "Assessment of the theoretical demand response potential in Europe." In: *Energy* 67, 1–18.

– **(2015)**. "Balancing of intermittent renewable power generation by demand response and thermal energy storage". PhD thesis. Universität Stuttgart.

– **(2016)**. "Economic potential for future demand response in Germany – Modeling approach and case study." In: *Applied Energy* 162, 401–415.

Göke, L. (Nov. 2021). "A graph-based formulation for modeling macro-energy systems." In: *Applied Energy* 301, 117377.

Göransson, L., Goop, J., Unger, T., Odenberger, M., and Johnsson, F. (2014). "Linkages between demand-side management and congestion in the European electricity transmission system." In: *Energy* 69, 860–872.

Marañón-Ledesma, H. and Tomasgard, A. (2019). "Analyzing Demand Response in a Dynamic Capacity Expansion Model for the European Power Market." In: *Energies* 12.15.

Misconel, S., Zöphel, C., and Möst, D. (2021). "Assessing the value of demand response in a decarbonized energy system – A large-scale model application." In: *Applied Energy* 299, 117326.

Müller, T. and Möst, D. (2018). "Demand Response Potential: Available when Needed?" In: *Energy Policy* 115, 181–198.

Palensky, P. and Dietrich, D. (2011). "Demand Side Management: Demand Response, Intelligent Energy Systems, and Smart Loads." In: *IEEE Transactions on Industrial Informatics* 7.3, 381–388.

Roos, A. and Bolkesjø, T. F. (2018). "Value of demand flexibility on spot and reserve electricity markets in future power system with increased shares of variable renewable energy." In: *Energy* 144, 207–217.

Schill, W.-P. and Zerrahn, A. (2018). "Long-run power storage requirements for high shares of renewables: Results and sensitivities." In: *Renewable and Sustainable Energy Reviews* 83, 156–171.

Strbac, G. (2008). "Demand side management: Benefits and challenges." In: *Energy Policy* 36.12. Foresight Sustainable Energy Management and the Built Environment Project, 4419–4426.

Zamora Blaumann, A. et al. (2021). *The potential of sufficiency measures to achieve a fully renewable energy system - A case study for Germany : A case study for Germany*. Tech. rep. Technische Universität Berlin.

Zerrahn, A. and Schill, W.-P. (2015). "On the representation of demand-side management in power system models." In: *Energy* 84, 840–845.

– **(2017)**. "Long-run power storage requirements for high shares of renewables: review and a new model." In: *Renewable and Sustainable Energy Reviews* 79, 1518–1534.

A. Appendix

A.1. Load profile plots from direct Demand Response formulation

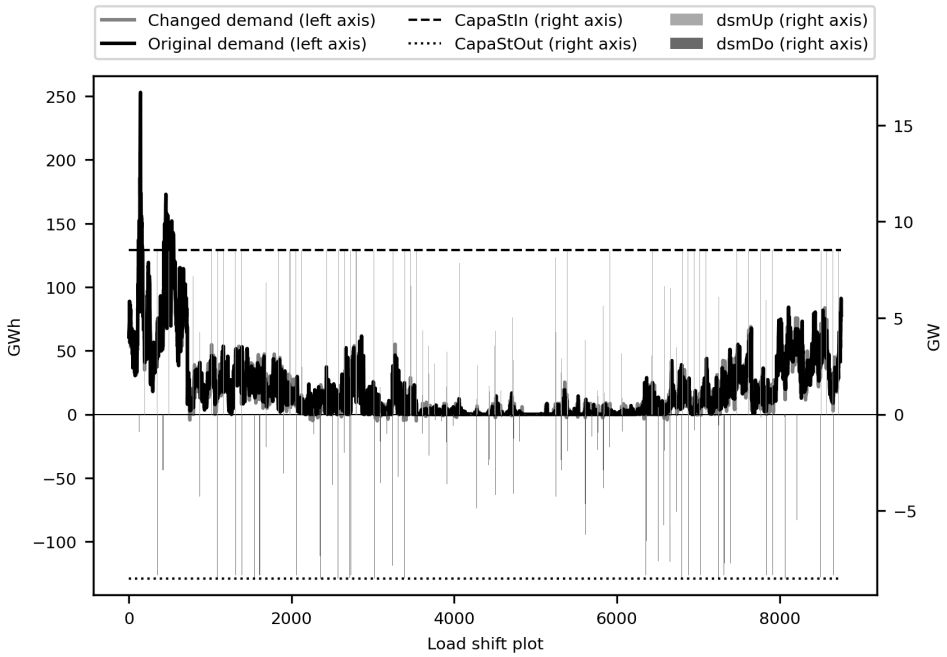

Figure 56: Load profile for DR_{Half} time-step 0-8760, *Heat Storage*

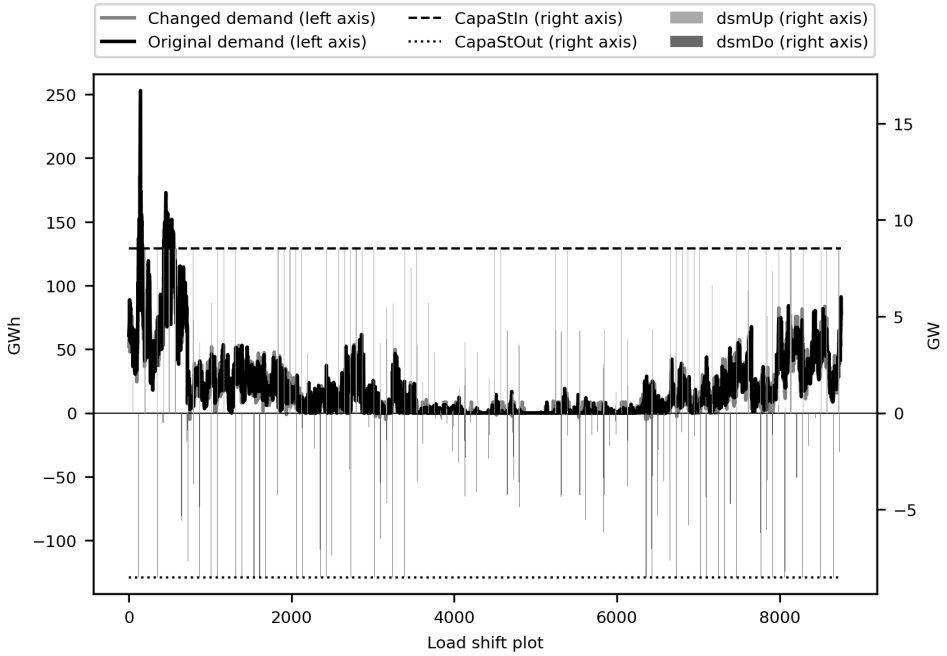

Figure 57: Load profile for DR_{Double} time-step 0-8760, *Heat Storage*

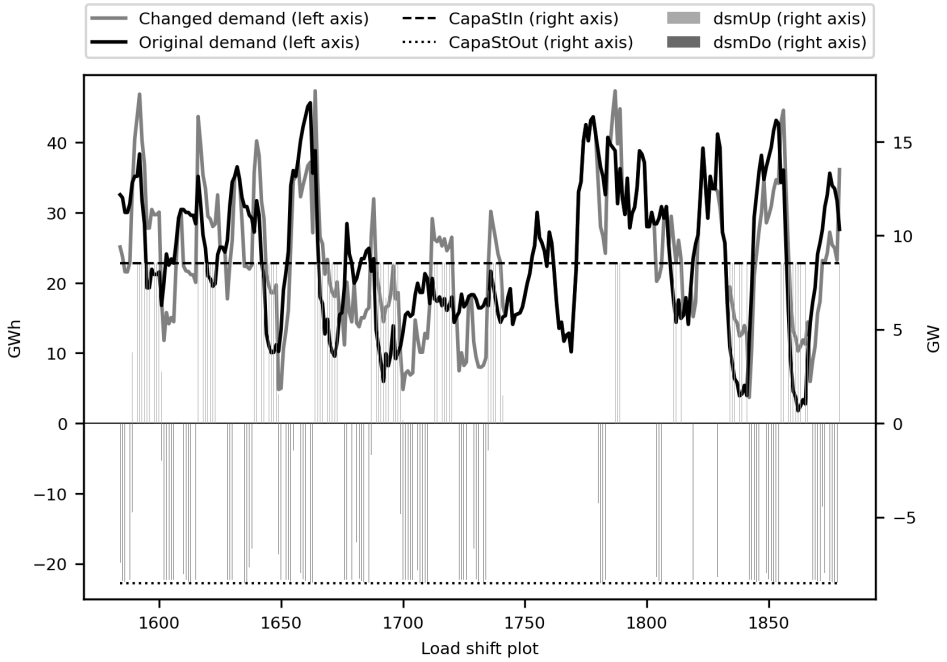

Figure 58: Load profile DR_{Half} time-step 1584-1880, *Heat Storage*

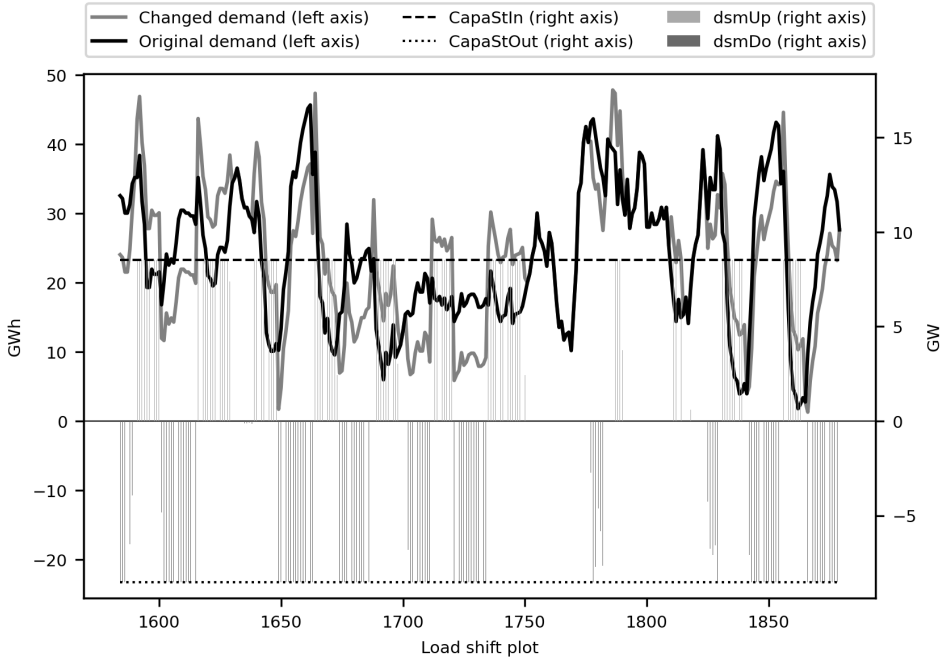

Figure 59: Load profile for DR_{Double} time-step 1584-1880, *Heat Storage*

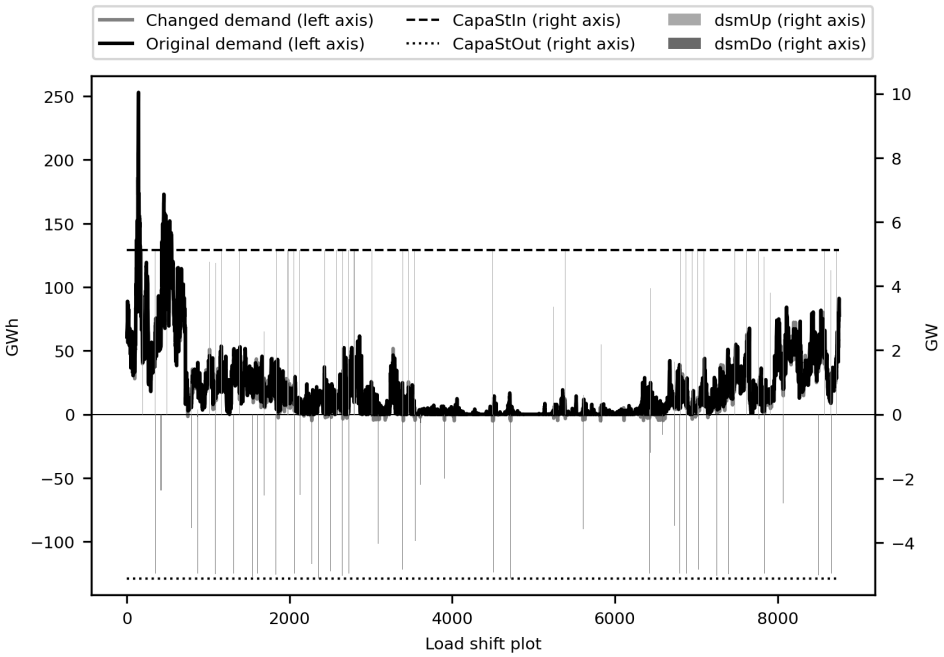

Figure 60: Load profile for DR_{Base} time-step 0-8760, $Heating\ AC$

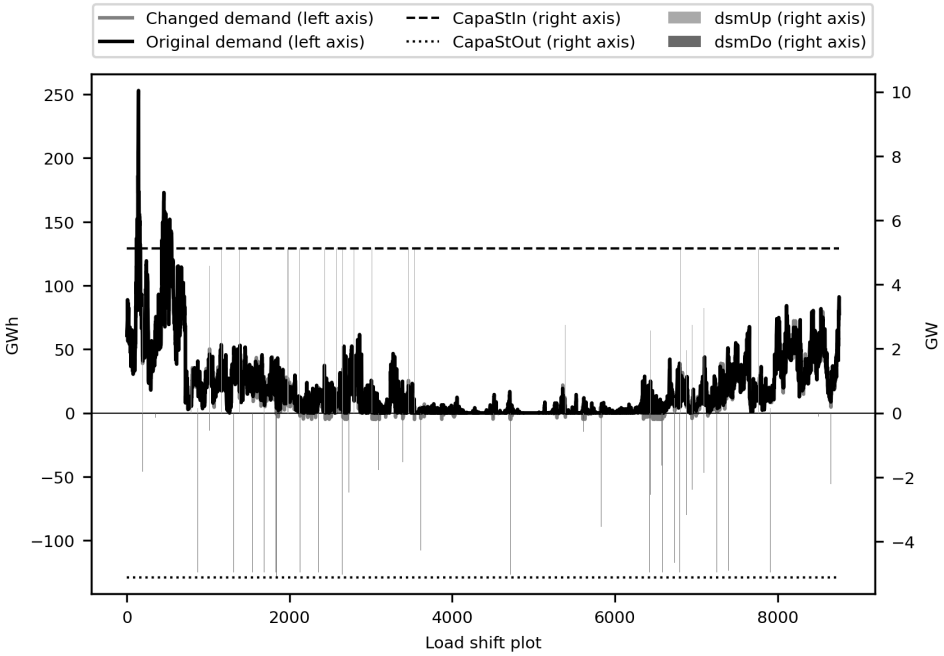

Figure 61: Load profile for DR_{Half} time-step 0-8760, $Heating\ AC$

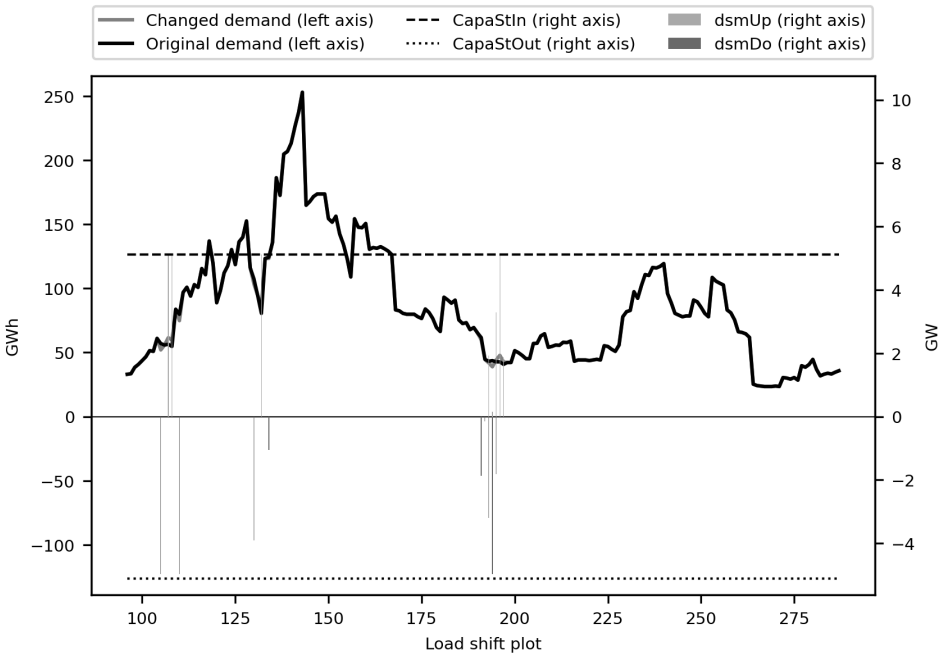

Figure 62: Load profile for DR_{Half} time-step 96-288, $Heating\ AC$

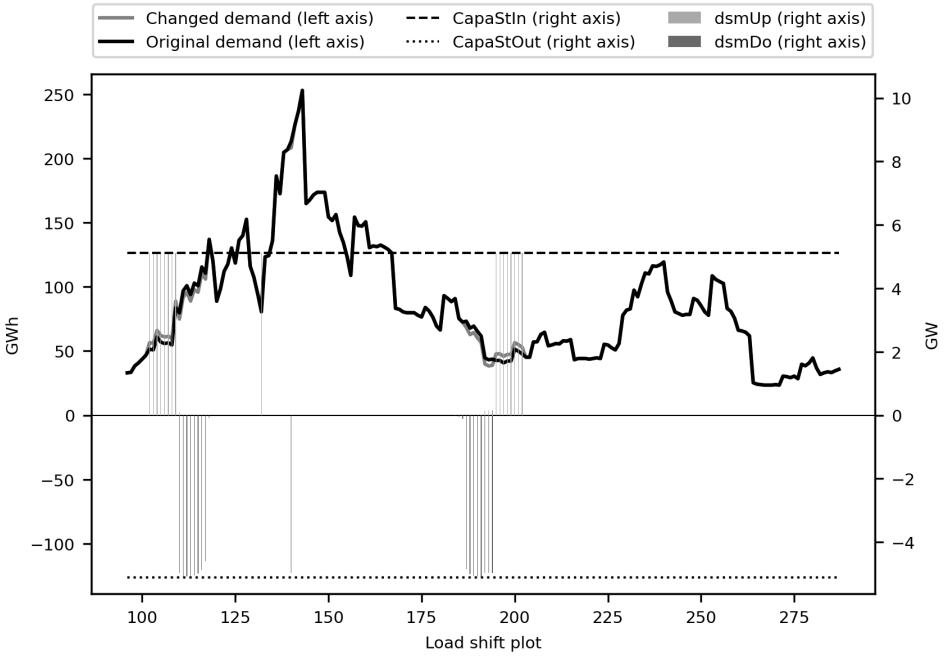

Figure 63: Load profile for DR_{Double} time-step 96-288, $Heating\ AC$

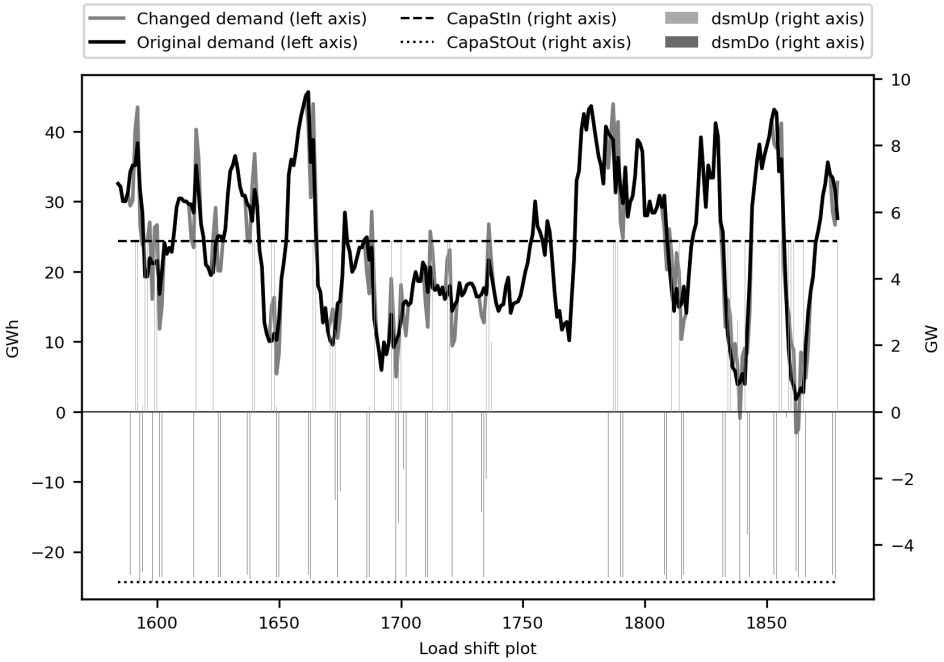

Figure 64: Load profile for DR_{Half} time-step 1584-1880, $Heating\ AC$

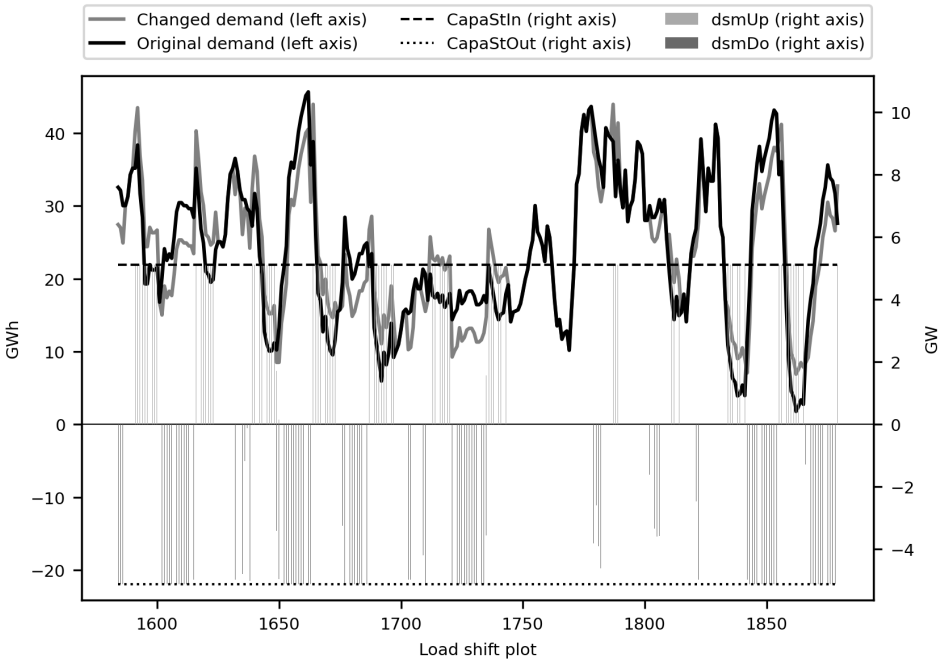

Figure 65: Load profile for DR_{Double} time-step 1584-1880, $Heating\ AC$

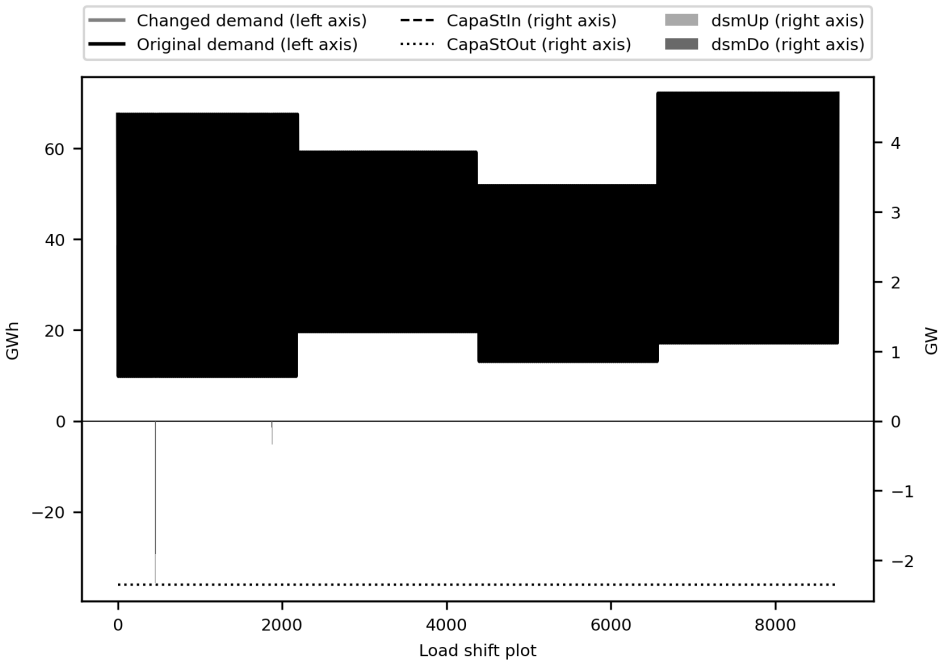

Figure 66: Load profile for DR_{Half} time-step 0-8760, $Process\ shift$

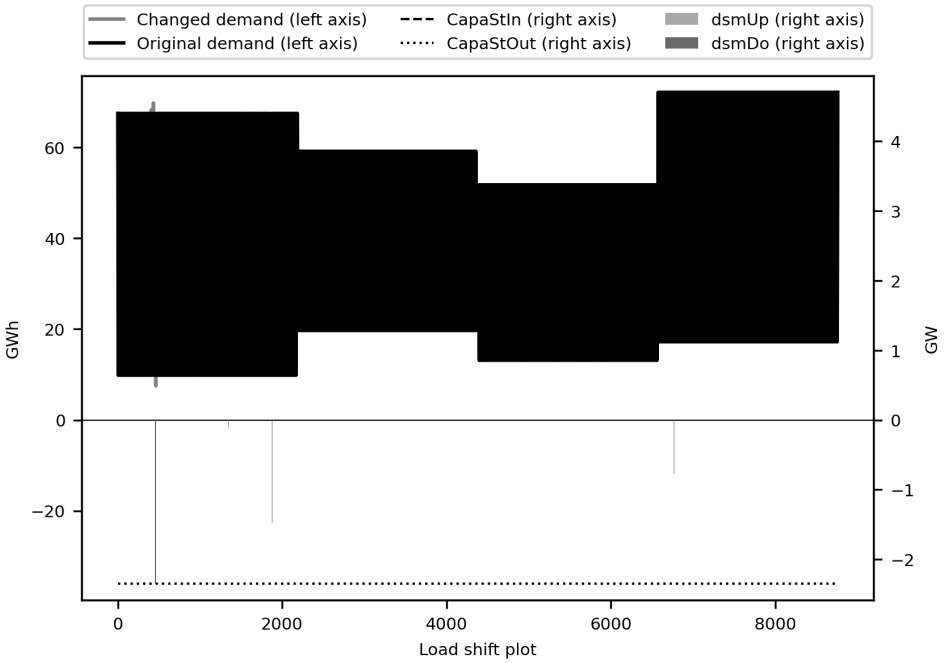

Figure 67: Load profile for DR_{Double} time-step 0-8760, $Process\ shift$

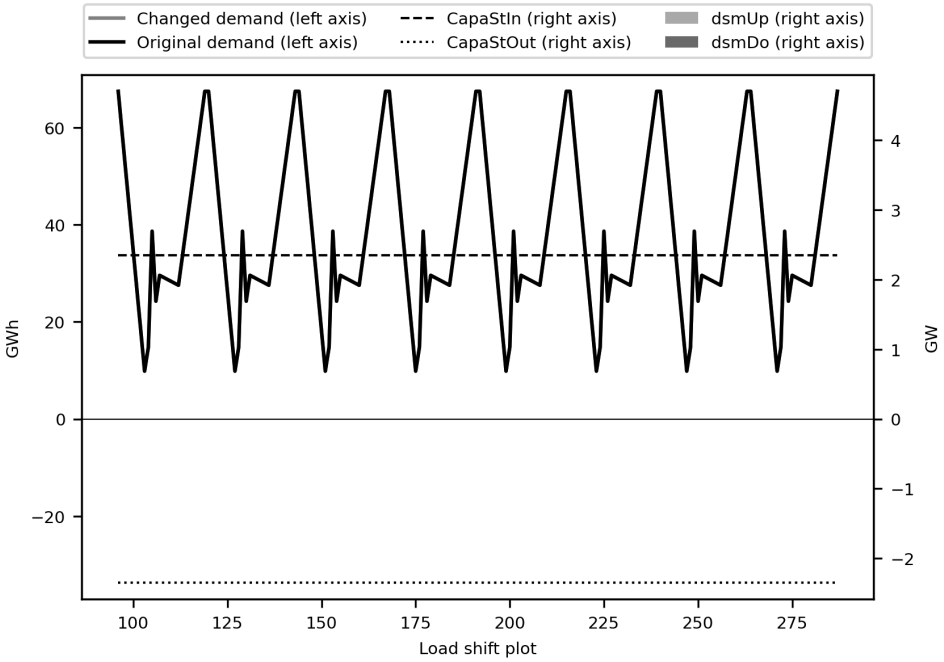

Figure 68: Load profile for DR_{Half} time-step 96-288, $Process\ shift$

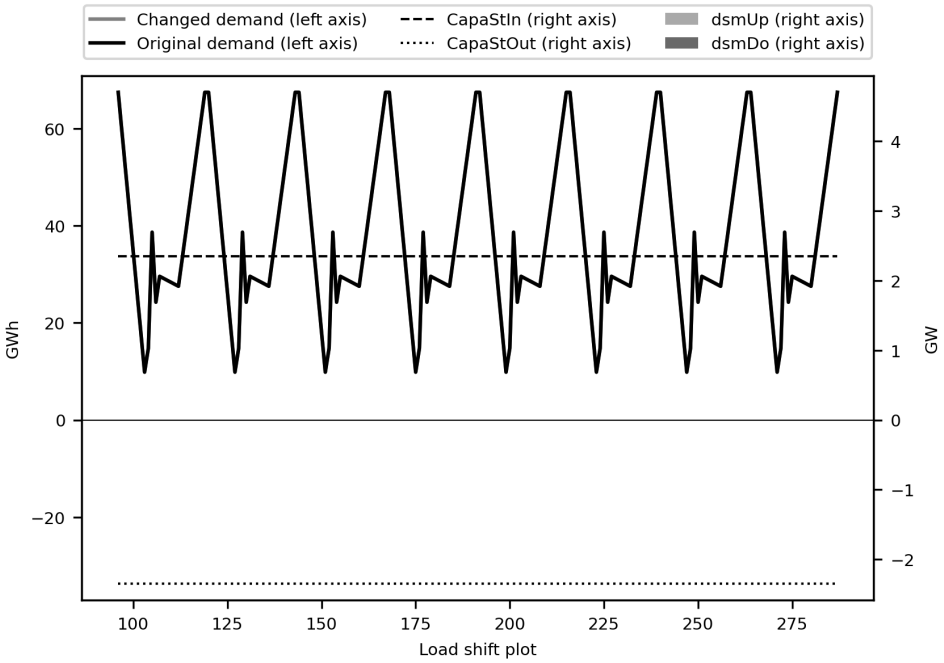

Figure 69: Load profile for DR_{Double} time-step 96-288, $Process\ shift$

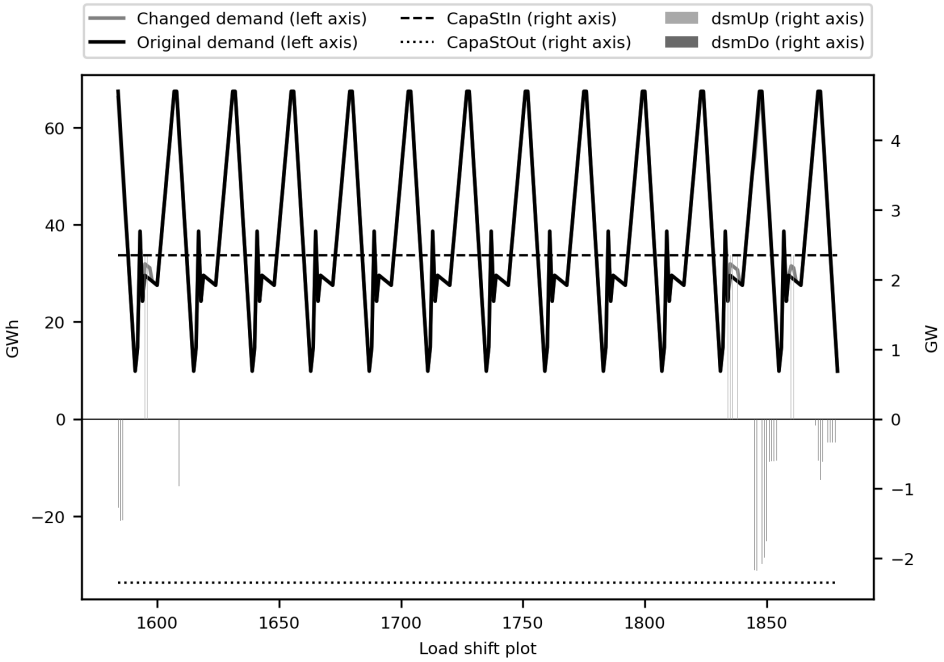

Figure 70: Load profile for DR_{Half} time-step 1584-1880, $Process\ shift$

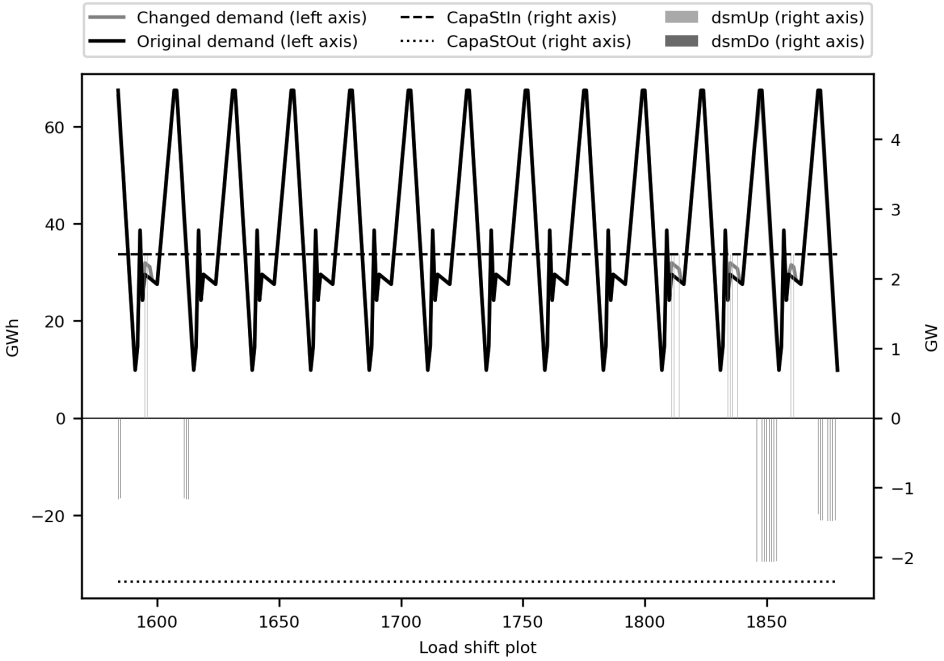

Figure 71: Load profile for DR_{Double} time-step 1584-1880, $Process\ shift$

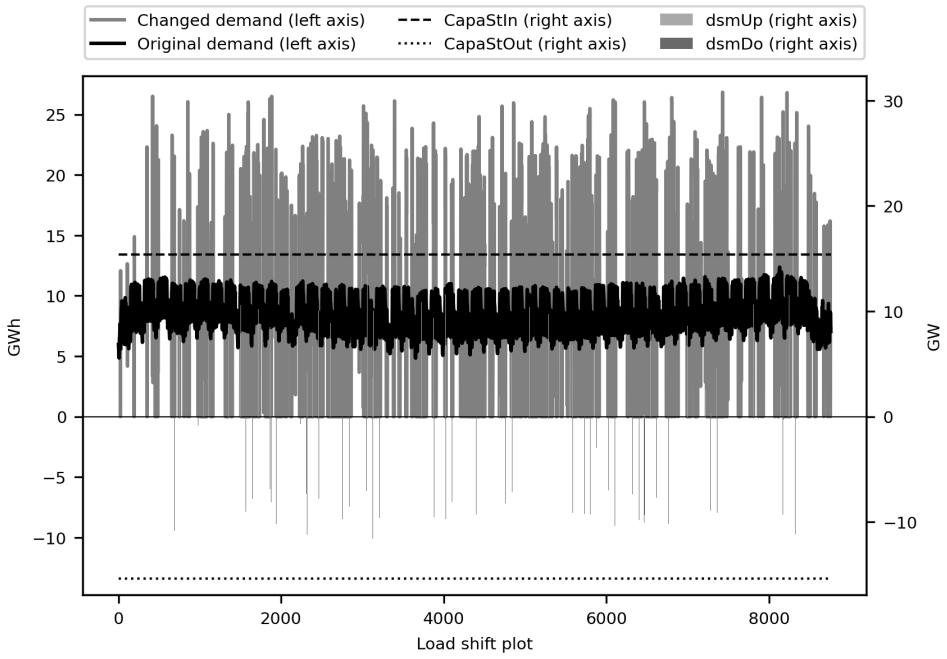

Figure 72: Load profile for DR_{Half} time-step 0-8760, *Washing Appliances*

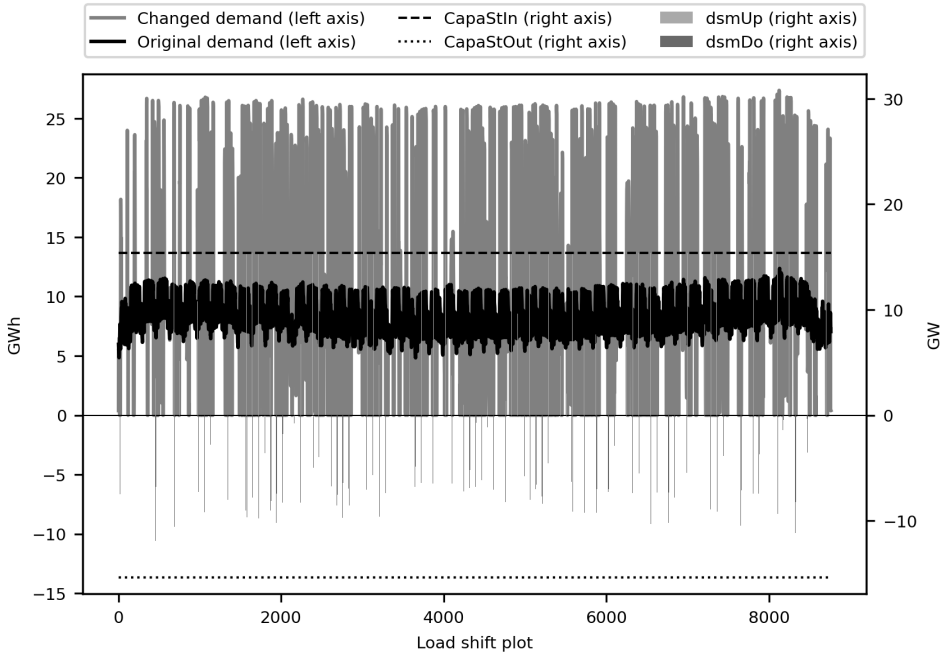

Figure 73: Load profile for DR_{Double} time-step 0-8760, *Washing Appliances*

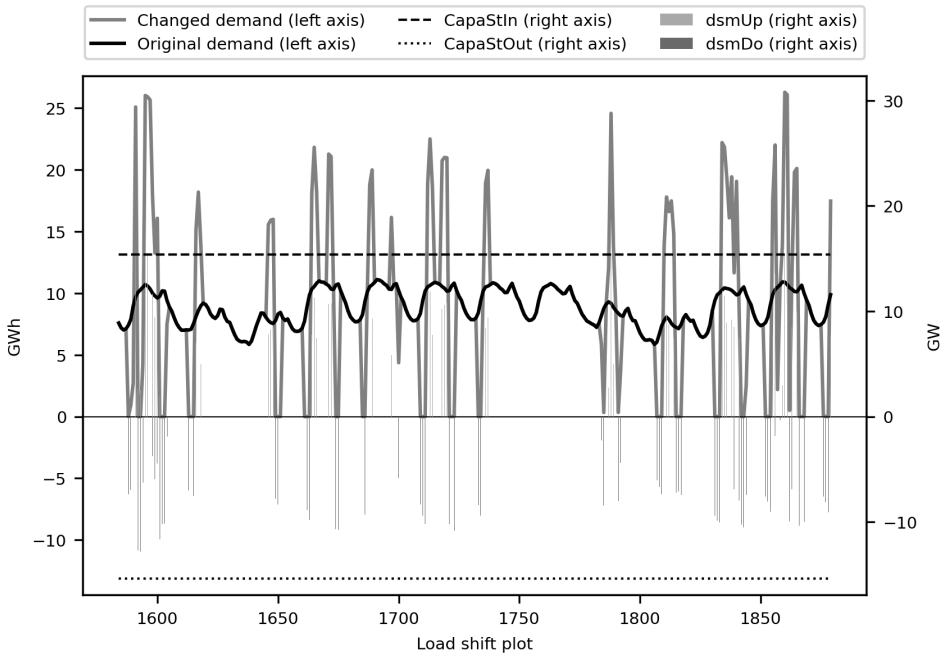

Figure 74: Load profile for DR_{Half} time-step 1584-1880, *Washing Appliances*

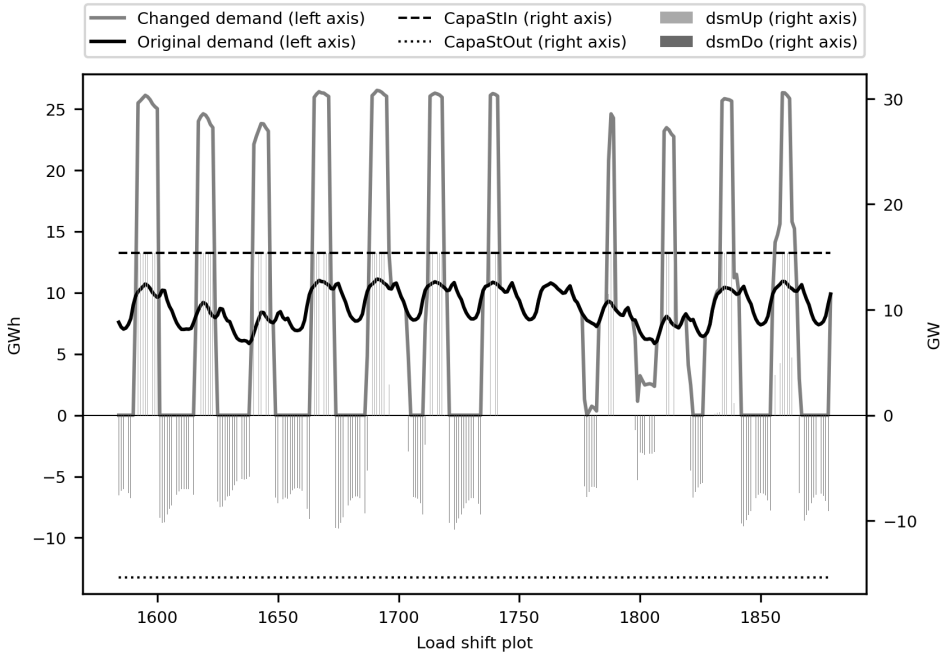

Figure 75: Load profile for DR_{Double} time-step 1584-1880, *Washing Appliances*

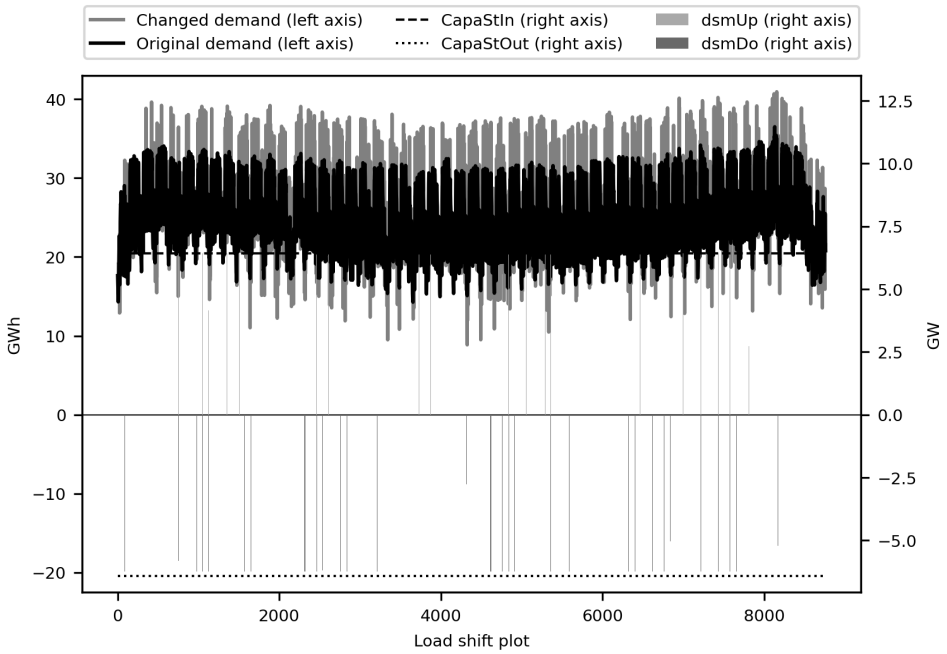

Figure 76: Load profile for DR_{Half} time-step 0-8760, $HVAC$

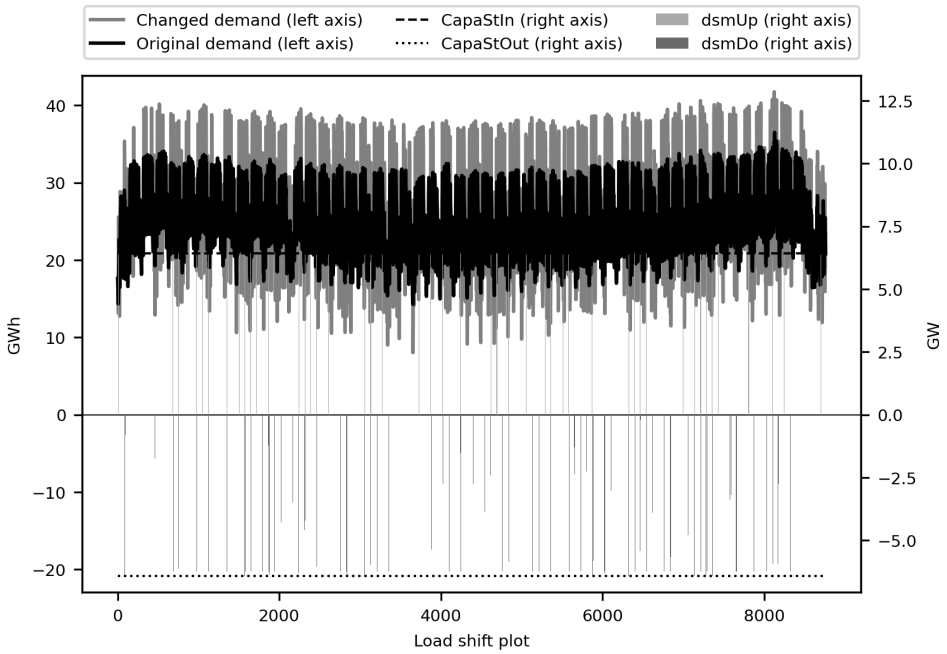

Figure 77: Load profile for DR_{Double} time-step 0-8760, $HVAC$

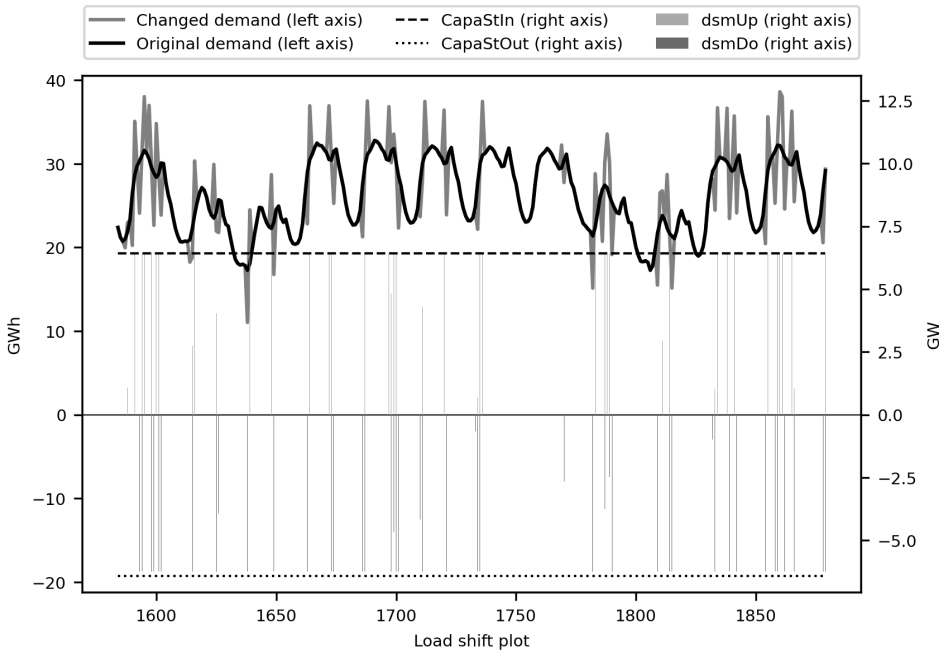

Figure 78: Load profile for DR_{Half} time-step 1584-1880, $HVAC$

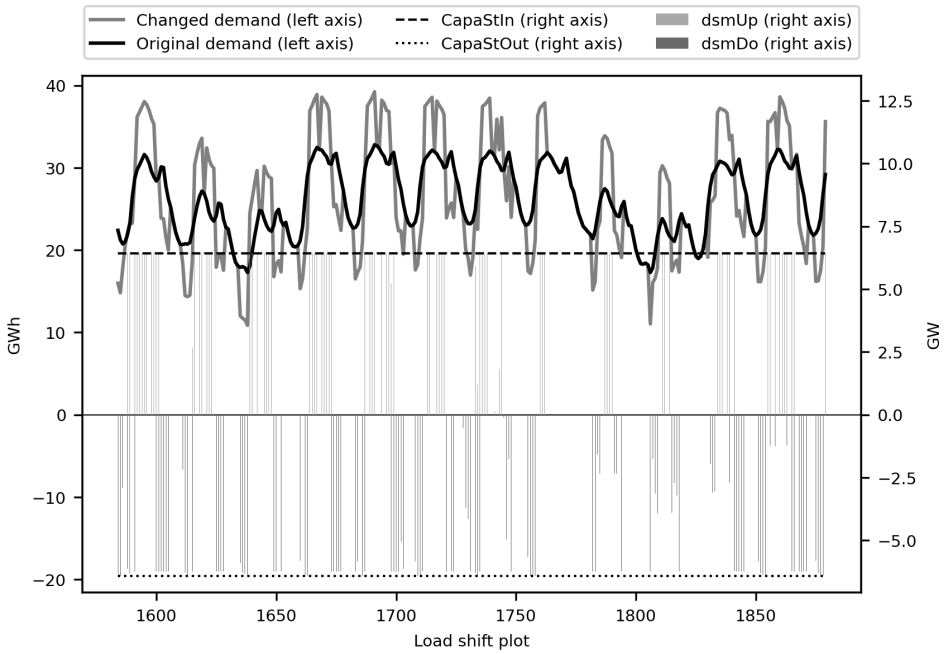

Figure 79: Load profile for DR_{Double} time-step 1584-1880, $HVAC$

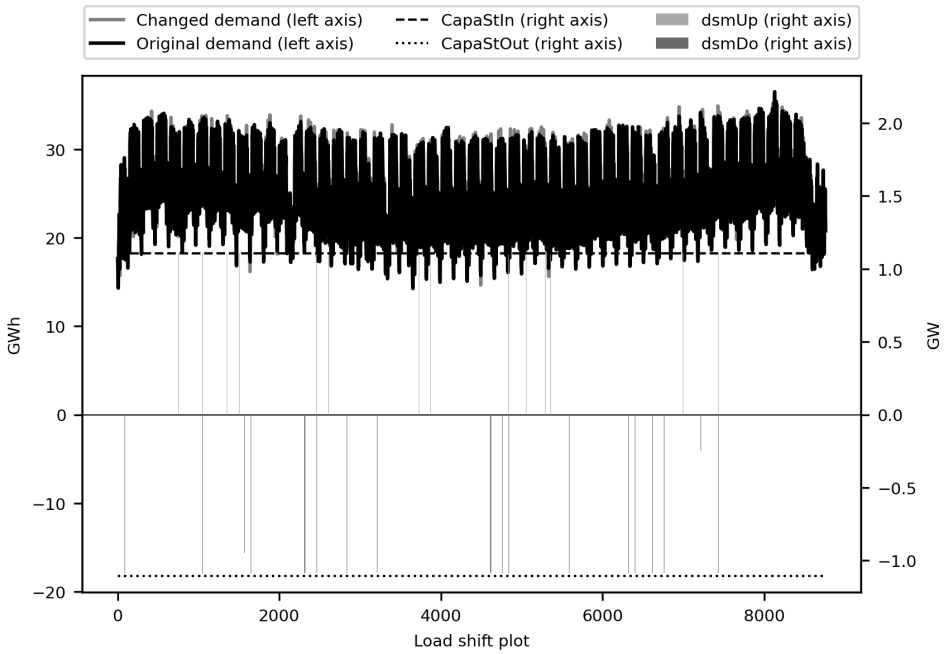

Figure 80: Load profile for DR_{Half} time-step 0-8760, *Cooling and water*

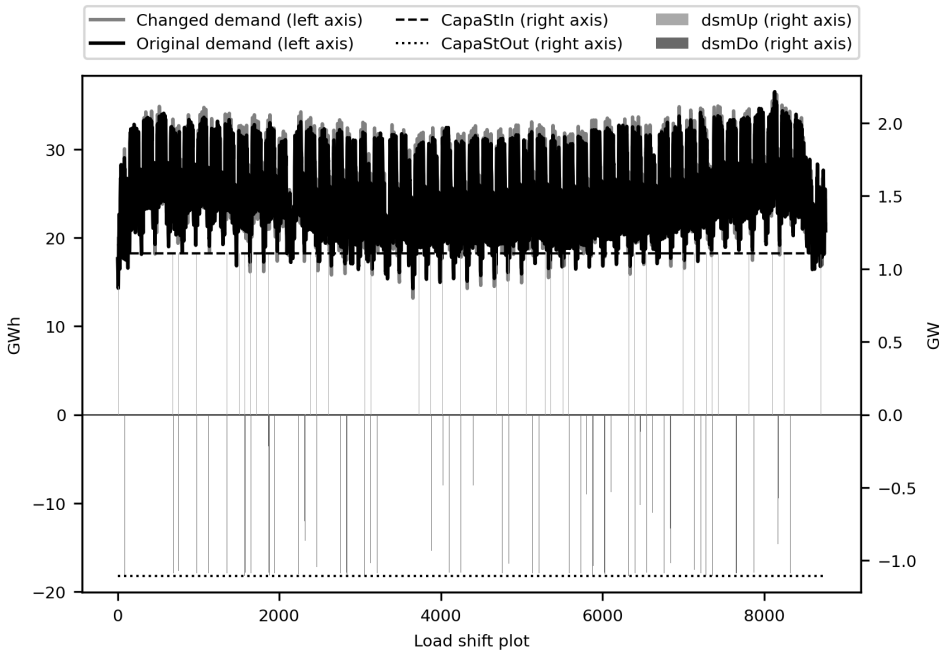

Figure 81: Load profile for DR_{Double} time-step 0-8760, *Cooling and water*

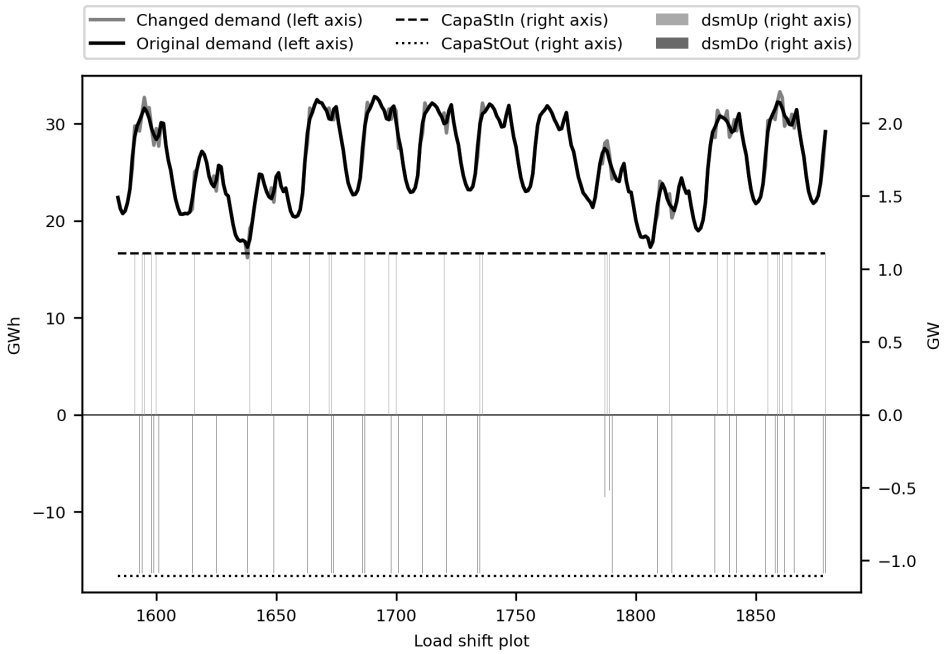

Figure 82: Load profile for DR_{Half} time-step 1584-1880, *Cooling and water*

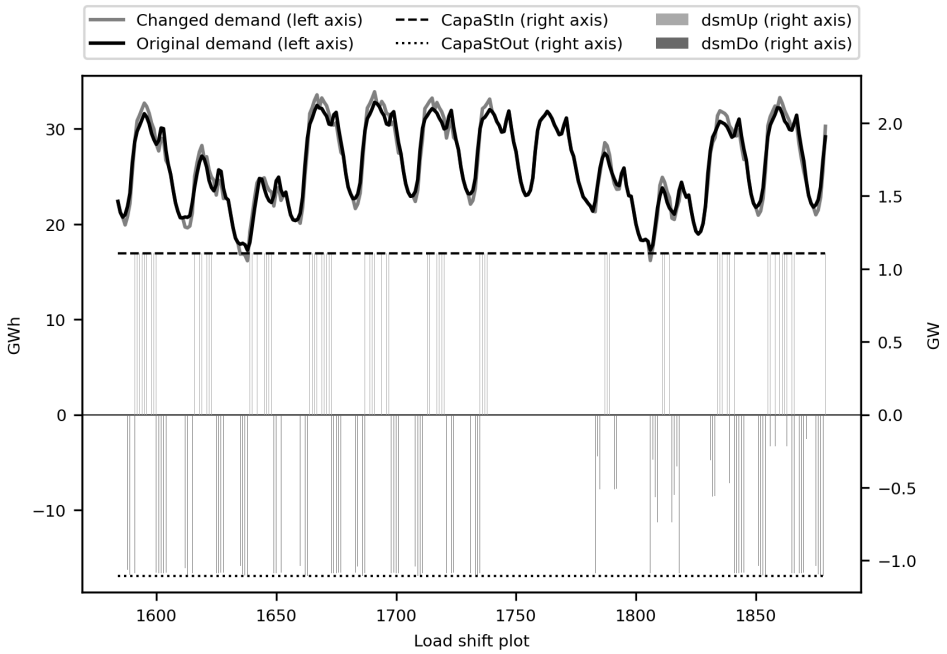

Figure 83: Load profile for DR_{Double} time-step 1584-1880, *Cooling and water*

A.2. Load profile plots from indirect Demand Response formulation

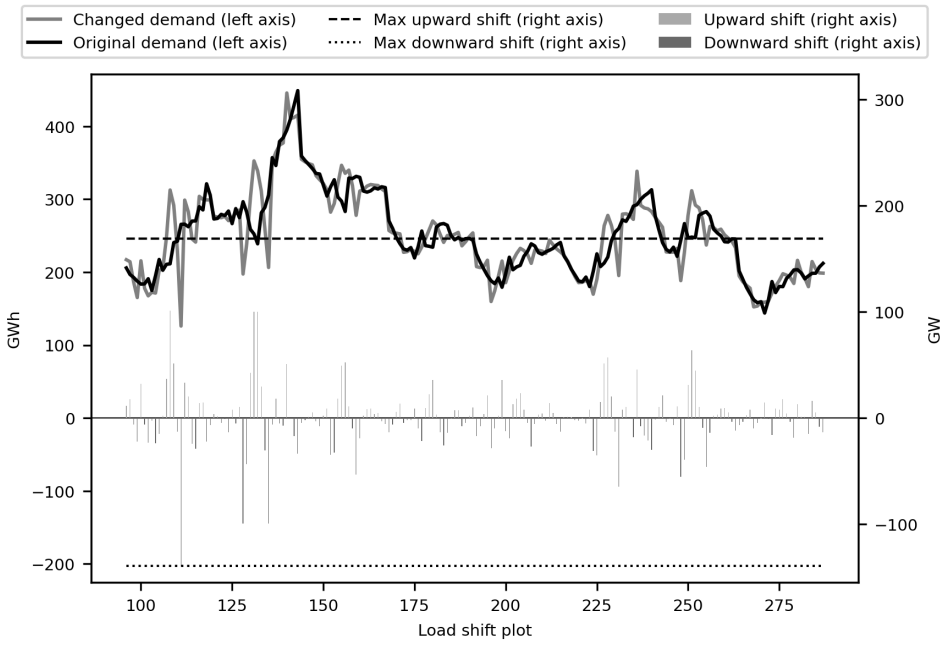

Figure 84: Load profile for TR_4 time-step 96-288

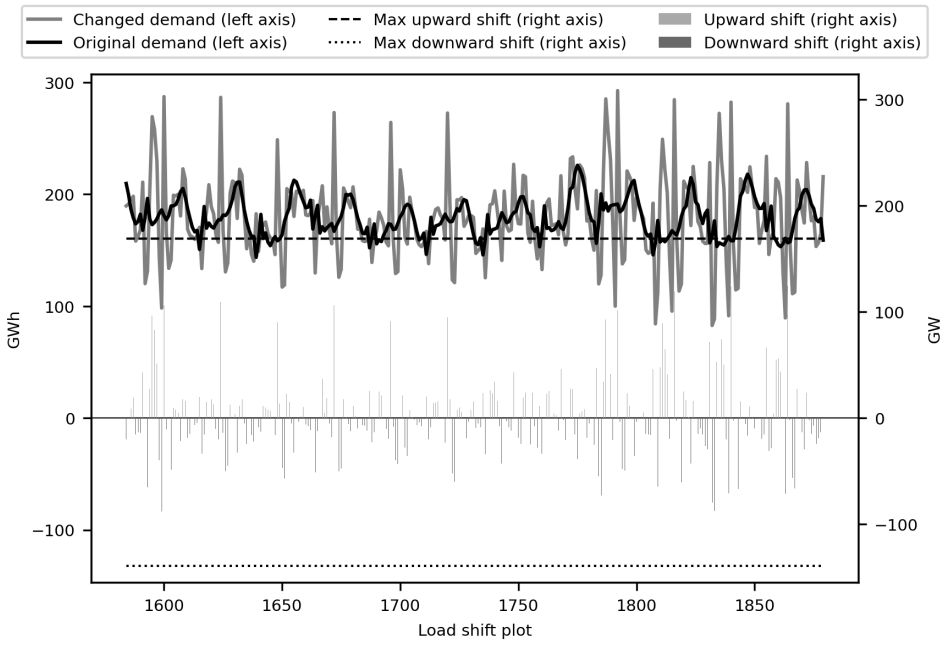

Figure 85: Load profile for TR_4 time-step 1584-1880

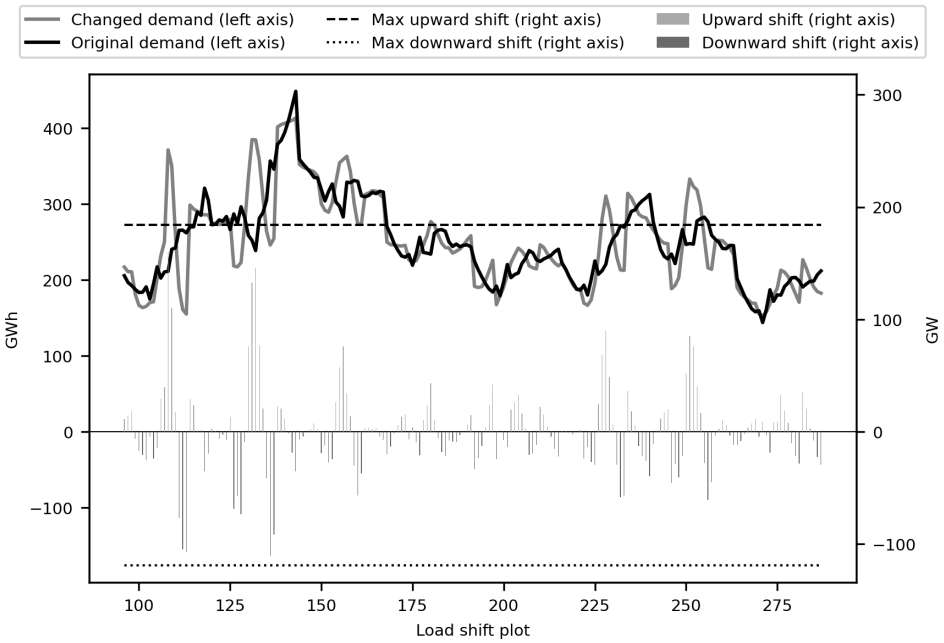

Figure 86: Load profile for TR_6 time-step 96-288

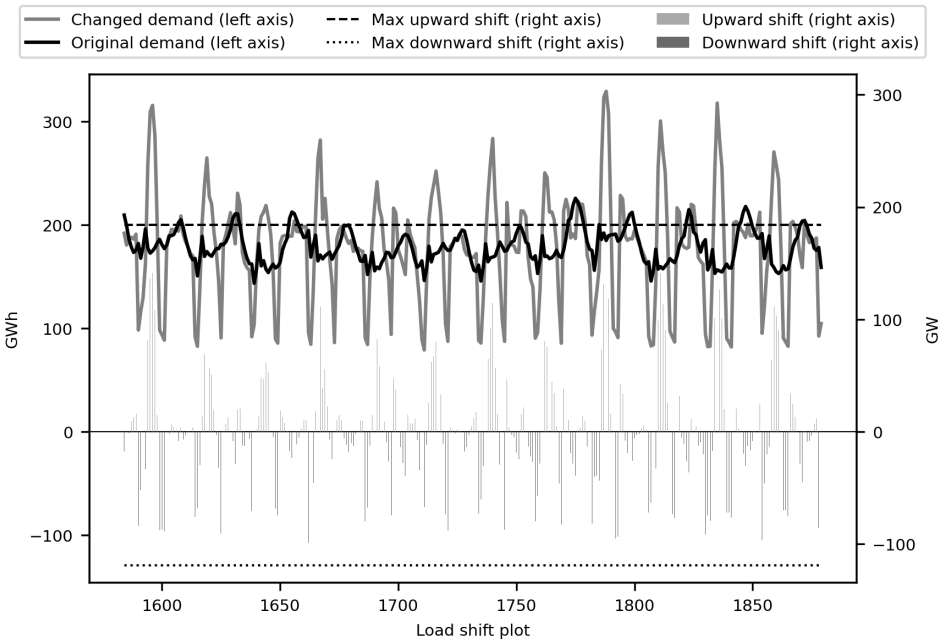

Figure 87: Load profile for TR_6 time-step 1584-1880

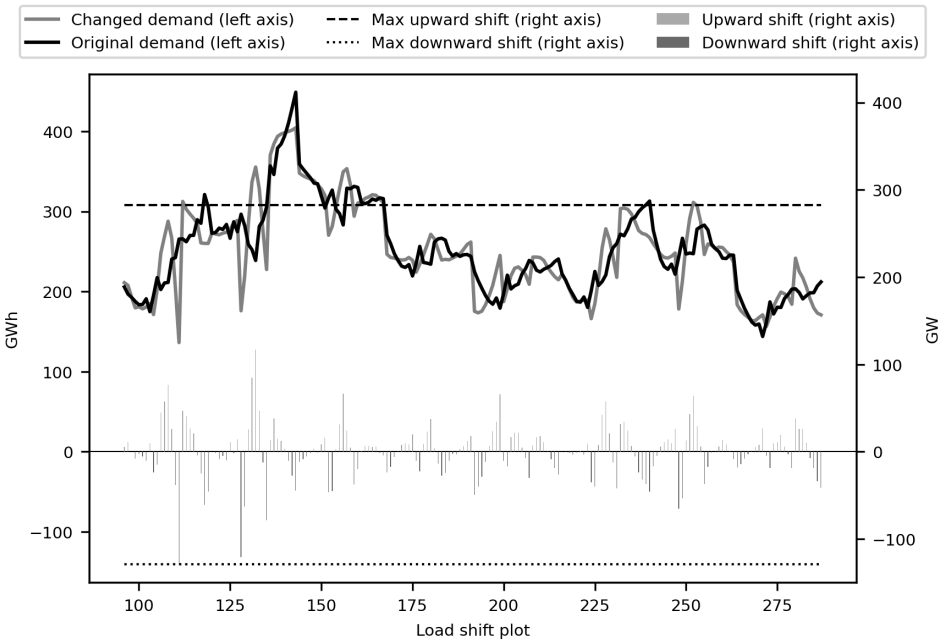

Figure 88: Load profile for TR_8 time-step 96-288

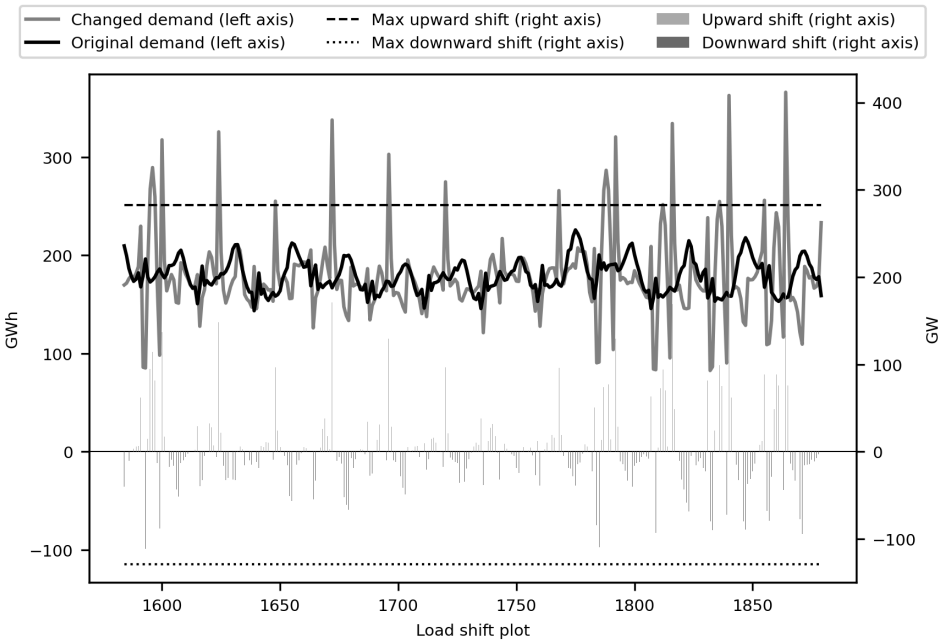

Figure 89: Load profile for TR_8 time-step 1584-1880

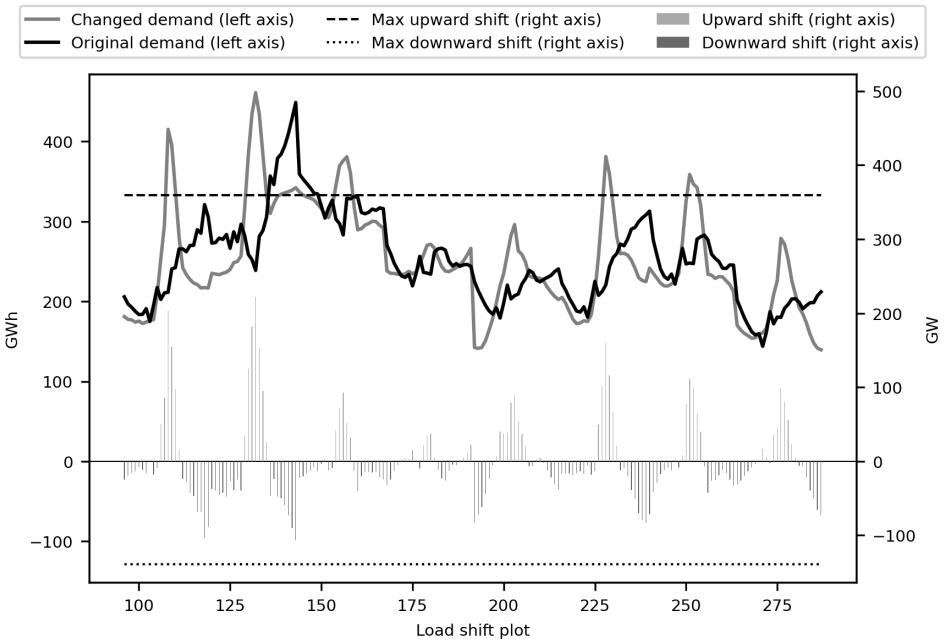

Figure 90: Load profile for TR_{12} time-step 96-288

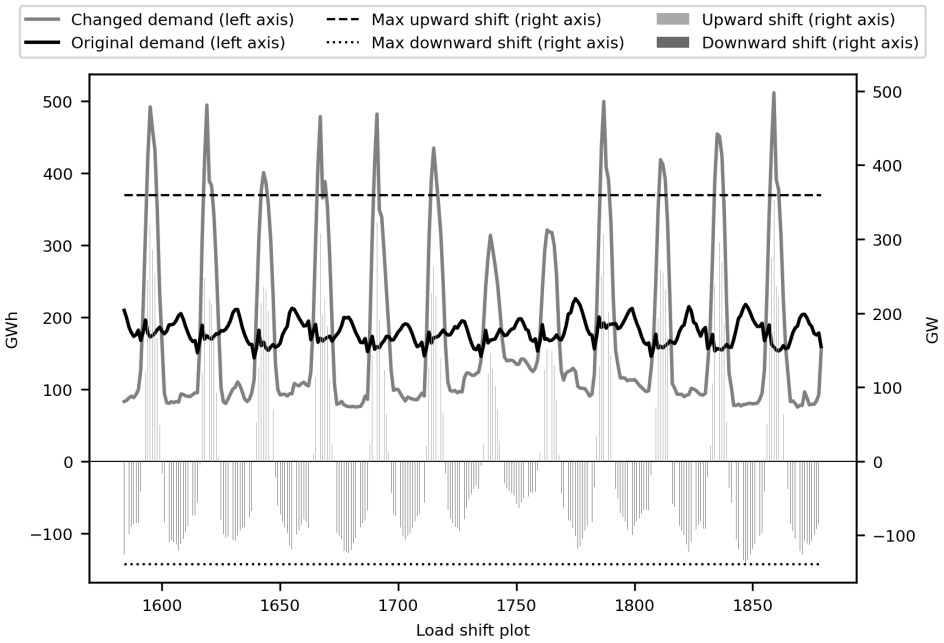

Figure 91: Load profile for TR_{12} time-step 1584-1880